Synthesis of Antimalarial Antifolates

Hanna Francesca Klein

A dissertation submitted to the Faculty of Science, University of the Witwatersrand, Johannesburg

In fulfillment of the requirements for the Degree of Master of Science

September 18, 2013

Declaration

I declare that the work presented in this dissertation was carried out exclusively by myself under the supervision of Dr A.L. Rousseau and Professor C.B. de Koning. It is being submitted for the degree of Master of Science in the University of the Witwaterstrand, Johannesburg. It has not been submitted before for any degree or examination in any other University.

Signed: .....

September 18, 2013

Abstract

Malaria, a widespread disease caused by the protozoan parasite of the genus *Plasmodium*, was responsible for an estimated 216 million infections and 655 000 deaths worldwide in 2010, with the vast majority occurring in Africa (91%) in children under 5 years of age. Parasitic resistance greatly undermines the current combination therapy treatment regimen such that the synthesis of new antimalarial drugs with high efficacy and low toxicity is crucial for future hopes of combating the disease. This is especially true for the antifolates, which remain one of the most important areas for antimalarial drug discovery today. The malarial parasite relies heavily on folate derivatives such as cellular cofactors for the biosynthesis of purines, pyrimidines and certain amino acids, which in turn are required for cellular replication and protein synthesis respectively. Folate derivatives can be produced by the folate salvage pathway or alternatively by the *de novo* pathway, a route unique to the parasite.

In this project, novel antifolates targeting malarial folate metabolism were developed using two approaches, both of which aimed to alleviate the costs of drug development, an important consideration in antimalarial research.

In the first instance, compounds based on already existing drugs, namely the well-known anticancer drugs methotrexate (MTX) and pemetrexed, were synthesised. Cancerous cells are associated with abnormal and frequent mitotic divisions and thus require folate derivatives for cellular growth and replication in a similar manner to rapidly dividing malarial cells. These are acquired *via* a salvage folate pathway, which contains many of the enzymes common to the parasite's own folate salvage pathway, and hence can also be targeted with antifolate therapy. Despite this, chemotherapeutic drugs and, methotrexate in particular, are not used in the treatment of malaria as they are considered too toxic. We aimed to address the issue of toxicity by synthesising precursors of methotrexate and pemetrexed which lack a glutamic acid residue. These molecules, which contain a terminal aromatic carboxylic acid, could potentially be glutamated *in situ* by enzymes of the parasite's *de novo* pathway to afford the active drugs, methotrexate and pemetrexed. In this way, the concentration of the active compound present in the bloodstream would be kept to a minimum. Furthermore, the drug would only be formed in infected cells as the *de novo* synthetic pathway is not present in humans. To this end, precursors of both methotrexate 4-(((2,4-diaminopteridin-6-yl)methyl)(methyl)amino)benzoic acid and pemetrexed 4-(2-(2-amino-4-oxo-4,7-dihydro-3H-pyrrolo[2,3-d]pyrimidin-5-yl)ethyl)benzoic acid were synthesised over 7 and 6 steps in overall yields of 2.2% and 3.2% respectively. Antimalarial testing was conducted *in vitro* in a whole cell *P. falciparum* screen against a cycloguanil

resistant/CQ sensitive Gambian FCR-3 strain. The methotrexate precursor was found to exhibit antimalarial activity (IC_{50} 2.478μM) whereas the pemetrexed precursor was inactive and did not inhibit parasitic growth.

The second approach for the synthesis of novel antimalarial antifolates made use of chemical modification of molecular scaffolds of known antimalarial activity. Using this strategy, a series of flexible pyrimidine compounds were designed by the structural simplification of a dihydrotriazine antifolate hit compound generated from a previous study. Disconnection of the pyrimidine ring into its corresponding α-cyano ketone and guanidine compounds indicated a possible route towards their synthesis. Initially, a control study was conducted in which the more rigid pyrimethamine analogue: 5,6-diphenylpyrimidine-2,4-diamine was synthesised over three steps in an overall yield of 46%. We then applied this methodology to the synthesis of the targeted pyrimidine compounds. Starting from the appropriately substituted phenol, the bromoether of each analogue was successfully synthesised by alkylation with 1,4-dibromobutane. Functional group interconversion of the bromide to the nitrile group, followed by the addition of ethyl benzoate at the α-cyano position afforded a series of α-cyano ketone compounds in yields of 9-68%. The enol ether intermediates were formed using diazomethane instead of the experimental conditions employed in the control study (using triethylorthoformate and an acid catalyst) which had resulted in low yields and the formation of alternative products. By contrast, the high yielding, relatively clean methylation reaction using diazomethane allowed for an attempt of the final step such that the pyrimidine ring was formed on reaction with guanidine in DMSO, affording the 5-(3-(4-chlorophenoxy)propyl)-6-phenylpyrimidine-2,4-diamine over five steps, in an overall yield of 5%. In this way, we had proved the viability of the synthetic route towards the targeted series of flexible, pyrimidine analogues.

Acknowledgements

Firstly, I would like to thank my supervisor Dr A.L. Rousseau without whom this project would not have been possible. Thank you for your kindness and constant willingness to help. I feel very fortunate to have been able to work with you over the last two and a half years and am quite sure I will be the first of many students to come. Thank you to my co-supervisor Professor C.B. de Koning for his invaluable advice, clear explanations and unyielding sense of humor. It has been most comforting to be around someone so approachable and experienced. I would also like to thank Professor J.P. Michael and Dr M. Bode for their assistance. They have both been very helpful.

Thank you to Dr R. Mampa for running numerous NMR spectra. I have really appreciated your generosity of time and the wealth of knowledge regarding NMR spectroscopy you were always willing to impart.

Thank you to Professor R. van Zyl for conducting antimalarial testing on the compounds synthesised.

A special thank you to the members of the Wits organic research group. Thank you to Adushan, Priya, Myron, Stefania, Kathy, Bhakolise, Siyanda, Jimmy, Jean and Tlabo. I have so enjoyed working in your company. I would also like to acknowledge the work contributed by Kamogelo as part of her Honors project. It was a pleasure working with you and I am very grateful for the progress made towards the series of flexible pyrimidine compounds synthesised.

Thank you to the National Research Foundation (NRF) for the funding received during my postgraduate studies.

Finally, thank you to my family. I certainly would not have been able to complete my MSc studies without your support. Thank you for the overdose of love, patience and encouragement which has carried me here.

Contents

Chapter 1

Introduction

Malaria is a widespread disease caused by the protozoan parasite of the genus *Plasmodium*, which is carried and transmitted to humans *via* a female *Anopheles* mosquito vector. There are five different *Plasmodium* species, namely: *P. falciparum*, *P. vivax*, *P. ovale*, *P. malariae* and *P. knowlesi*. *P. falciparum* (Fig. 1.1) is the most virulent *Plasmodium* species and, due to its comparably longer life-span, is particularly effective in transmission[1]. Furthermore, *P. falciparum* is the most predominant form of malaria in sub-saharan Africa[1].

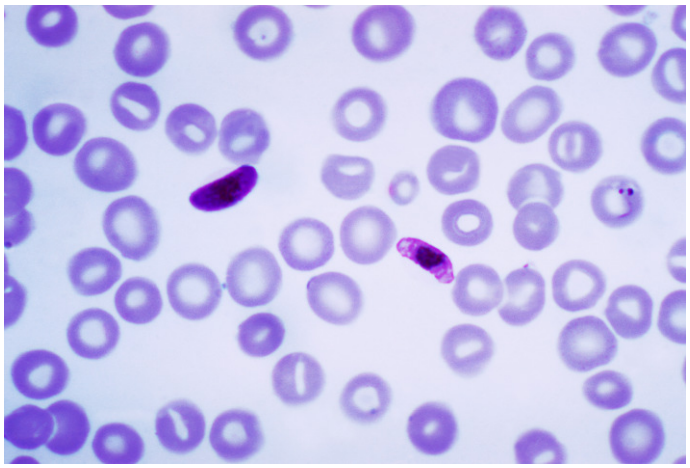

Fig. 1.1 Photomicrograph of a blood smear containing gametocytes of the *P. falciparum* parasite[2]

The *Plasmodium* parasite is introduced into the human bloodstream *via* the female vector mosquito's salivary glands on taking a blood meal (Fig. 1.2). In the first stage of the disease, parasitic sporozoites travel to the liver where they multiply by mitosis within the liver cells or hepatocytes forming thousands of merozoites, a differentiated form of the parasite. This period of asymptomatic dormancy is followed by cell rupture and the onset of the second stage of the disease, in which most of the merozoites enter red blood cells where they continue to multiply asexually, consume intracellular protein and cause cell lysis. This stage of infection, involving

the periodic invasion, multiplication and cell lysis, is characterised by cyclical bouts of fever; a symptom which has been associated with the disease throughout human history. The minority of merozoites, which do not partake in this stage of infection, differentiate into gametocytes which can be ingested by a mosquito during a subsequent blood meal[3]. The ingested gametocytes mate within the mosquito, ultimately resulting in the formation of parasitic sporozoites which travel to the mosquito's salivary glands to complete the lifecycle.

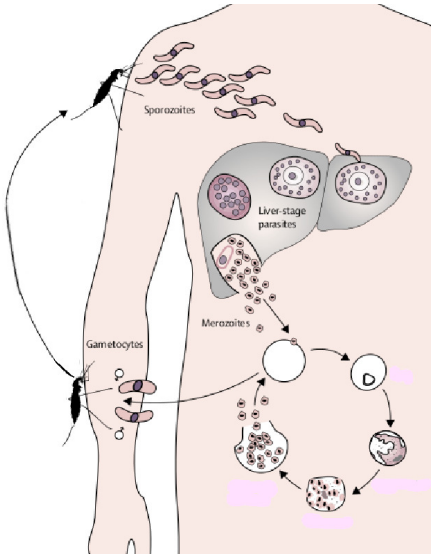

Fig. 1.2 Life cycle of the *P. falciparum* parasite[4]

The geographical distribution of the disease is vast, occurring predominantly in sub-Saharan Africa but also in South-East Asia and the Eastern Mediterranean (Fig. 1.3). The malarial parasite thrives in areas of high temperature and humidity as well as those with high rainfall, as this creates sites of stagnant water which are ideal for mosquito larvae to mature and breed. Furthermore, the period before mosquito to human transmission in which the parasite matures and becomes infectious is substantially shorter at higher temperatures making human infection more likely[5]. Although this explains the predominance of the parasite in tropical and subtropical regions, it does not consider other social and economic factors such as war, climate change, deforestation, changing agricultural practices, the HIV epidemic and most importantly, drug resistance, all of which have been cited as possible reasons for the poor control of malaria in sub-Saharan Africa since the 1990s[4],[5].

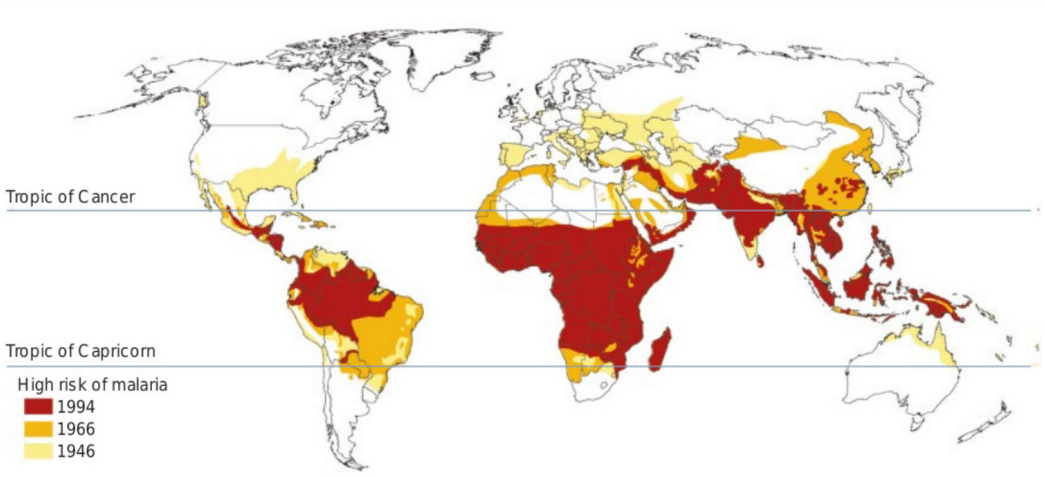

Fig. 1.3 Global distribution of malaria from 1946 to 1994[5]

1.1 Strategies for malarial control and treatment

Malaria was responsible for an estimated 216 million infections and 655 000 deaths worldwide in 2010[6] with the vast majority occurring in Africa (91%) in children under 5 years of age[6]. Past and current strategies used to combat the disease include malarial vector control, the use of pesticides, the development of an effective vaccine and the synthesis of new antimalarial drugs.

1.1.1 Malarial vector control strategies including the use of pesticides

Before World War II, malaria was controlled by environmental management schemes involving the large-scale larvicidal treatment of breeding sites. This effectively reduced the parasite's habitat and prevented the maturation of the *Anopheles* species which, when combined with seasonal variation found in more temperate environments, eradicated the disease from Europe, Asia and the Americas[7]. Despite these achievements, by the late 1940s these vector control practices were abandoned and, in the wake of the discovery of dichlorodiphenyltrichloroethane (DDT) **1**, replaced by the use of synthetic insecticides, a strategy which only targeted adult mosquitoes[7].

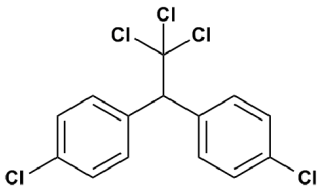

1

Initially, the potent insecticidal properties of DDT were thought to be enough to eradicate the disease and indeed, this proved to be the case in southern Europe, the USSR, Taiwan, North America, and parts of the Caribbean, Venezuela, China, Madagascar and South Africa[8],[9],[10]. However, this strategy proved inadequate in the tropics, especially in sub-Saharan Africa, where limited resources, poor healthcare infrastructure, political turmoil, population pressure and ideal environmental conditions for vector maturation and transmission, prevented eradication of the parasite. These factors worsened with the worldwide and copious use of DDT in the agricultural industry from the 1940s to the 1960s, which led to the emergence of DDT-resistant parasites. By 1962, the environmental impact of DDT as a persistant organic pollutant became apparent, bioaccumulating in the fatty tissues of aquatic organisms and predatory birds[11]. This led to it being banned in 1972 for agricultural use in the US and subsequently, worldwide[12]. More recent studies have pointed to its effects on human health including genotoxicity and endocrine disruption[13].

Today, the use of DDT is restricted to residual indoor spraying and the majority of vector control techniques rely on the use of insecticide-treated bednets, which prevent infection and consequently, have been shown to be effective in decreasing child mortality in malaria endemic areas[14]. Unfortunately, these interventions pose little threat to the highly virulent *Anopheles gambiae* mosquito, which can readily detect and avoid many domestic insecticides, such that the overall vector population remains relatively unaffected[15],[16]. In addition, the poor availability and delivery of insecticide treated nets in sub-Saharan Africa make them inaccessible to many of the local populace[7],[17] further exacerbating the problem. Hence, in order to be effective, these vector control strategies would have to be used in conjunction with alternative strategies as part of a more integrated approach to eradicating the disease.

1.1.2 Antimalarial vaccine development

Current antimalarial research has focused on the development of an effective vaccine. A recent study using radiation-attenuated mosquitoes to inject *P. falciparum* sporozoites into human volunteers found that over 90% of the volunteers were protected[18]. This was followed by the landmark studies completed by the Manhica Health Research Centre (CISM) in Mozambique

in collaboration with GSK, whose RTS,S vaccine was found to reduce the risk of infection in children aged one to four years by 45% over the first six months (compared with children who received a control vaccine)[19] and by 29% after 18 months[20]; both results promoting the feasibility of developing a vaccine against malaria.

Although these results remain promising, the development of a multi-stage vaccine on a large scale remains to be accomplished. In fact, the RTS,S vaccine remains the only identified candidate since the idea of developing a vaccine against malaria was first proposed by Nussenzweig *et al.*[21] in 1967. An effective vaccine will probably have to incorporate multiple antigens from various stages of the parasite's life cycle[22], which may prove to be a difficult task as the immune response required for protection remains to be elucidated[23]. Furthermore, there are over five thousand parasitic genes from which to select an antigen and only thirteen of these have entered clinical testing[24]. Other obstacles adding to the complexity behind vaccine development include variability in protein expression, which is dependent on the stage of the parasite's life cycle, as well as the possibility of competition between the antigens making up a multi-component vaccine[22]. Additional issues such as costs and limited resources to conducting sound, clinical trials also slow down the process significantly.

1.1.3 Antimalarial drugs

In light of these concerns, chemotherapy and more specifically, the synthesis of new antimalarial drugs, still remains the primary approach to malarial control.

1.1.3.1 Quinine and Quinolines

The first antimalarial compound, the alkaloid quinine **2** was serendipitously discovered in Peru from the bark of the cinchona tree [25]. The native Quechua people ground the bark into a powder and used it as an antipyretic for fevers long before its distribution as a medication against malaria throughout Europe in the 1640s. However, it was not until 1820 that the active compound was isolated by the French pharmacists, Pier Joseph Pelletier and Joseph Bienaime Caventou. This work allowed for a quantitative and qualitative analysis of the bark as well as the creation of a dosing regime such that quinine quickly became the first and primary treatment against malaria.

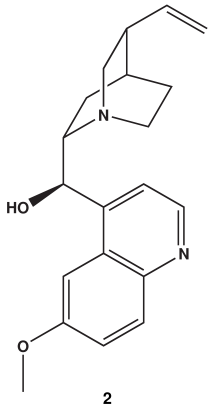

2

As the only available treatment against malaria, quinine was in high demand by the French, British and Dutch who all had colonies in malaria-infested areas[25]. However, the extraction of the antimalarial compound from its only natural source of cinchona bark meant that it was constantly in short supply. Thus, there was much incentive to direct research towards the synthesis of an alternative drug. This came during World War I in the structurally similar compounds, chloroquine **3** and later, amodiaquine **4**, both of which are synthetic compounds[26]. The pharmacological profile of these 4-aminoquinoline compounds was a marked improvement when compared to their aryl alcohol counterparts, as these antimalarials were found to be less toxic, inexpensive and easily administered, thereby encouraging greater compliance[27].

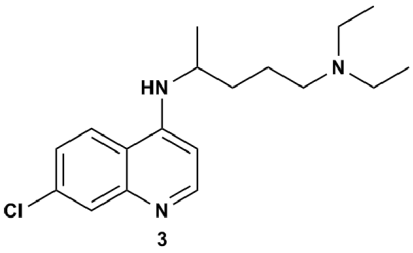

3

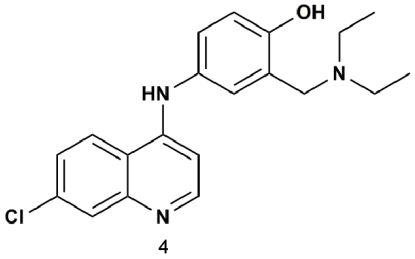

4

The potency of chloroquine stemmed from its ability to accumulate within the acidic food vacuole of the malarial parasite. Although the definitive mechanism responsible for its antimalarial activity remains unclear, many convincing hypotheses based on interference of the parasite's digestion of host cell hemoglobin during the erythrocytic stage of its lifecycle, have been put forward[28]. Using various protease enzymes, the malarial parasite degrades hemoglobin into ferric heme (FPIX) and globin. The globin is further digested into small peptide chains, amino acids and essential nutrients, all of which are required for adequate parasitic growth. The FPIX compound, on the other hand, cannot be further digested and is necessarily detoxified by the parasite by polymerisation to an insoluble, crystalline compound known as hemozoin. Chloroquine takes advantage of the parasite's vulnerability to FPIX which, on failing to be detoxified, would lead to parasitic death. To this end, it irreversibly binds to the free FPIX

molecule forming a stable complex which cannot be converted to the hemozoin polymer. The consequent build-up of the FPIX-chloroquine complex leads to toxicity and resulting parasitic death. Chloroquine was particularly effective due to the improbability of the malarial parasite developing resistance to it. That is, chloroquine does not target the malarial parasite directly and heme, being host specific, does not genetically mutate in the presence of the drug, making parasitic resistance less likely to occur. This allowed the quinoline drug to remain as an effective first-line antimalarial therapy for decades[29]. However, the malarial parasite eventually evolved by genetic modifications of the DNA coding for its digestive vacuole transmembrane protein, PfCRT[30], increasing the rate of chloroquine efflux and thus, preventing accumulation of chloroquine within its vacuole. As a result, by the 1950s chloroquine resistant parasites were observed in Southeast Asia and South America[28] and have since become widespread.

1.1.3.2 Artemisinin-based drugs

The antimalarial effects of artemisinin have been known since 200 BC when Chinese herbalists first recorded using it from the leaves of *Artemisia annua* or sweet wormwood. The Chinese traditional medicine was used for the treatment of malaria as well as various other medical conditions. However, the drug was only isolated in 1972 after the Chinese government, in the face of developing resistance to chloroquine, initiated a secret, nation-wide research program to discover new antimalarial drugs for use in the North Vietnamese war against the United States of America. This involved screening synthetic chemicals as well as traditional Chinese remedies for antimalarial activity[31], culminating in the discovery of artemisinin **5** after isolation from its original herbal source. Several semi-synthetic derivatives of artemisinin **5**, a sesquiterpene lactone, have since been developed including artemdiethyl ether **6**, artedimethyl ether **7** and artesunate **8** [32]. The defining peroxide bridge of the artemisinins bestow a short-half life to the drugs which have to be used in combination with other antimalarial compounds in order to be effective and limit the development of resistance. Artemisinin-based combination treatments (ACTs) are used as the primary choice of treatment in many countries[33], however, resistance against ACTs has been reported and poses a threat to the efficacy of the current treatment regimen. Hence, the development of new drugs remains a crucial part of current malarial research.

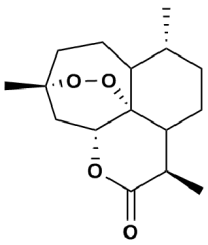

5

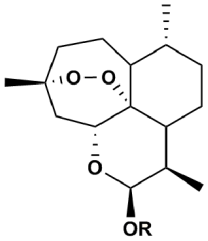

6 R = Me
7 R = Et
8 R = $CO(CH_2)_2CO_2H$

1.1.3.3 Antifolate drugs

This project focuses on the third and most widely used class of antimalarial drugs today: the antifolates. In the section to follow, we will describe the mechanism by which they exhibit antimalarial activity, the problem of parasitic resistance and how this has shaped design and development.

1.2 Development of antifolate drugs

The development of antifolate drugs remains one of the most important areas for antimalarial drug discovery today. Unlike the plant-derived quinolines and artemisinins, the antifolates were developed by a chemical synthetic approach; the product often being similar in structure to existing drugs or other biological molecules. The basis for this work therefore relies on a sound knowledge of the malarial parasite's cell biology, particularly folate metabolism.

1.2.1 Folate metabolism and the malarial parasite

The malarial parasite relies heavily on folate derivatives as cellular cofactors for the biosynthesis of purines, pyrimidines and certain amino acids[34] which in turn are required for cellular replication and protein synthesis respectively. Folate derivatives can be produced *via* the folate salvage pathway or alternatively *via* the *de novo* pathway, a route unique to the parasite.

1.2.1.1 The folate salvage pathway

The folate salvage pathway (Scheme 1.1) is present in both humans and the malarial parasite and allows the parasite to regenerate or "salvage" the key intermediate dihydrofolate (DHF) **9** as follows: DHF is reduced to tetrahydrofolate (THF) **10**, with the concurrent oxidation of NADPH to NAD^+, by the *dihydrofolate reductase* domain of the *dihydrofolate reductase-thymidylate synthase* (DHFR-TS) enzyme. The THF intermediate is then converted by *serine*

hydroxymethyl transferase (SHMT) to methylene THF **11**, which in turn is responsible for the alkylation of deoxyuridine monophosphate (dUMP) **12** to deoxythymidine monophosphate (dTMP) **13**, an essential precursor for DNA synthesis. This reaction regenerates the folic acid derivative, DHF **9** which can then re-enter the salvage pathway at the reductive step.

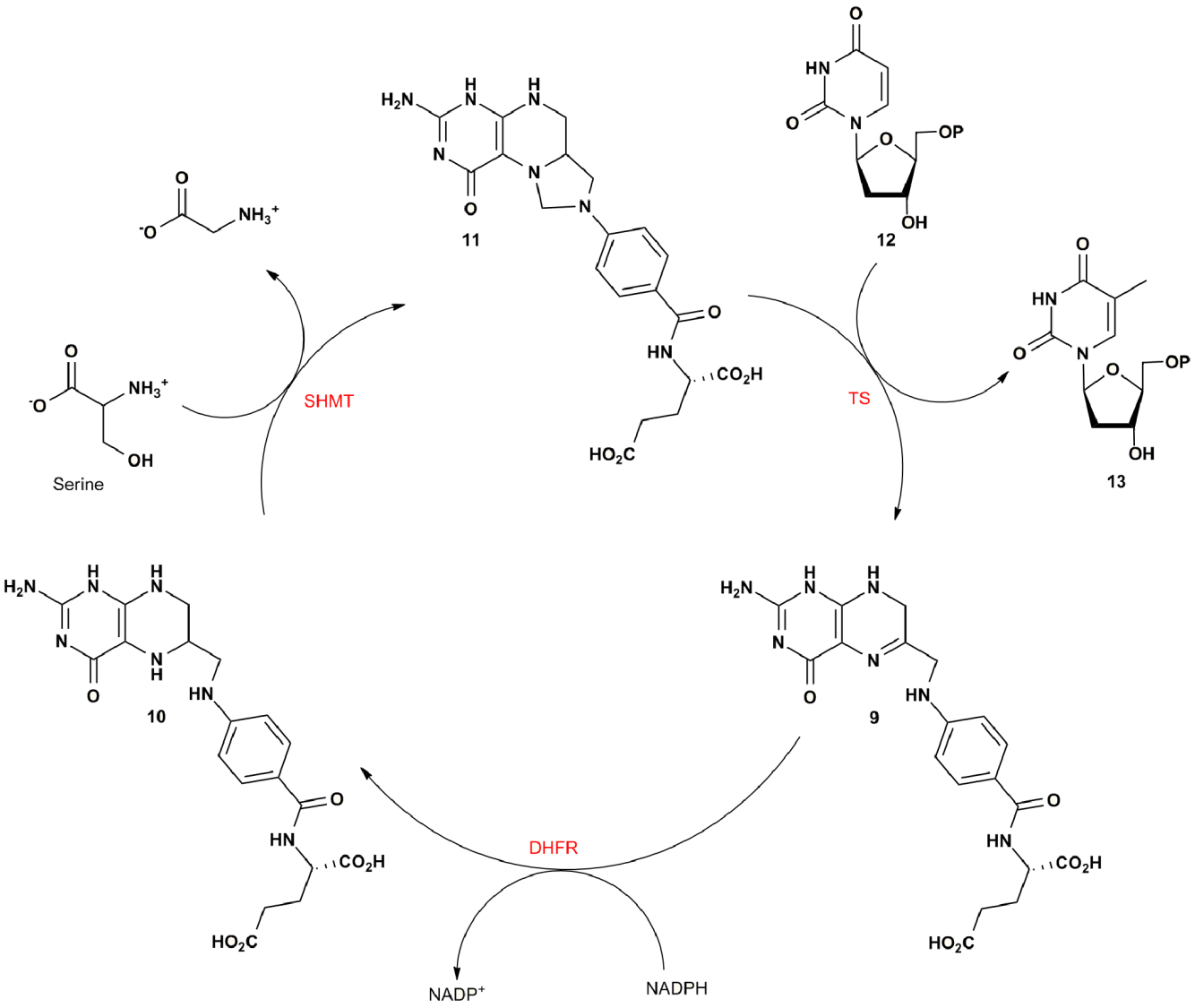

Scheme 1.1 The folate salvage pathway present in both humans and the malarial parasite

1.2.1.2 The *de novo* pathway

Unlike humans, who acquire DHF from their diet, the malarial parasite is also able to synthesize DHF in six steps *via* the *de novo* pathway (Scheme 1.2). The phosphorylated purine nucleoside, guanosine triphosphate (GTP) **14** is converted to dihydroneopterin triphosphate (DHNTP) **15** by *GTP-cyclohydrolase*. The enzymes catalysing the next two reactions, namely *dihydroneopterin triphosphate pyrophosphohydrolase* (DHNTPase) and *dihydroneopterin aldolase* (DHNA), are responsible for the dephosphorylation of dihydroneopterin triphosphate (DHNTP) **15** to the free hydroxyl form, dihydroneopterin (DHN) **16** and subsequent cleavage to form hydroxymethyl-7,8-dihydropteridine (DHPT) **17**. The phosphorylation of DHPT to hydroxymethyl-7,8-dihydropteridine diphosphate (DHPT-PP) **18** followed by the formation of 7,8-dihydropteroate (DHP) **20** by condensation with *para*-amino benzoic acid (PABA) **19**, is achieved by the bifunctional enzyme, *dihydrohydroxymethylpterin pyrophosphokinase-dihydropteroate synthase* (HPPK-DHPS)[35]. The parasitic enzyme *dihydrofolate synthase* (DHFS) glutamates DHP to afford the key intermediate DHF **9**. DHF is then further glutamated by *folylpolyglutamate synthase* (FPGS), which exists as a bifunctional enzyme complex with DHFS, before feeding into the folate salvage pathway. Polyglutamation ensures a high DHF-enzyme affinity[36] and infers a negative charge to the folate substrate, thereby preventing leakage into the extracellular compartment[37].

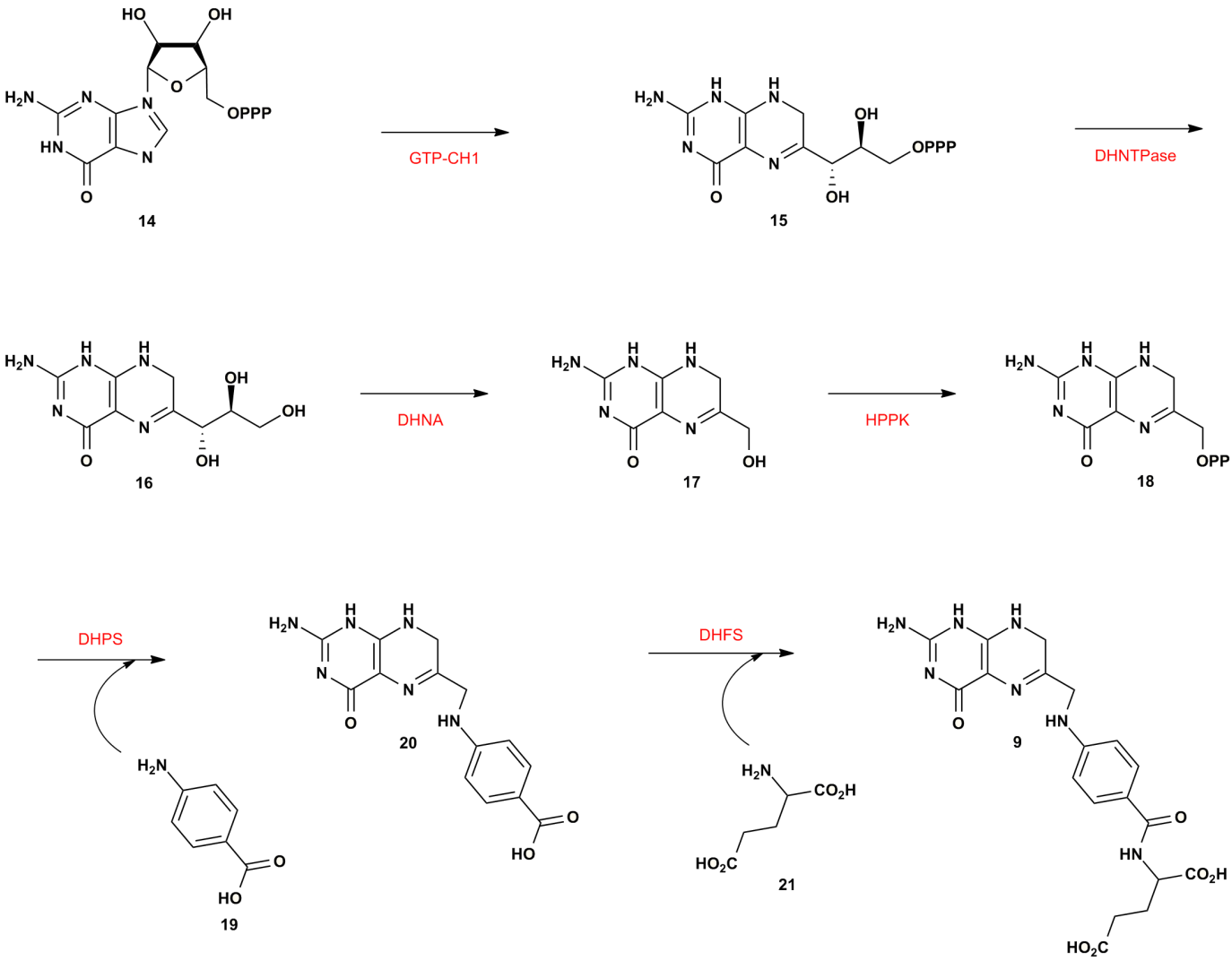

Scheme 1.2 The *de novo* pathway unique to the malarial parasite

1.2.2 The folate pathway as a target for antimalarial therapy

The folate pathway has been successfully targeted by compounds which inhibit folate synthesis and/or conversion [38]. These antifolates were developed alongside other synthetic malarial compounds in response to the shortage of quinine during World War II. They were structurally based on pyrimidine, which was known to be both a constituent of nucleic acids and involved in protein synthesis[39], and target key enzymes of the folate pathway: PfDHFR-TS and DHPS. By contrast, progress towards designing inhibitors of other enzymes of the folate pathway, including SHMT, GTP-CH1, DHNA, HPPK and PfDHFS-FPGS has been limited.

1.2.2.1 Inhibitors of *P. falciparum* dihydrofolate reductase-thymidylate synthase (PfDHFR-TS)

The vast majority of antifolate compounds target DHFR, a key enzyme in the folate salvage pathway (Scheme 1.1) which acts on DHF, a derivative of folic acid, reducing it to THF, which in turn is needed for the synthesis of the nucleosides and amino acids required for adequate DNA/RNA replication and protein synthesis. The inhibition of DHFR prevents these processes occurring, thereby resulting in a rapid reduction of cell growth and multiplication, ultimately leading to cell death. This strategy is also used in the treatment of cancer as well as other bacterial and fungal infections; all of which are marked by rapidly dividing, folate-dependent cells[34].

Unlike humans, who possess monomeric forms of both DHFR and TS, the malarial parasite expresses DHFR and TS as a bifunctional enzyme[34], the crystal structure of which has been solved[40]. This structural information, which provides insight into interdomain interactions between DHFR and TS as well as enzyme-ligand binding conformations, has significantly aided in the development of new antifolate compounds[41],[42].

The first antifolate compounds to be developed were the DHFR inhibitors, proguanil **22** and chlorproguanil **23** [3].

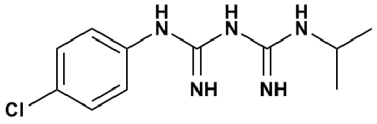

22

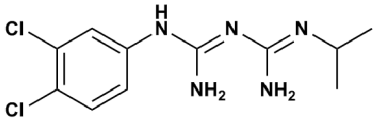

23

These compounds do not inhibit DHFR directly but are metabolised in the liver to the corresponding active compounds cycloguanil **24** and chlorcycloguanil **25**.

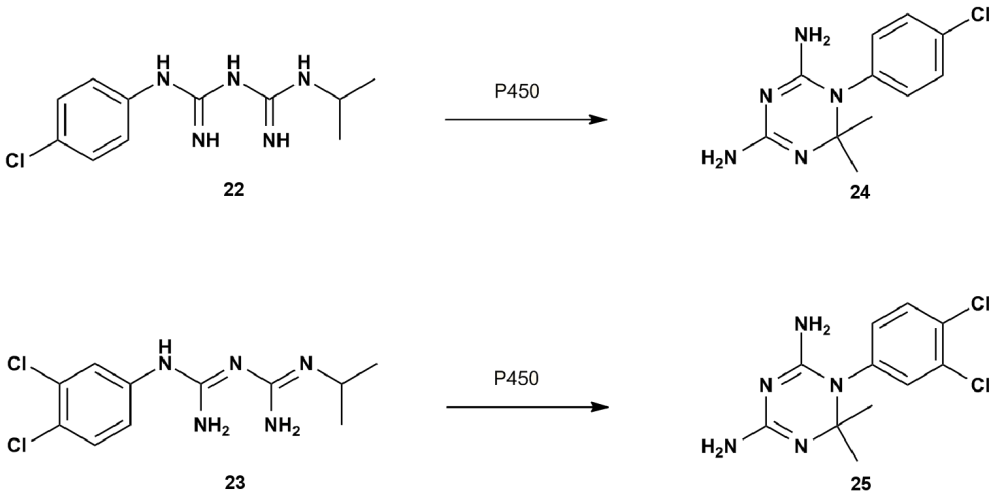

22 24 23 25

Although initial reports of its effectiveness seemed promising[43], the ubiquitous use of proguanil as a prophylactic drug for plantation workers in Southeast Asia and elsewhere soon resulted in the development of wide-spread parasitic resistance to the drug[3]. This was shortly followed by the development of the DHFR inhibitor, pyrimethamine **26** which proved effective even against chloroquine-resistant parasites[3].

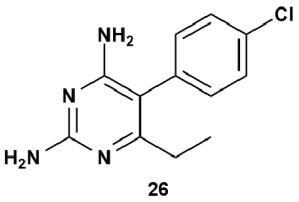

26

Unfortunately, as in the case of proguanil, it was not long before parasitic resistance to pyrimethamine emerged in the late 1940s and early 1950s. This led to the development of more flexible antifolates such as trimethoprim (TMP) **27** which was primarily used in combination with the DHPS inhibitor, sulfamethoxazole. The combination drug, known as Co-trimoxazole was used as a common antimalarial but its clinical use was restricted in 1995 due to bone marrow toxicity caused by sulfmethoxazole[44]. Trimethoprim (not in combination) has been available since 1980 but has since become the least potent of the antimalarial DHFR inhibitors[45].

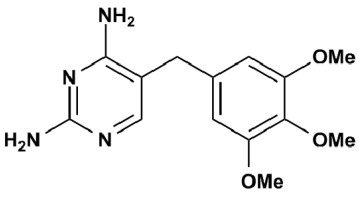

27

1.2.2.2 Inhibitors of dihydropterate synthase (DHPS)

Unlike DHF and TS, DHPS is limited to the parasite's *de novo* pathway and is thus a particularly attractive target for antimalarial chemotherapy, eliminating toxicity associated with targeting enzymes common to both the host and invading parasite. Despite this, far less inhibitors have been developed against DHPS than DHFR. This is mainly due to the parasite being able to acquire folate from the exogenous medium or regenerate DHF using the folate salvage pathway[38]. This class of antifolates tend to therefore be used in combination with other antimalarials, most notably the DHFR inhibitors.

The first DHPS inhibitor to be developed was the antifolate, prontosil **28** in 1932.

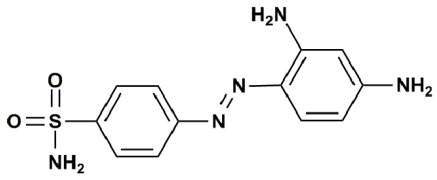

28

The azo dye was converted to its active form of sulfonamide *in vivo* which led to the development of other sulfonamide-based compounds including, dapsone **29**, sulfalene **30** and, most notably sulfadoxine **31**.

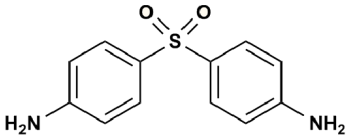

29

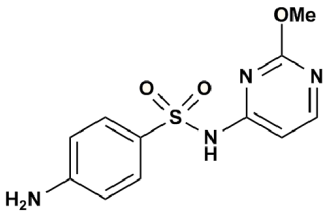

30

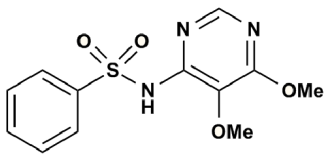

31

Sulfadoxine had a longer half-life and improved toxicity profile than prontosil, however, it was considerably slower in eradicating parasitemia when compared to other antimalarial agents. Moreover, it was found that the majority of sulfur-based drugs could not be used as effective monotherapies against malaria. High dosages were required for adequate activity, leading to correspondingly high levels of induced toxicity. In the case of sulfadoxine, this was overcome by using it in combination with the DHFR inhibitor, pyrimethamine **26** as studies suggested the existence of a synergistic effect between the two compounds[46] due to the DHFR inhibitor acting on both the parasite's *de novo* and salvage pathways in the presence of a DHPS inhibitor[38]. In this way, the "salvaging" of exogenous DHF by the parasite was effectively inhibited. Indeed,

the combination drug, commercially known as Fansidar, was found to be more effective than both chloroquine or either drug used alone[47], and as such became the alternative antimalarial drug to chloroquine.

1.2.2.3 Other enzymes of the folate pathway

Other enzymes of the folate pathway, including SHMT, GTP-C1, DHNA, HPPK and PfDHFS-FPGS, also have the potential to act as targets for antimalarial agents. All, with the exception of SHMT, act within the parasite's *de novo* pathway such that inhibitors of these enzymes could potentially bring about synergy with known DHFR inhibitors, thereby making them favorable candidates for drug design[38]. Despite this, the majority of structural and mechanistic information regarding these enzymes has been derived from bacterial sources, and as yet, has not been explored in the *P. falciparum* parasite. Thus, progress towards developing inhibitors against these enzymes has been limited and indeed, no antifolate outside the realm of the DHFR-TS and DHPS inhibitors currently exists[48].

.

1.2.2.4 Combination therapy

Combination therapy has become the primary approach towards the treatment of malaria, as it is a useful strategy for slowing down the pace at which the parasite develops resistance towards antimalarial agents[38]. Combinations of antifolate drugs, usually one DHPS inhibitor and one DHFR inhibitor, have been widely used for the treatment of malaria. Despite this, resistance to antifolate combination therapy such as Fansidar (pyrimethamine/sulfadoxine) has been reported in South East Asia, South America[39] and East Africa[49], [50]. This led to the development of Lapdap, a combination of chloroproguanil and dapsone. Unfortunately, resistance to the drug was reported in South East Asia[38] even before it was withdrawn in 2008 due to toxicity issues: hemolysis associated with patients with glucose 6-phosphate dehydrogenase deficiency[51]. Other antifolate combination therapies include Maloprim, a combination of pyrimethamine and dapsone, which is used together with chloroquine as a prophylactic against chloroquine resistant parasites[34] and Metakelfin, a combination of pyrimethamine and sulfalene, whose clinical use has been limited.[38]. Cotrimoxazole, a combination of TMP with the DHPS inhibitor, sulfamethoxazole has also been considered for treating *P. falciparum* malaria, however, *in vitro* results suggest that resistance is likely to occur with its wide-spread use[52].

Current antimalarial combination therapy is focused on the addition of an artemisinin derivative to well-known antifolate drugs. The artemisinins have been shown to exhibit potent activity against *P. falciparum* when used together with other well-known antimalarial agents or

combination therapies[53]. This includes combination of artemisinin derivatives with the prophylactic drug Malarone itself, a combination of atovaquone and proguanil hydrochloride, as well as Fansidar. These combinations are highly efficacious in practice[54], however, in both cases resistance has been reported[55], [56]. Lapdap with artesunate has also been considered for chemotherapy but was found to exhibit inadequate efficacy[57] prior to the withdrawal of Lapdap due to the toxicity of dapsone[58]. Other combinations under investigation involve combining the antifolates, Fansidar with the quinoline derivative, amodiaquine and similarly combining chlorproguanil and dapsone with artesunate [53]. It is hoped that such combination drugs will either exhibit synergistic or additive antimalarial activity and/or slow down the pace of resistance to new drugs. In this way, they might be effective enough to act as a first-line treatment for malaria in Africa and other areas with wide-spread drug resistance.

1.2.3 Parasitic resistance

The spread of resistance to current combination therapy regimens has highlighted the need for new approaches to drug design and discovery. Parasitic resistance to antifolates arises by genetic point mutations at various amino acids within and surrounding the parasite's PfDHFR-TS and DHPS active sites[59], preventing adequate inhibitor binding and thus, lowering drug efficacy. Recently solved crystallographic data pertaining to both the wildtype and mutant forms of PfDHFR-TS complexed with pyrimethamine or the potent cycloguanil analogue WR99210 **32** respectively, have given insight into both the molecular target as well as the mutated amino acids responsible for drug resistance[41]. This has allowed a more directed approach towards the design and development of new folate inhibitors with the potential to overcome resistance.

The dimeric PfDHFR-TS enzyme contains two active sites, formed on contact between the closely associated TS subunits (Fig. 1.4). The amino acid residues responsible for catalysis have been identified to be Asp54, Trp48, Ala16, Ser108 and Phe58 [42], [41]. These residues partake in H-bonding and other electrostatic interactions with the substrate and/or NADPH coenzyme , ensuring the substrate binds in the correct orientation. Other important residues include Ile14, Ile164, and Thr185. Genetic mutations of these amino acids are thus limited so as to maintain enzyme functionality. This constraint to enzyme mutation allows scientists to continue to use the folate pathway as viable target for the design of antimalarial compounds.

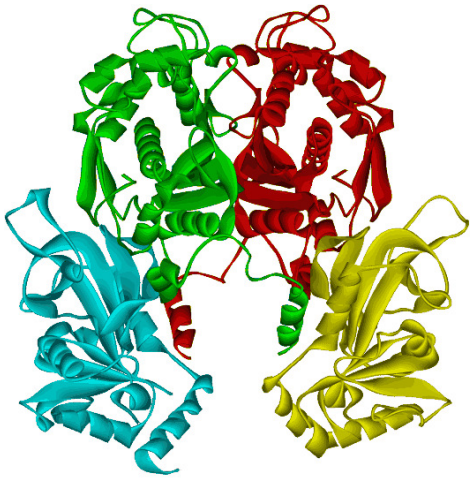

Fig. 1.4 Ribbon diagram of PfDHFR-TS showing the DHFR and TS domains in blue and yellow, and green and red repectively.[1]

Mutations responsible for resistance have been identified at amino acids Ala16, Cys50, Asp54, Phe223, Asn51, Cys59, Ser108 and Ile164, all of which are located within or near the active site [42], [41]. The effect of these mutations on binding with WR99210 and pyrimethamine is visible in the crystal structures of the wild-type and mutant forms of the PfDHFR-TS enzyme complexed with these inhibitors (Fig. 1.5).

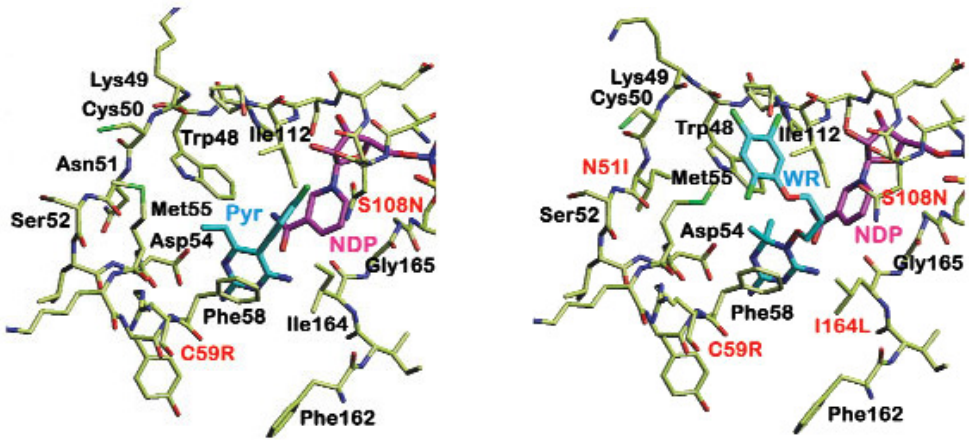

(a) Double mutant PfDHFR-TS complexed with pyrimethamine

(b) Quadruple mutant PfDHFR-TS complexed with WR99210

Fig. 1.5 Comparisons of interactions between mutant PfDHFR-TS with (a) pyrimethamine and (b) WR99210. The residues responsible for resistance are labelled in red.

[1]image generated using accelrys discovery studio software (version 2.1) courtesy of Dr A.L. Rousseau and colleagues at the CSIR

Mutations affect substrate/inhibitor binding by either changing the enzyme cavity size or creating greater steric hindrance within the active site. The Ser223 mutation allows Glu54 to form hydrogen bonds with the substrate such that enzyme functionality is maintained but the cavity size of the active site is increased, preventing smaller-sized inhibitors from binding adequately[42]. Mutation of Ser108 for bulkier amino acids Asn, Thr, Gln and Cys has also been shown to affect the binding of smaller inhibitors by creating steric hindrance between the mutant residue and the *p*-chlorophenyl group present in pyrimethamine, cycloguanil and other structurally rigid DHFR inhibitors. This in turn affects binding of both the inhibitor and NADPH coenzyme[42], [60]. This can be seen in the complex between the double mutant (C59R/S108N) PfDHFR-TS and pyrimethamine (Fig. 1.5a) in which the side chain of mutant Asn108 makes close contact with both the nicotinamide ring of NADPH and the *p*-chlorophenyl group of pyrimethamine.

Unlike the rigid inhibitors of pyrimethamine and cycloguanil, the potent cycloguanil analogue WR99210 **32** adopts a conformation which fits well within the active site of mutant enzymes. Indeed, the dihydrotriazine-based compound was found to bind to the double mutant PfDHFR-TS enzyme 10-fold more when compared to pyrimethamine[41]. Its potency is thought to arise from its 5-atom linker, located between the heterocycle and aromatic ring, which bestows a greater degree of flexibility to the molecule. This allows it to bind with greater affinity within the PfDHFR enzyme active site by avoiding unfavorable contacts with mutant amino acids in this area. This can be seen in the complex between the quadruple mutant (51I/C59R/ S108N/I164L) PfDHFR-TS and WR99210 (Fig. 1.5b) in which the flexible side chain of WR99210 is orientated so as to avoid the sterically bulky mutant Asn108 residue in addition to other mutations. Moreover, WR99210 is able to form alternative hydrophobic interactions, accounting for its high affinity within the active site[41].

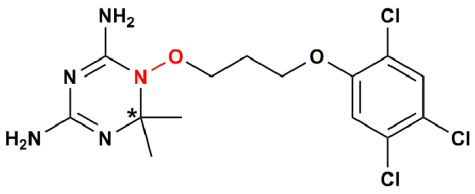

32

The antimalarial activity of WR99210 has been known since its discovery in 1985 when it was found to inhibit all known mutant forms of DHFR *in vitro* in the nanomolar range[3], [61]. Unfortunately, it was never developed further into a viable, antimalarial agent due to concerns over toxicity, especially gastrointestinal tract (GIT) effects. In addition, it was found to have poor bioavailability and an unacceptable pharmacokinetic profile, probably stemming from its labile N-O bond[62]. Therefore, to address these issues of toxicity, a biguanidine precursor,

PS-15 **33** was developed as a prodrug to WR99210. However, PS-15 had to be abandoned due to cross-resistance with cycloguanil and pyrimethamine[45].

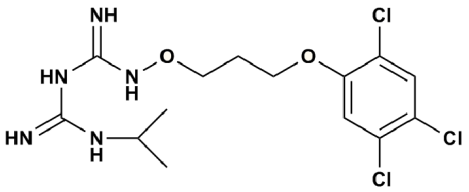

33

Analogues of WR99210 and PS-15 have recently been synthesised[63]. Electron donating methoxy and electron withdrawing nitro groups were added onto the phenyl ring in order to minimise metabolic degradation. Triazine metabolites **34**, **35** and **36** were found to exhibit high *in vitro* activity against the K-1 strain of *P. falciparum*, whereas the biguanide prodrugs, **37** and **38**, were found to match and, in the case of the PS-33 compound **37**, exceed the *in vivo* antimalarial activity of PS-15 against the W-2 strain of *P. falciparum*, which is resistant to chloroquine, quinine, sulfadoxine, and pyrimethamine. Although these results remain promising, the toxicity profile of these compounds remains to be established.

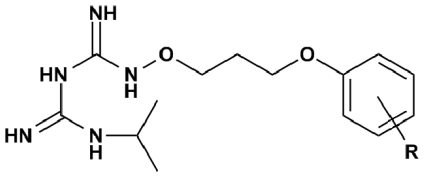

37 R = 4-Cl
38 R = 3,4-Cl

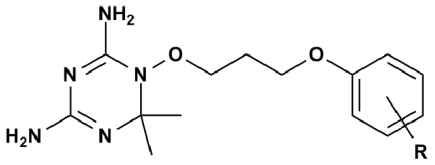

34 R = 4-NO_2
35 R = 4-OMe
36 R = 3,4,5-OMe

1.2.4 Design and development of new antifolates

The need for novel antimalarial antifolate compounds with high efficacy and low toxicity remains crucial if we are to overcome the burgeoning problem of drug resistance. Chemotherapy remains one of the most important strategies in the prophylaxis and treatment of malaria, however, progress towards the development of new antifolate compounds with potent antimalarial activity and a favorable therapeutic index remains limited.

This is partly due to the strict criteria placed on antimalarial drugs which, given the demographics of the disease, have to be both relatively easy to administer and cost effective[33]. Cost considerations are of particular importance as the majority of infected populations live

in poverty-stricken, developing countries and as such antimalarial drugs must be inexpensive in order to be distributed widely and routinely available. Indeed, inexpensive drugs such as chloroquine, which cost less than $0.1 per treatment[53], are still used in some countries as the primary choice of treatment for malaria[28], despite their decreasing effectiveness resulting from widespread resistance. Alternative drugs were found to be more expensive, difficult to administer, and with higher levels of toxicity, in addition to encountering resistance of their own[28].

Progress towards the development and discovery of new antimalarial compounds has also been hampered by a lack of investment resulting from limited marketing opportunities in third world countries. Thus, antimalarial research must be particularly innovative when compared to other, more competitive and industrial-sized drug development and discovery programs, so as to circumvent the problems associated with limited funding. Current efforts include the discovery of natural products, the evaluation of drug resistance reversers, the consideration of new chemotherapeutic targets, the use of compounds that were originally used to treat other diseases and developing analogues of existing drugs[53],[64]. These latter strategies, being relevant to the current project, are discussed.

1.2.4.1 Antifolate drugs used in the treatment of other diseases as potential antimalarial agents

Antifolate compounds used in the treatment of both malaria and another disease could target an enzyme common to both diseases or alternatively, may act by an entirely different mechanism[53]. Given the financial constraints associated with antimalarial research, this strategy is particularly attractive as it could significantly lower the costs of drug development by avoiding uneccessary *in vivo* and *in vitro* studies which have already been completed for these compounds. There are numerous instances of this approach to drug discovery: for example, the antimalarial drug, quinine is used for the treatment of muscle cramps[65], while the hydroxylated analogue of chloroquine is used in the treatment of rheumatoid arthritis and systemic lupus erythematosus[66]. However, oxidising drugs have not been targeted towards malaria[64], and this project aims to use this concept in the development of antifolate drugs against the *P. falciparum* parasite, in particular by making use of the anticancer drugs, methotrexate (MTX) **39** and pemetrexed **40**.

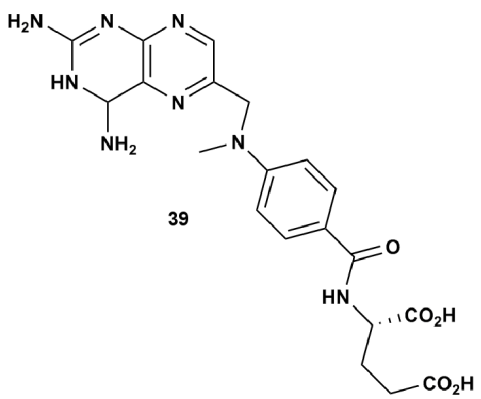

39

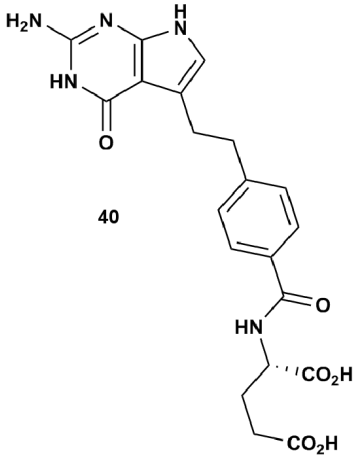

40

Cancerous cells are associated with abnormal and frequent mitotic divisions and thus require high levels of folate derivatives for cellular growth and replication. This is also true for rapidly dividing malarial cells. The folate derivatives are acquired *via* a salvage folate pathway which contains many of the enzymes common to the parasite's own folate salvage pathway (Scheme 1.1), and hence can also be targeted with antifolate therapy. Indeed, recent *in vitro* studies found the antifolate MTX, a potent DHFR and TS inhibitor, to be effective against both chloroquine-senstitive and multidrug-resistant *P. falciparum* strains[67], exhibiting IC_{50} values of 0.32nM and 48.02nM respectively. Other studies using pyrimethamine (PM)-senstitive and PM-resistant laboratory strains and field isolates of the *P. falciparum* parasite showed that MTX exhibited an IC_{50} <85nM[58] against the parasite. Similarly, the chemotherapeutic agent, pemetrexed has been shown to be active against *P. falciparum in vitro*, exhibiting an IC_{50} <50nM[64]. Pemetrexed also targets folate pathway enzymes TS and DHFR[34] and, although not as intensively studied as MTX, this work suggests that it too could potentially act as a new antimalarial antifolate.

Despite these results, anticancer drugs, and MTX in particular, are not used in the treatment of malaria as they are considered too toxic[64]. In cancer treatment, high doses of MTX of 5-12g/m^2 (dose/body surface area) or 5000mg (oral dose/adult) per week for several weeks are required resulting in plasma concentrations of >1000μM. If used in the long term, these doses could be fatal[33]. However, recent *in vitro* studies indicate that the MTX dosage for antimalarial treatment would most likely be much lower than that required for anticancer therapy[68], as even peak *in vivo* plasma concentrations of 10^3-10^4nM occur at low doses of MTX 25-100mg/m^2[67].

Furthermore, MTX has been used in the treatment of other diseases such as rheumatoid arthritis[69] at much lower doses of 0.1-0.35mg/m^2 (LD-MTX)[70], which amounts to a weekly oral/intramuscular dose of 7.5-30mg per adult[64]. At this dose, the chronic use of the drug

is safe, efficacious and well tolerated[71] and as such has become the secondary drug for the treatment of rheumatoid arthritis after nonsteroidal, anti-inflammatory drugs. In addition, LD-MTX is increasingly being used for the treatment of juvenile idiopathic arthritis (RJA) in children, multiple sclerosis and psoriasis[70],[72], suggesting its potential as a therapeutically viable antimalarial agent.

It should however be noted that MTX is a potent DHFR inhibitor and when used chronically at doses of >30mg per week can cause toxic side effects[64], including gastrointestinal toxicity, stomatitis, alopecia, marrow suppression, and liver function abnormalities[71]. These result directly from the inhibition of the DHFR enzyme in normal cells, which in turn affects the normal synthesis of purines and pyrimidines. MTX toxicity has been counteracted with the use of chemical modulators such as folic acid (FA), folinic acid (FNA), THF and 5-methylene-tetrahydrofolate (Me-THF) which, when used after several hours of treatment with MTX, are able to restore cell growth, thereby lowering toxicity, without affecting drug efficacy[73]. This strategy of using a modulator to increase the therapeutic life of a drug could potentially be used in the case of MTX for the treatment of malaria. However, limitations persist: the antifolate/folate derivative treatments currently used for cancer and rheumatoid arthritis are administered parenterally[33] and a potential antimalarial drug would have to be made orally available to meet the criteria for a drug to be widely accepted in rural areas of third world countries. Hence, the main limitation in developing these drugs would concern the oral availability of folate analogues, which might be compromised in an oral formulation.

1.2.4.2 Chemical modifications of existing drugs

Another approach to antimalarial chemotherapy is to develop analogues of existing drugs by chemical modifications[53]. This strategy is particularly apt for malarial research as the mechanism of action or the biological target of the existing drug is already known, thus significantly lowering development costs. Furthermore, since the synthesis of the parent drug has already been completed, the synthesis towards novel analogues is potentially simplified. There are several examples of current antimalarial drugs which were developed in this manner, including chloroquine, primaquine **41** and mefloquine **42** which were all developed through modifications of quinine[53].

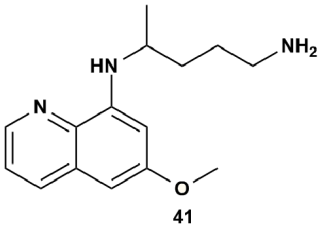

41

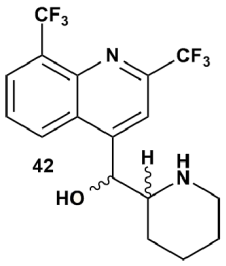

42

Primaquine has been further developed resulting in the discovery of tafenoquine **43**, a chemoprophylactic antimalarial agent[74], [75]. Similarly, the potency of chloroquine was improved by modifications to form short chain chloroquine analogues or 4-aminoquinolines such as **44**, **45** and **46**, which are effective against chloroquine-resistant parasites[76].

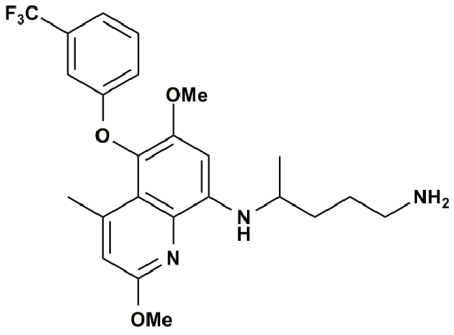

43

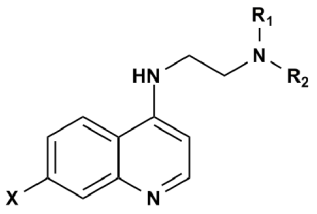

44 X = Cl, R_1 = H, R_2 = *t*-Bu
45 X = CF_3, R_1, R_2 = alkyl
46 X = CF_3, R_1 = H, R_2 = *t*-Bu

This strategy has also been used in the synthesis of analogues of cycloguanil, pyrimethamine and TMP; the parent compounds no longer being clinically useful due to resistance. Gordon Lowe, at Isis Innovation recently reported the synthesis of a number of cycloguanil analogues[77], [78]. Both methyl groups were replaced for a hydrogen atom and aryl substituted group respectively. The compounds were tested against both the wildtype and and double mutant (A16V, S108T) PfDHFR-TS enzyme. Eight compounds were found to inhibit both the wild type and mutant enzymes better than cycloguanil with compounds **47**, **48** and **49** yielding the best results.

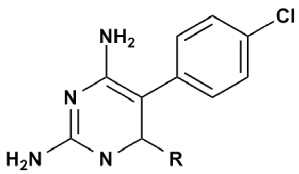

47 R = *p*-phenoxyphenyl

48 R = *m*-phenoxyphenyl

49 R = *p*-benzyloxyphenyl

Further modification of the *p*-Cl group for a *m*-Cl group resulted in the synthesis of compounds **50**, **51** and **52**[77]. The IC_{50} values of these compounds was found to be within the nanomolar range when exposed to a chloroquine/cycloguanil resistant *P. falciparum* FCR3 strain *in vitro*.

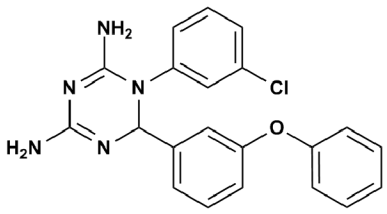

50

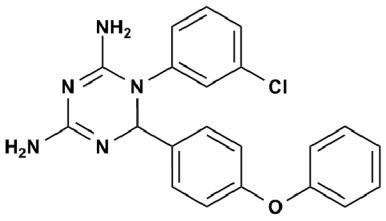

51

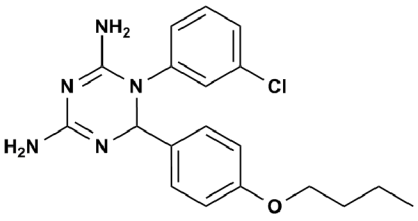

52

Analogues of both pyrimethamine (**53-56**) and TMP (**57** and **58**) have recently been synthesised[79] by varying substituents on both the pyrimidine and phenyl rings. Compounds bearing a *m*-Cl group (compound **56**) as well as those containing an unsubstituted 5-phenyl group and a long 6-alkyl substituent (compounds **53-55**) were found to be 10-25 times more effective than their parent compounds, exhibiting IC_{50} values against the resistant parasite within the micromolar range. TMP derivatives, **57** and **58** were found to exhibit equally good antimalarial activity. In addition, the binding affinity of some of these compounds for both wildtype, single mutant (S108N) and double mutant (C59R, S108N) PfDHFR-TS is significantly higher than that for the original compounds, indicating their potential as antimalarial agents.

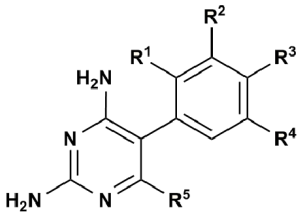

53 R^1-R^4 = H; R^5 = Et

54 R^1-R^4 = H; R^5 = hex^n

55 R^1-R^4 = H; R^5 = $(CH_2)_3C_6H_5$

56 R^1, R^3, R^4 = H; R^2 = Cl; R^5 = $(CH_2)_3C_6H_4$(MeO-*p*)

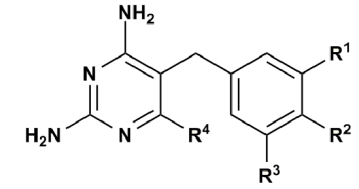

57 R^1 = OEt; R^2 = OCH_2-[3,4,5-$(OMe)_3$]C_6H_2; R^3, R^4 = H

58 R^1 = OPr^n; R^2 = OCH_2-[3,4,5-$(OMe)_3$]C_6H_2; R^3, R^4 = H

More recently, novel DHFR inhibitors were designed by the chemical modification of the potent cycloguanil derivative, WR99210 [62], [80]. Researchers at the Council for Scientific and Industrial Research (CSIR) in South Africa used crystallographic data of wild-type PfDHFR and mutant PfDHFR complexed with pyrimethamine and WR99210[41] to aid the design of a library of flexible cycloguanil analogues (Fig. 1.6)[62], [80].

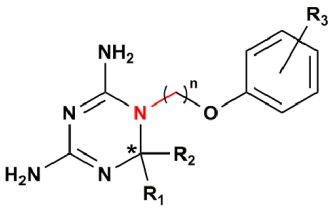

n = 1-4

R_1-R_3 = Me, Ph, H

Fig. 1.6

They replaced the labile N-O bond of WR99210 with the more stable N-C bond and, while changing the functionality around the stereogenic center and substituted phenyl ring, investigated the effect of varying the length of the flexible tether linking the 1,2-dihydro-1,3,5-triazine-4,6-diamine heterocycle and the substituted phenyl ring. They found that, when tested against a cycloguanil-resistant strain of *P. falciparum* (Gambian FCR-3), compounds bearing 1,2,3 and 5-atom linkers displayed antimalarial activity comparable with that of cycloguanil i.e. in the low micromolar range. In contrast, compounds bearing a 4-atom flexible tether exhibited activity in the nanomolar range, with two compounds, **59** and **60**, exhibiting activity in the subnanomolar range with IC_{50} values of 0.4 and 0.1nM respectively[80].

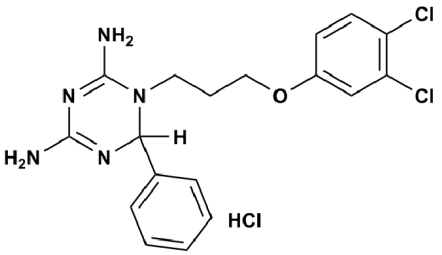

59

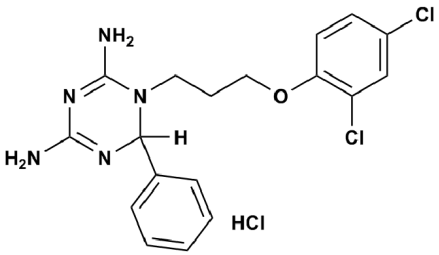

60

Although these results remain promising, the original synthesis of these compounds is not trivial and, in fact was initially found to result in the formation of isomers (Fig. 1.7) such that the flexible tether was attached to the exocyclic nitrogen atom (N-6) as opposed to the desired endocyclic N-1 of the 1,2-dihydro-1,3,5-triazine-4,6-diamine heterocycle. This led to the adoption of a more difficult synthetic route in which the yields were comparatively lower[62]. Moreover, the synthesis was not enantioselective and as such enantiomeric mixtures were screened for antimalarial activity.

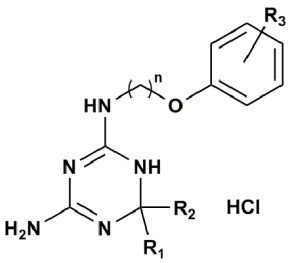

Fig. 1.7

The synthetic difficulties of this series of flexible cycloguanil analogues would have to be improved in order for them to be considered as potential antimalarial drugs for future development. This led us for the purposes of this MSc to pursue the synthesis of a series of novel DHFR inhibitors, structurally based on these compounds but chemically modified enough to potentially simplify their synthesis. In this way, we planned to develop new antifolates using two approaches. The first made use of the already existing chemotherapeutic agents, MTX and pemetrexed which have been shown to exhibit antimalarial activity[67], [58], [64]. In the second approach, chemical modification was used to structurally simplify the dihydrotriazine antifolate compound **60**, generated in the above study, providing a route towards the synthesis of novel, potentially potent DHFR inhibitors.

1.3 Aims for this project

1.3.1 The synthesis of antifolate precursors which could potentially be utilised by enzymes of the parasite's *de novo* pathway to form potent DHFR inhibitors *in situ*

In this project we aim to synthesize novel antimalarial, antifolate compounds based on the already existing chemotherapeutic agents, MTX and pemetrexed. This could alleviate the costs of drug development, an important consideration in antimalarial research.

We plan to investigate an alternative approach to addressing the issue of MTX and pemetrexed toxicity by synthesising precursors of these compounds which lack a glutamic acid residue, **61** and **62** and, assess whether such molecules would be glutamated *in situ* by the enzymes of the parasite's *de novo* pathway. We hypothesize that such precursors, being structural analogues of DHP and containing a terminal carboxylic acid, could be glutamated within infected cells by the parasitic enzyme, DHFS, *via* the *de novo* pathway to form the active antimalarial drug MTX or pemetrexed *in situ*. Upon death of the parasite, the active drug would be released into the bloodstream, however, the relative concentration would be low enough to reduce toxic side effects. This could potentially improve the therapeutic index of the drug as the concentration of the active compound present in the bloodstream would be lowered. Furthermore, the drug would only be synthesised in infected cells as the *de novo* synthetic pathway is not present in humans.

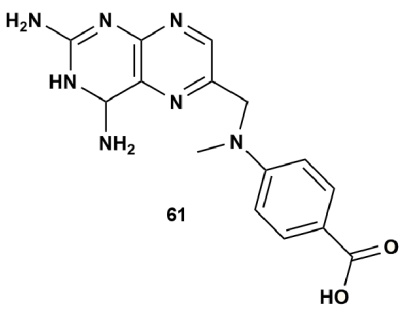

61

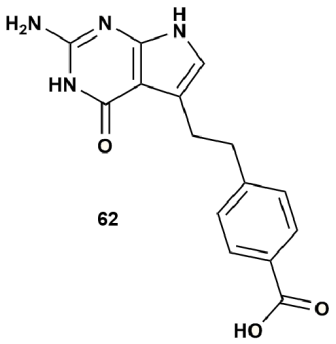

62

This strategy of using the parasite's enzymes to synthesise potent antimalarials from precursors *in situ* has been explored to a limited extent using 2,4-diamino-6-hydroxymethyl-pteridine (DAP) **63** and 2,4-diaminopteroic acid (DAPA) **64**, which are precursors of the chemotherapeutic drug, aminopterin as well as 2,4 diamino-N10-methyl-pteroic acid (DAMPA) **61**, a precursor of MTX[81]. They were found to exhibit antimalarial activity in the micromolar range; DAMPA being more active than DAP and DAPA. However, whether DAMPA acts directly on DHFR

or is built up into MTX *in situ*, which in turn inhibits DHFR, is unknown.

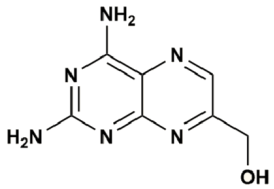

63

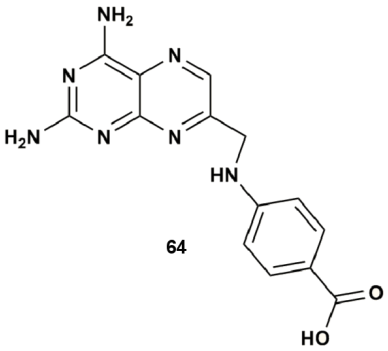

64

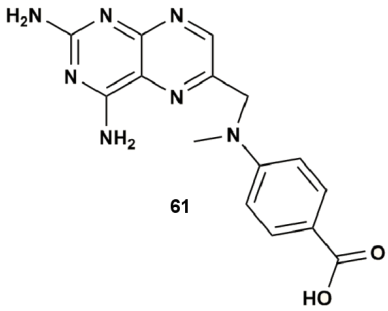

61

We hope to extend this idea to include precursors of greater structural variety by synthesising various analogues of pemetrexed. Structural differences will be introduced into the phenyl moiety as highlighted (Fig. 1.8). In contrast, only one precursor of methotrexate will be synthesised as several studies concerning the synthesis and antimalarial activity of methotrexate and its analogues have already been investigated[34]. Precursors of MTX and pemetrexed will be synthesised using reported synthetic routes while the synthesis of the analogues will be based on variations of these.

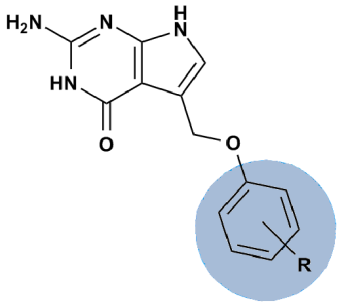

Fig. 1.8 Analogues of Pemetrexed where R is a halogen (particularly Cl or F) or electron donating OMe or OH group

Some of these compounds do not contain an aromatic, terminal carboxylic acid and, as such, cannot be glutamated *in situ* but, will be synthesised for comparison with the MTX and pemetrexed precursors which can be glutamated. All synthesised compounds will be assessed *in vitro* in a whole cell, *P. falciparum* screen for biological activity.

1.3.2 The synthesis of novel DHFR inhibitors based on molecular scaffolds with known antimalarial activity

Secondly, we aim to synthesize a series of novel, flexible pyrimidine analogues (compounds **65a-d**) which are structurally based on the dihydrotriazine antifolate hit compound **60**, generated from a previous study on the synthesis of flexible cycloguanil analogues[82], [80].

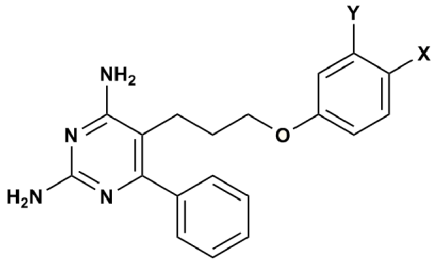

65a: X=H, Y=H
65b: X=Cl, Y=H
65c: X=H, Y=CF_3
65d: X=Cl, Y=Cl

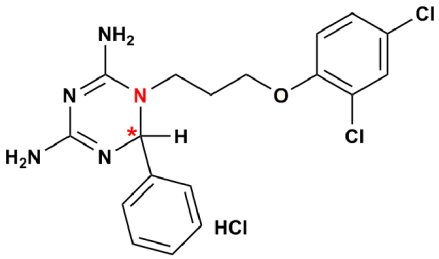

60

Given the difficulties and complexity associated with the synthesis of these dihydrotriazine compounds, this project aims to synthesise pyrimidine analogues of the hit compound so as to eliminate the problem of enantioselectivity. In this approach we will replace the N-C bond with a C-C bond so as to restore aromaticity to the compound. We envisaged the synthesis of these flexible pyrimidine analogues to be comparably easier than their dihydrotriazine equivalents, thereby reducing development costs, an important consideration in the design of animalarial agents.

The viability of the synthetic route will be tested by initially synthesising the more rigid 5,6-diphenylpyrimidine-2,4-diamine **69** under the same reaction conditions. The experimental methodology will then be applied to the novel system.

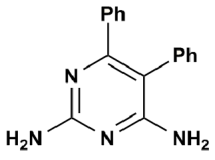

69

All novel compounds will be assessed *in vitro* in a whole cell, *P. falciparum* screen for biological activity. Using these two approaches, we hope to identify novel antimalarial compounds based on existing molecular scaffolds with known antimalarial activity and to explore new ways to

effectively utilise known, potent antifolates for antimalarial chemotherapy.

Chapter 2

Results and Discussion

2.1 Planned approach towards the methotrexate precursor

Methotrexate, or amethopterin as it was known, was discovered as an analogue of aminopterin; a folic acid derivative first synthesised by Subbarao and coworkers in 1947[83]. Since its discovery, numerous studies have been conducted regarding both the biological activity and synthesis of methotrexate and its analogues [84], [85], [86], [87], [88]. Many of the proposed synthetic routes towards the potent antifolate compound are problematic, resulting in low yields[89] and the formation of impurities which are difficult to separate from the desired product[90]. In light of these concerns, we decided to follow the method employed by Boyle and Pfleiderer who were able to synthesise the central pteridine scaffold, **63** in a good yield[91].

A retrosynthesis of the target molecule's central 2,4-diamino-6-(hydroxymethyl)pteridine scaffold **63** (Scheme 2.1) suggests it can be disconnected to 2,4,5,6-tetraaminopyrimidine **70** and the commercially available compound, dihydroxyacetone **71**.

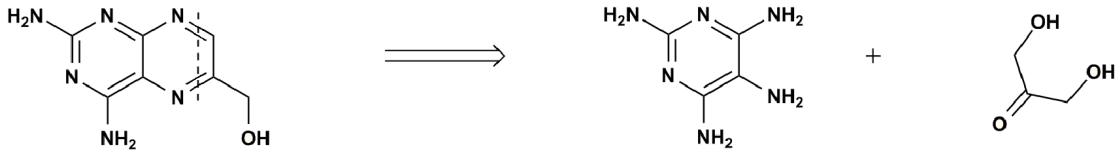

Scheme 2.1

The forward synthesis is shown in Scheme 2.2. 2,4,5,6-Tetraaminopyrimidine **75** would be made in three steps, as described by Traube, starting from the commericially available compounds, guanidine hydrochloride **72** and malononitrile in the presence of a suitable base[92]. Nitrosation

at the C5 position was chosen to facilitate the introduction of the fourth amine as the nitroso group could be reduced to afford the desired 2,4,5,6-tetraaminopyrimidine sulfate **75**. This would lead us to the key ring closing step to be carried out by the condensation of compound **75** with dihydroxyacetone **71** under oxidising conditions to form the pteridine. This method for the synthesis of pteridines unfortunately also results in the formation of alternative methyl and hydroxymethyl derivatives, and as such, partial purification through the conversion to the hydrobromide salt **77**, using hydrobromic acid, would be necessary. The bromomethyl functionality would then be introduced by reaction with bromine in the presence of triphenylphosphine. The resulting brominated product **78** would not be isolated but carried directly into the final step of the synthesis. Reaction with the aromatic amine, *N*-methyl PABA *in situ* would thus afford the desired methotrexate precursor **61**.

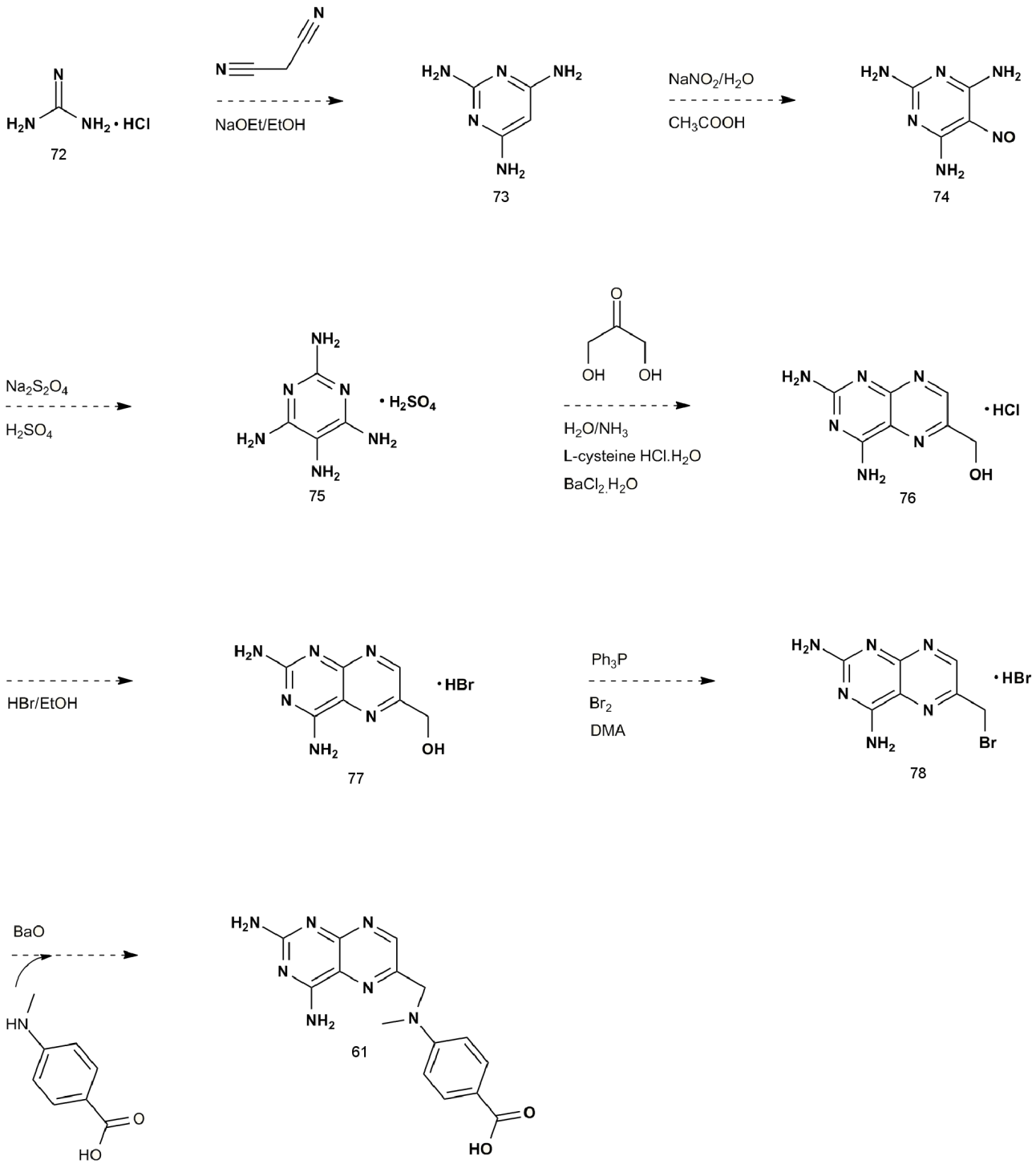
72
NaOEt/EtOH
73
NaNO2/H2O
CH3COOH
74
Na2S2O4
H2SO4
75
H2O/NH3
L-cysteine HCl.H2O
BaCl2.H2O
76
HBr/EtOH
77
Ph3P
Br2
DMA
78
BaO
61

Scheme 2.2

2.2 Synthesis of the methotrexate precursor

2.2.1 Synthesis of 2,4,6-triaminopyrimidine 73

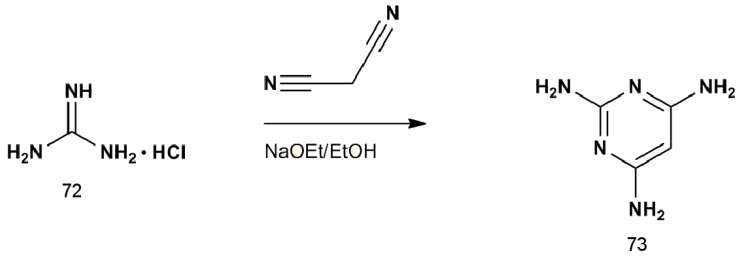

The synthesis of the methotrexate precursor **61** was commenced with the neutralisation of guanidine hydrochloride salt by sodium ethoxide and subsequent reaction with malononitrile **72** as reported[93]. To this end, the two starting materials were dissolved in a solution of sodium ethoxide in ethanol and refluxed overnight. The resulting reaction mixture was filtered to yield the pyrimidine product **73** as a creamy, brown solid in a quantitative yield.

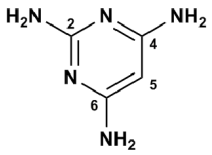

The ^{1}H NMR spectrum was fairly simple with only three signals, all appearing downfield of 5ppm. The singlet at 5.54ppm accounted for the only aromatic H5 proton. The remaining two signals were assigned to the amine functionalities with the equivalent C4 and C6 NH_2 groups appearing as a broad singlet at 7.20ppm and the C2 NH_2 appearing slightly downfield of this, as a singlet at 8.44ppm. These results preliminarily suggested we had in fact formed the pyrimidine ring, however, the presence of guanidine could still not be ruled out. The ^{13}C NMR spectrum was more conclusive with the signal for aromatic carbon C5 appearing at 76.0ppm, an observation characteristic of pyrimidines. Signals at 152.7ppm and 157.2ppm were assigned to aromatic carbons C2 and the equivalent C4 and C6 respectively. Mass spectroscopy results supported the NMR spectroscopic data with a molecular ion appearing at 126.0774amu, matching the molecular formula of our molecule ($C_4N_5H_7$). The high melting point 249-251°C was identical to the literature value[94] and also confirmed the absence of lower melting, starting materials.

2.2.2 Synthesis of 2,4,5,6-tetraaminopyrimidine sulfate 75

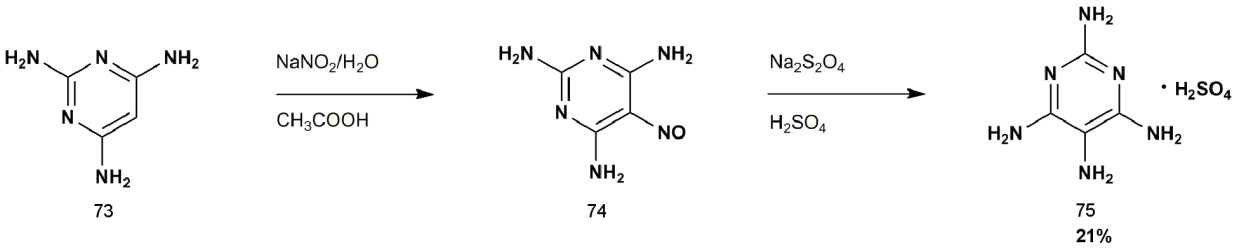

An electron withdrawing nitroso group was then introduced at the C5 position to form intermediate **74** *en route* to 2,4,5,6-tetraaminopyrimidine **75**. Nitrosation was attempted under classical conditions: the triaminopyrimidine starting material **73** was dissolved in glacial acetic acid to which aqueous sodium nitrite solution was added[95], [96]. After 2 hr, the product **74** precipitated out of solution as a water-insoluble, pink solid which was subsequently collected by filtration. The nitroso product **74** was immediately carried into the next step without further purification or characterisation. With the nitroso group in place, the formation of the desired tetraminopyrimidine **75** was readily accomplished by reduction. The starting material **74** was suspended in water and treated with sodium dithionite and sulfuric acid at 110°C. After cooling overnight, the crude product had precipitated out of solution as a yellow solid. This solid was filtered off and purified by recrystallisation from methanol, to afford the tetraaminopyrimidine sulfate product **75** as a beige powder in a disappointing yield of 21%.

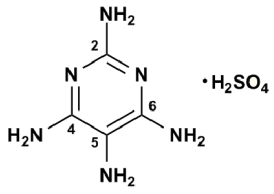

The IR data fitted well with that reported for the commercially available compound. The melting point was found to be well over 300°C in line with the literature value[93].

2.2.3 Synthesis of 2,4-diamino-6-(hydroxymethyl)pteridine hydrobromide 77

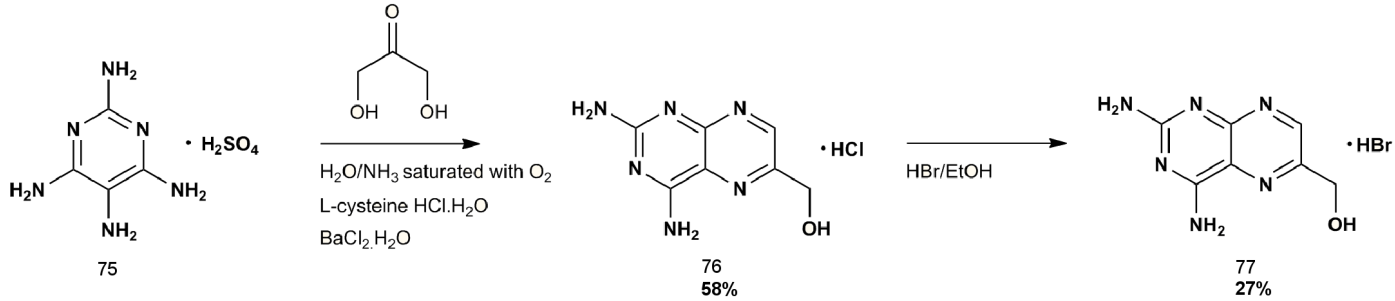

The key step of the synthesis, pteridine formation, was achieved by condensation of starting material **75** with 1,3-dihydroxyacetone in an aqueous ammonia solution in the presence of cysteine and oxygen, as reported by Boyle and Pfleiderer[91]. Partial purification of the 2,4-diamino-6-(hydroxymethyl)pteridine hydrochloride intermediate **76** was accomplished by recrystallisation of the hydrobromide salt **77** from ethanol containing hydrobromic acid, as reported by Piper and Montgomery[97].

The reaction mechanism for pteridine formation is shown in Scheme 2.3. Nucleophilic addition of the 5-amino group of compound **75** to the carbonyl group of dihydroxyacetone results in the formation of compound **79**. The schiff base **80** is formed at the 5-amino position following dehydration across the hemiaminal functionality. Isomerisation of the double bond converts the methyl alcohol group **81** to its corresponding aldehyde **82** which, following nucleophilic addition by an aromatic amine, results in ring closure and consequent formation of the desired pteridine substructure **63**.

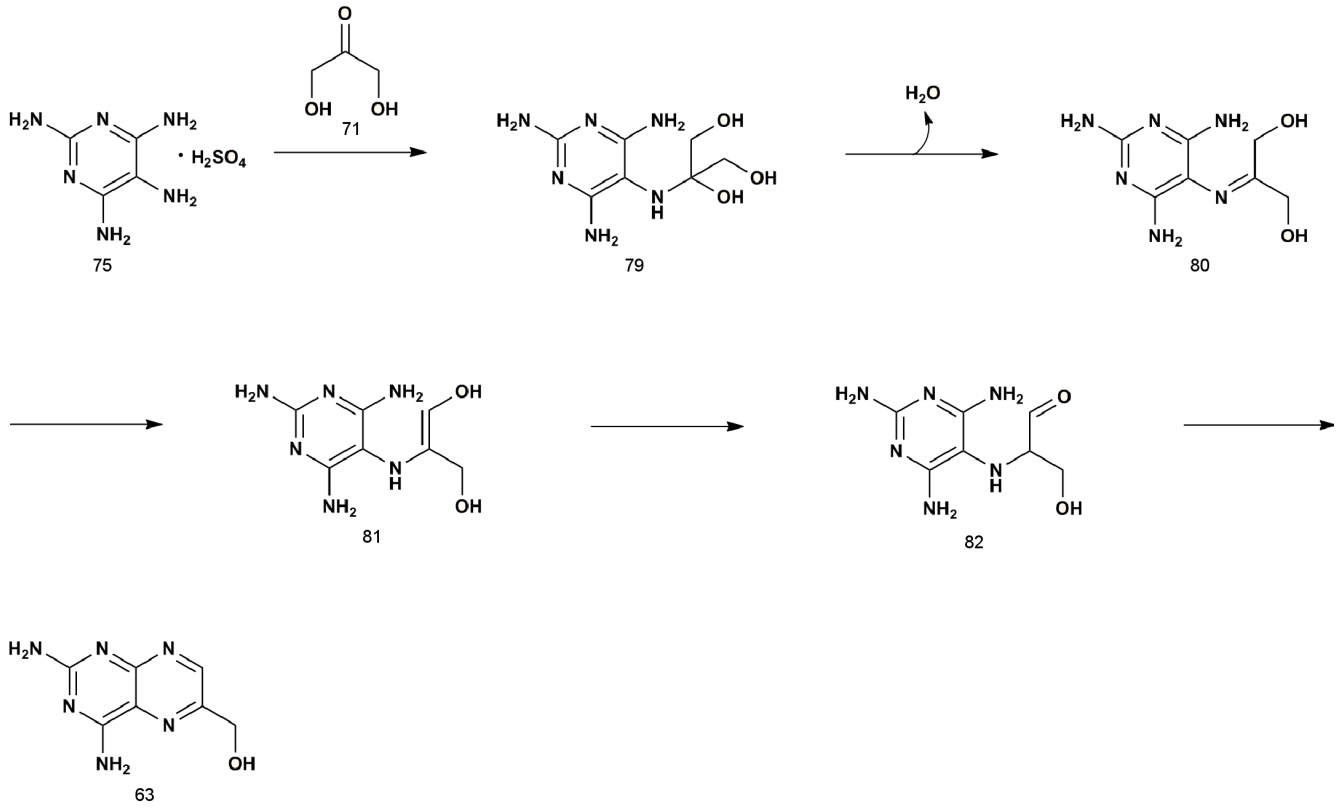

Scheme 2.3

Reported difficulties stem from the formation of various alternative products including the 7-substituted pteridine compound **83** as well as methyl derivatives, **84** and **85**.

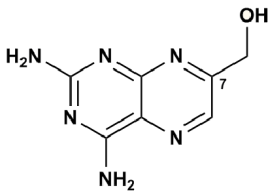

83

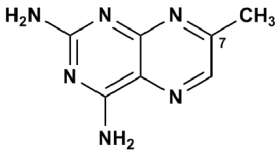

84

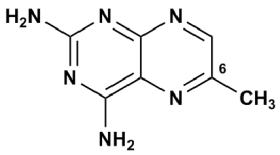

85

Compound **83** results directly from the lack of control of the orientation in which the starting material reacts with dihydroxyacetone. That is, reaction of the C5-$N\mathrm{H}_2$ group results in the desired 6-substituted pteridine product **63**, whereas reaction of either the neighboring C4-$N\mathrm{H}_2$ or C6-$N\mathrm{H}_2$ groups form the alternative 7-substituted pteridine product **83**. By contrast, the mechanism by which methyl derivatives **84** and **85** form remains unknown[85]. It has been suggested that under the given experimental conditions, the dihydroxyacetone reagent undergoes a side reaction to form a methylglyoxal intermediate **90**[85]. Mechanistically, this has been proposed to occur by a Lobry de Bruyn-van Ekenstein transformation followed by dehydration, as shown in Scheme 2.4. If this were to occur prior to condensation with 2,4,5,6-tetraaminopyrimidine sulfate **75**, it certainly would provide an explanation for the formation of the methylpteridine coproducts.

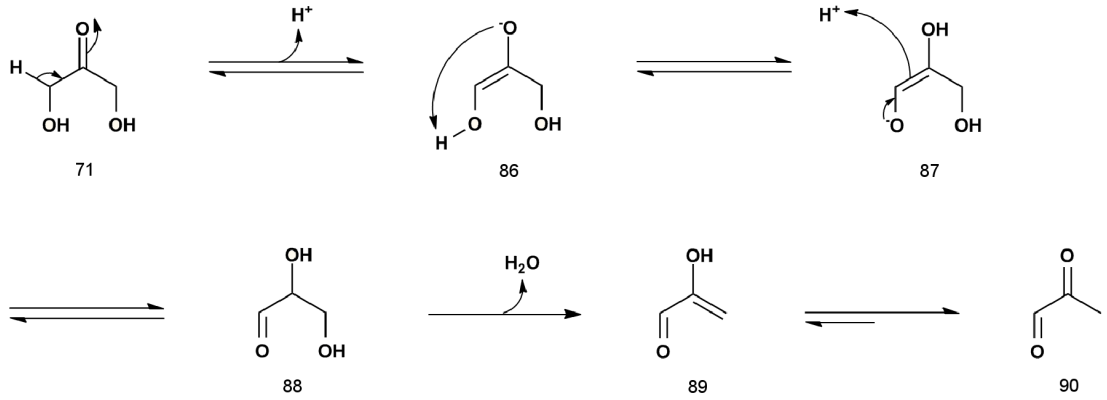

71 86 87 88 89 90

Scheme 2.4

The chosen reaction conditions were therefore paramount to eliminating the possibility of side reactions, while facilitating pteridine formation. Accordingly, the pteridine hydrochloride salt **76** was first acquired by heating the reduced product **75** with barium chloride dihydrate in water. This resulted in the displacement of the sulfate counterion with hydrochloride and the simultanous formation of the byproduct barium sulfate, which was easily removed by filtration. The hydrochloride salt of **75**, present within the collected filtrate, was then reacted

with dihydroxyacetone in the presence of L-cysteine hydrochloride in an aqueous ammonia solution. Slightly oxidising reaction conditions were provided by a steady but slow stream of oxygen which was bubbled through the reaction solution for the duration of the experiment. After 45 hr at room temperature, the oxygen flow was stopped and the reaction mixture refrigerated, allowing for the crude product to precipitate out of solution. Following filtration and recrystallisation from ethanol and water, the intermediate compound **76** was obtained as a yellow powder in a yield of 58%. Pleasingly, this was was found to be within the upper end of the range reported by Shaw *et al.* (50-60%)[85]. In the crude ^{1}H NMR spectrum, we were delighted to observe that the desired product **76** had formed in preference to both the 7-substituted pteridine and methyl derivatives in ratios of 29:1 and 23:1 respectively. Previous attempts to form the pteridine product in the absence of oxygen had resulted in far poorer ratios with the alternative products forming over one third of the mixture. Interestingly, the 6-methyl-2,4-pteridinediamine coproduct appeared to have formed preferentially to its 7-methyl derivative which was not at all detected.

Having successfully formed the pteridine ring substructure of methotrexate, we moved onto partially purify the 2,4-diamino-6-(hydroxymethyl)pteridine hydrochloride **76** from its methyl and 7-substituted coproducts prior to bromination. The starting material **76** was refluxed in an ethanol/hydrobromic acid solution for 5 min. After cooling to room temperature and refrigeration of the reaction mixture overnight, the product crystallised out of solution and was filtered off. In this way, the hydrobromide product was effectively separated from the crude product mixture to afford **77** as a yellow powder in a yield of 27%. Although low, this yield was comparable to that reported in the literature (34%)[97].

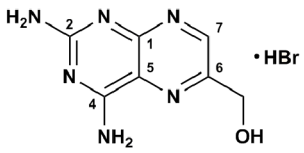

The success of the purification was evident in the ^{1}H NMR spectrum in which a barely detectable singlet at 3.03ppm indicated the presence of traces of the methylpteridine coproduct. In addition, the 7-substituted derivative could no longer be detected by NMR spectroscopy. The two signals for the desired product **77** had shifted slightly downfield in the presence of the electron rich hydrobromide group. Similarly, the ^{13}C NMR spectrum contained no signals for the coproducts, with a single peak at 68.7ppm owing to the CH_2 group and six peaks contained within the aromatic region accounting for the pteridine ring.

2.2.4 Synthesis of 4-[[(2,4-diamino-6-pteridinyl)methyl]methylamino] benzoic acid 61

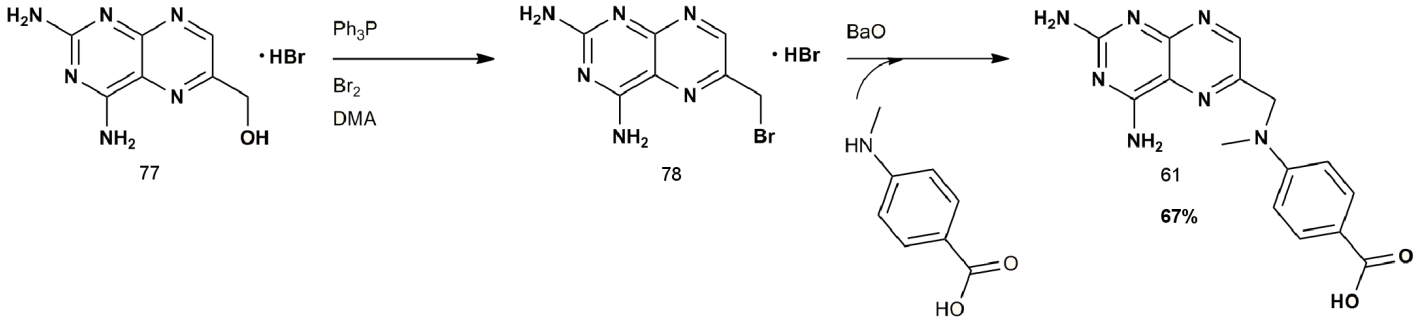

With the pure 6-(bromomethyl)-2,3-pteridine hydrobromide compound **77** in hand, we were ready to convert the alcohol to the bromomethyl functionality. Following methodology put forward by Rosowsky *et al.*, the starting material **77** was treated with dibromotriphenylphosphorane (Ph_3PBr_2) in *N,N*-dimethylacetamide (DMA) at 0-5°C[87]. The reaction was left to stir at room temperature overnight, under an argon atmosphere. The product **78** was not isolated but reacted with 4-(methylamino)benzoic acid *in situ* in the presence of barium oxide at 55°C. After 24 hr, the reaction mixture was cooled and the crude product recovered by filtration. Purification by recrystallisation from a methanol/water solution afforded the desired methotrexate precursor **61** as a dark yellow powder in a reasonable yield of 67%.

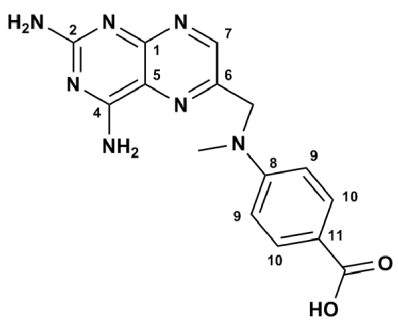

The ^{1}H NMR spectrum contained an additional three signals accounting for the 4-(methylamino)benzoic acid moiety. Two *ortho* coupled doublets in the aromatic region were assigned to the H10 and H9 protons of the *para*-substituted phenyl ring. The third signal owing to the NCH_3 group was clearly visible as a singlet integrating for three protons at 3.69ppm. The remainder of the spectrum resembled that of its precursor **77**, with slight differences being apparent in the comparably lower chemical shifts. The presence of the 4-(methylamino)benzoic acid moiety was also evident in the ^{13}C NMR spectrum which contained four new aromatic signals upfield from those previously assigned to the pteridine ring. In addition to these, two peaks at the upper and lower extremes of the spectrum, owing to the carbonyl and N-CH_3 groups respectively, were observed. The presence of the carbonyl group was also evident in the IR spectrum which showed a stretching band at $1652cm^{-1}$. The mass spectrum showed a molecular ion at 326.1471amu, matching the calculated value for the final product exactly.

Having synthesised the methotrexate precursor over 7 steps in an overall yield of 2.2% we pro-

ceeded to the synthesis of unglutamated analogues of the antifolate compound, pemetrexed.

2.3 Planned approach towards the pemetrexed precursor

The synthesis for the anticancer, antifolate compound, pemetrexed was first reported in 1992 by Taylor and coworkers[98]. Since then, more practical synthetic routes have been described upon which our synthesis towards the unglutamated precursor of pemetrexed **62** was based[99]. Using a retrosynthetic approach, the pyrrolo[2,3-*d*]pyrimidine ring system could be disconnected to a 2-amino-4-pyrimidone **91** and α-haloaldehyde **92** (Scheme 2.5).

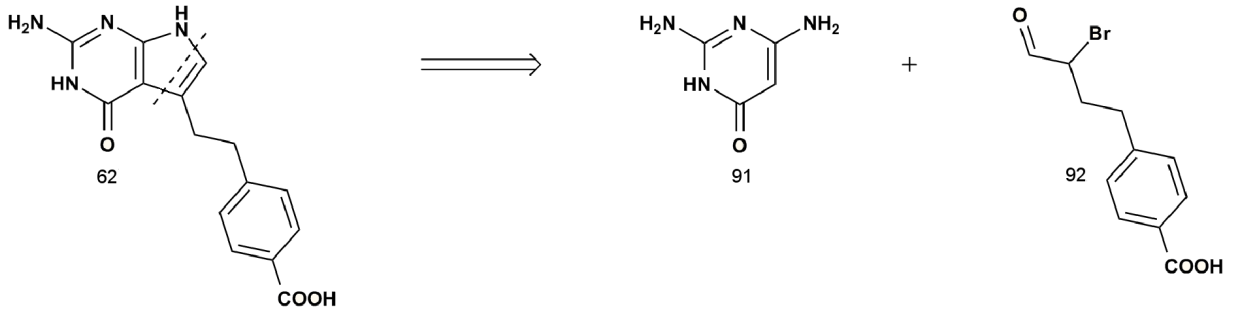

Scheme 2.5

As shown in Scheme 2.6, the aromatic aldehyde **94** would be synthesised in one step from 4-iodobenzoic acid methyl ester **93** and 3-buten-1-ol, using a palladium catalysed Heck-type reaction in the presence of a base and an appropriately bulky, phosphine ligand. Selective bromination of the aromatic aldehyde **94** at the α position followed by cyclocondensation with the commercially available 2-amino-4-pyrimidone would result in the formation of the pyrimidine ring affording the pemetrexed ester precursor **96**. Finally, conversion of the ester to the corresponding acid **62** would in turn be achieved by ester hydrolysis.

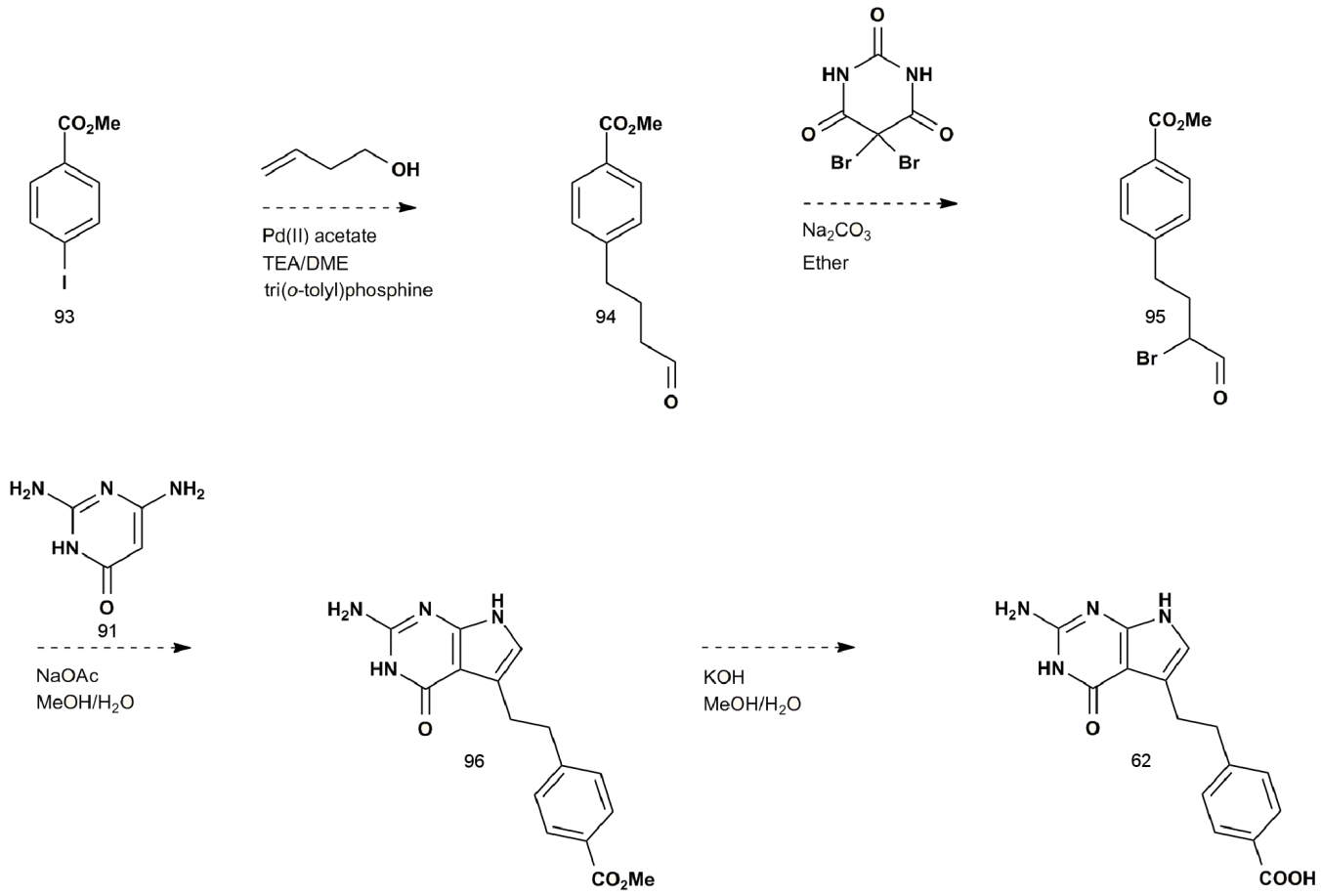

Scheme 2.6

2.4 Synthesis of the pemetrexed precursor

2.4.1 Synthesis of *E*-methyl 4-(4-hydroxybut-1-en-1-yl)benzoate 98

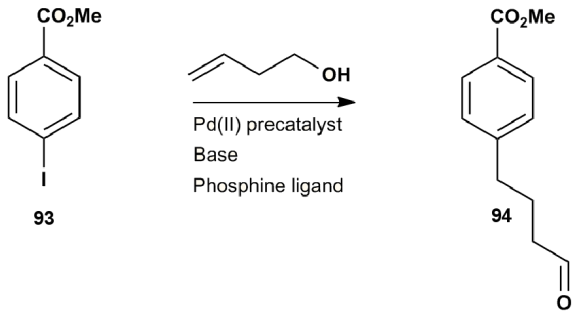

We began our synthesis of the pemetrexed precursor from the commercially available aromatic halide, 4-iodobenzoic acid methyl ester **93**, using classical, palladium-catalysed, Heck chemistry reported by Larock *et al.*[100] in their synthesis of arylaldehydes and ketones from aryl halides

and non-allylic alcohols. The starting material **93** would be coupled to alkene, 3-buten-1-ol using a base and Pd(II) precatalyst to afford the aromatic aldehyde **94**.

The Heck or Mizoroki-Heck reaction was discovered independently by Mizoroki[101] and Heck[102] in 1971 and 1972 respectively. The transformation was later developed by Heck to incorporate phosphine ligands[103], thereby forming the versatile palladium-catalysed reaction it is today. It essentially involves the catalytic arylation and alkenylation of olefins, which is useful for the formation of substituted olefins, dienes and other unsaturated compounds[104]. As outlined in Scheme 2.7, the palladium(0) compound can be generated *in situ* from the palladium(II) precatalyst *via* reduction by a phosphine ligand, L (*step A*). The activated palladium(0) catalyst then inserts itself into the arylhalide bond, R-X (*step B*). This is known as oxidative addition as Pd(II) is formed and is followed by coordination of the palladium catalyst with the alkene by π bonding. The R-Pd-X intermediate then inserts itself into the alkene in a *syn* addition step known as migratory insertion (*step C*). *Beta*-hydride elimination of the *trans* isomer forms a new palladium-alkene complex (*step D*) which is subsequently destroyed by reductive elimination in the presence of a base to release the desired olefin product and regenerate the palladium(0) catalyst.

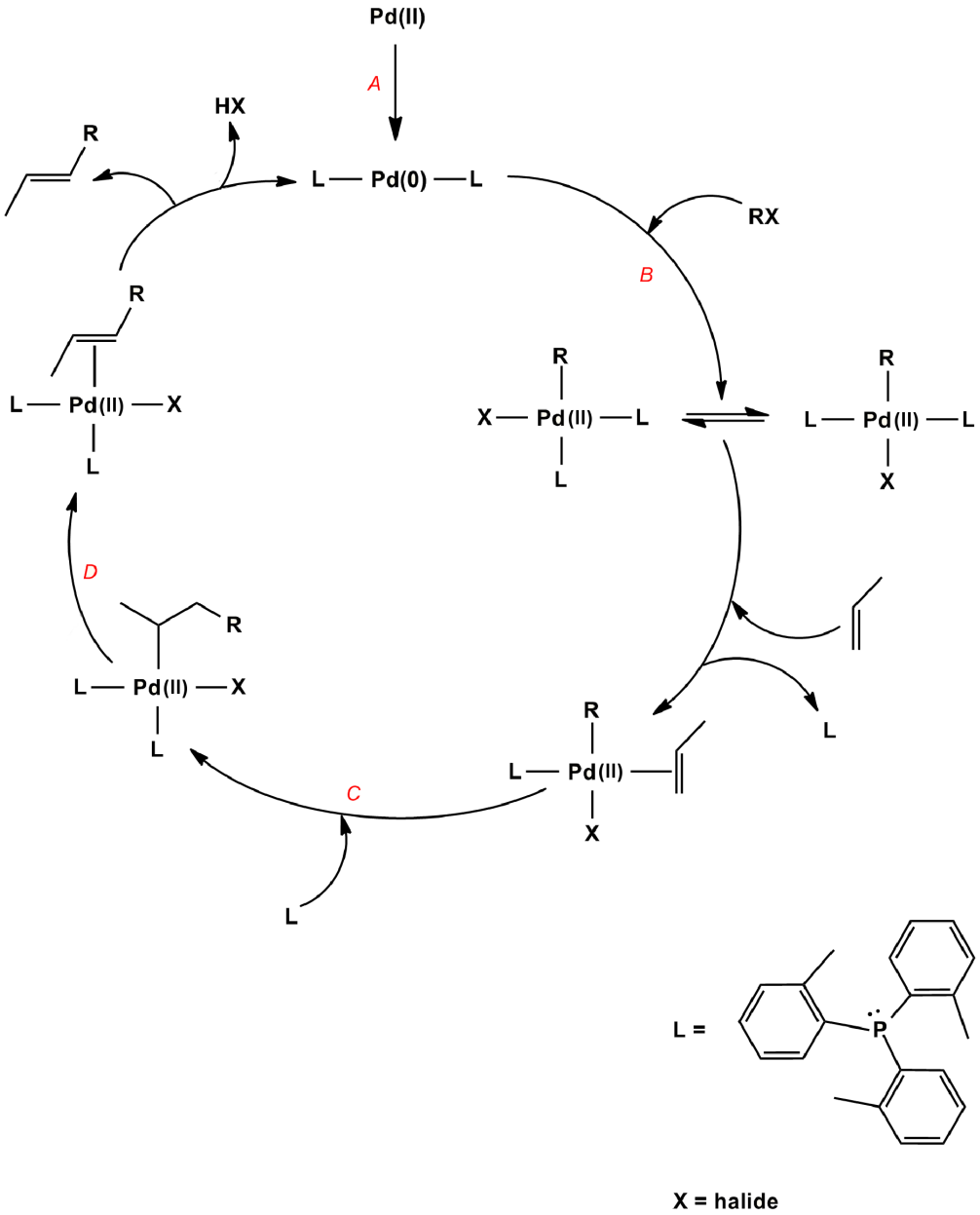

Scheme 2.7 Mechanism of the palladium-catalysed Heck reaction[104]

In the particular synthesis of arylaldehydes and ketones, the Heck reaction takes advantage of palladium's ability to migrate along carbon chains by palladium-hydride elimination and subsequent readdition [100]. In this way, the double bond is progressively shifted along the carbon chain with each subsequent catalytic cycle, until captured by the terminal alcohol functionality to form a carbonyl product [105]. Of course, the formation of other products including the isomeric aldehyde **97** and olefins, **98** and **99** are also possible. However, in the literature, these were reported to occur in low yields of 5% for **97** and 5% for **98** and **99** collectively, with the desired aromatic aldehyde **94** forming in a yield of 90% [106] (Scheme 2.8).

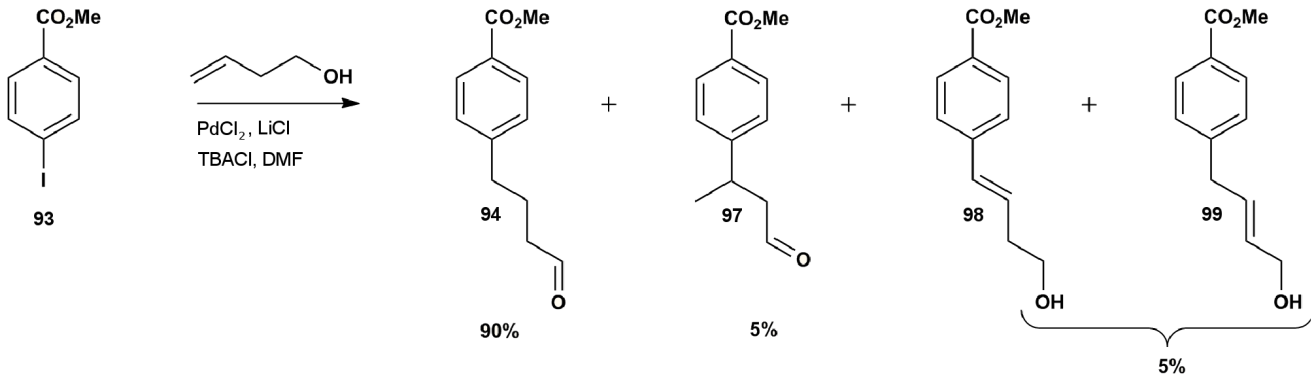

Scheme 2.8

We thus attempted to replicate these results using an experimental procedure based on that described by Stadler *et al.*[107] as this method was more appropriate for the smaller scale on which we were working. The commercially available starting material **93** and the tri(*o*-tolyl)phosphine ligand were dissolved in a TEA/DME solution and, after purging the reaction flask of air which could otherwise oxidise the Pd(0) catalyst, added to the palladium(II) acetate catalyst. The reaction mixture was heated to 60°C and left to stir under an argon atmosphere. After 18 hr of stirring under these conditions, the reaction did not go to completion and, instead of forming the aromatic aldehyde **94** in high yields, the formation of the aromatic alkene **98** was favored in a yield of 65% with only 10% of the starting material being converted to the desired product **94**. Interestingly, the formation of isomers and alternative olefins was not detected.

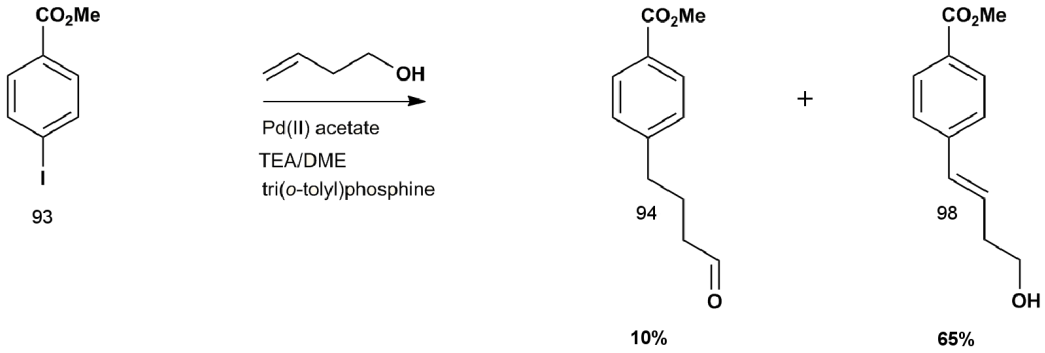

Given that the aromatic alkene **98** forms after only one catalytic cycle (Scheme 2.7), we decided to increase the experimental time in an attempt to improve the yield of aldehyde **94**. Unfortunately, this did not result in further transformation of the olefin to the desired product. Further attempts to improve the yield included using Larock's methodology [100] and later, conducting the reaction in the microwave reactor using Pd(II) acetate, tri(*o*-tolyl)phosphine and triethylamine (TEA) in both dimethoxyethane (DME) and a dimethylformamide (DMF)/acetonitrile (CH_3CN)/water (H_2O) mixture, however all attempts resulted in lower yields than those reported above, with the aromatic alkene **98** once again forming predominantly over the desired

product **94**.

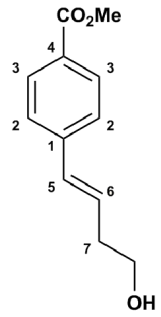

Two distinct, upfield signals in the ^{1}H NMR spectrum at 6.53ppm and 6.36ppm, each integrating for one proton, attested to the formation of the aromatic alkene **98**. In this case, the J value of 16Hz for coupling between H5 and H6 indicated the formation of the *trans* isomer only. The remainder of the spectrum was comprised of two doublets in the aromatic region, accounting for the two sets of *ortho* coupled ring protons, together with a singlet, triplet and, further upfield, multiplet owing to the methyl and two CH_2 groups. In the ^{13}C NMR spectrum, an downfield signal at 167.2 was immediately assigned to the C=O group. The presence of six signals between 148ppm and 128ppm accounted for four aromatic carbons (two being equivalent), and two belonging to the alkene functionality. The remaining three, upfield signals accounted for the two CH_2 groups and methyl group. In the IR spectrum, an OH stretch was observed at $3325cm^{-1}$ and the mass spectrum showed a molecular ion at 207.1027amu, which corresponded well with the calculated value of 207.0978amu for $C_{12}H_{15}O_3$.

At this point, given the poor yield of the desired product **94**, we decided to recover the aromatic alkene and extend the synthetic route by another two steps: hydrogenating the double bond to form the saturated compound **100** followed by oxidation of the terminal alcohol functionality to its corresponding aldehyde. In this way, we hoped to obtain the desired aromatic aldehyde **94** indirectly, while still maintaining the feasibility of the synthesis.

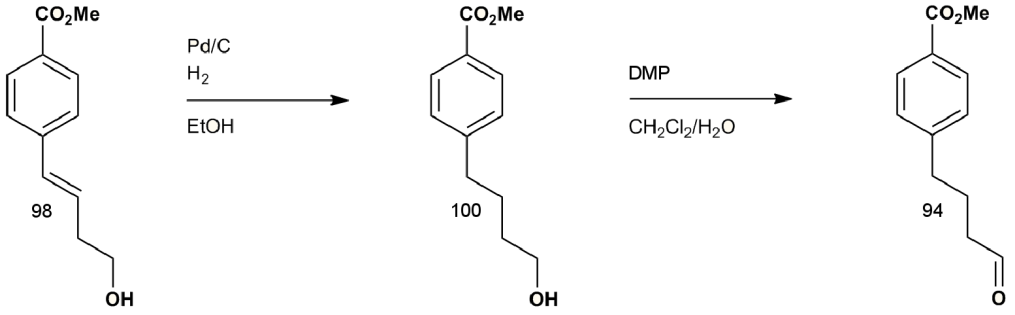

2.4.2 Synthesis of methyl 4-(4-hydroxybutyl)benzoate 100 [108]

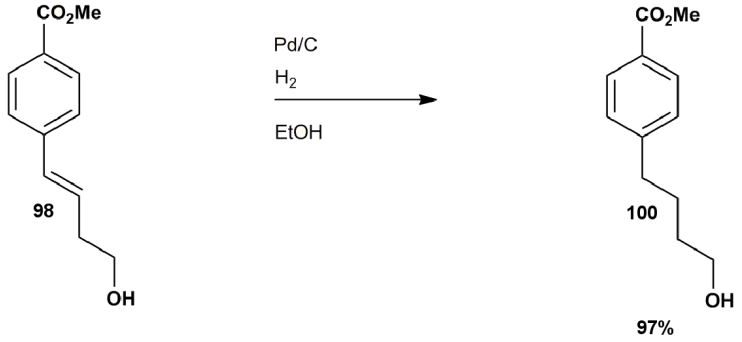

The hydrogenation of unsaturated compounds using hydrogen gas in the presence of palladium on carbon is well established in the Wits organic chemistry group and indeed, the hydrogenation of the aromatic alkene **98** was very successful, resulting in almost complete conversion to the hydroxybutyl ester **100**. The starting material **98** was dissolved in ethanol to which palladium on carbon was added. The reaction was monitored by TLC and after a few hours of stirring under hydrogen, a less polar product of higher R_f had begun to form. The reaction was left to stir for 36 hr to ensure complete conversion of the unsaturated compound, after which the reaction mixture was filtered and, following a workup, purified by column chromatography. The product **100** was obtained as a yellow oil in an almost quantitative yield of 97%.

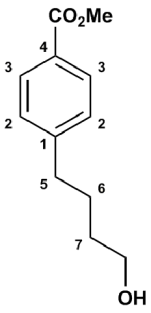

In the ^{1}H NMR spectrum, hydrogenation of the starting material was confirmed by the fact that the two signals for the alkene's protons, H5 and H6, were no longer present and instead replaced by a multiplet integrating for four protons at 1.80-1.50ppm. Moreover, the signal for the CH_2OH group had shifted slightly upfield as expected for a more saturated compound. In the ^{13}C NMR spectrum, the two signals for the alkene carbons, C5 and C6, were no longer present and replaced by two additional signals for the saturated CH_2 groups at 35.7ppm and 27.3 respectively.

2.4.3 Synthesis of methyl 4-(4-oxobutyl)benzoate 94

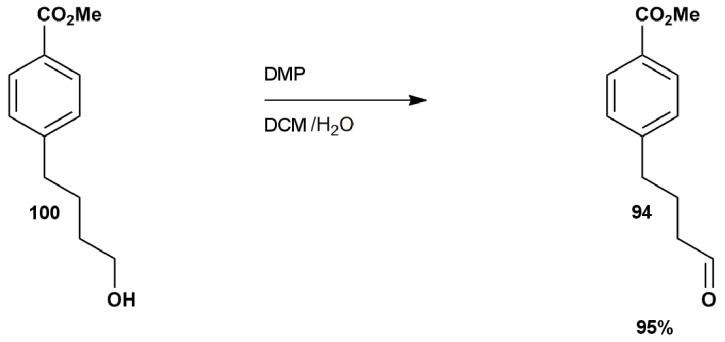

Having successfully obtained the saturated hydroxybutyl ester **100** in an excellent yield, we proceeded to synthesise the aromatic aldehyde **94** by oxidation of the terminal alcohol to a carbonyl group. Several oxidising agents were investigated, specifically pyridinium chlorochromate (PCC), oxalyl chloride (Swern oxidation) and Dess-Martin periodinane. Both PCC and oxalyl chloride proved unsuccessful in this respect and, when compared to DMP, required more complicated workups and/or generated more toxic waste. In contrast, DMP reacts under mild conditions and was found to be very effective in selectively complexing with the hydroxyl group. Interestingly, the use of dry dichloromethane resulted in poorer yields as the presence of water has been shown to speed up the reaction mechanism[109], shown in Scheme 2.9. The oxidising agent **101** chemoselectively complexes with the alcohol group to form a diacetoxyalkoxy periodinane intermediate **102**. This results in the loss of an acetate group which in turn acts as a base, deprotonating the alcohol's α-hydrogen and forming the carbonyl product **104** and byproducts, iodinane **103** and acetic acid.

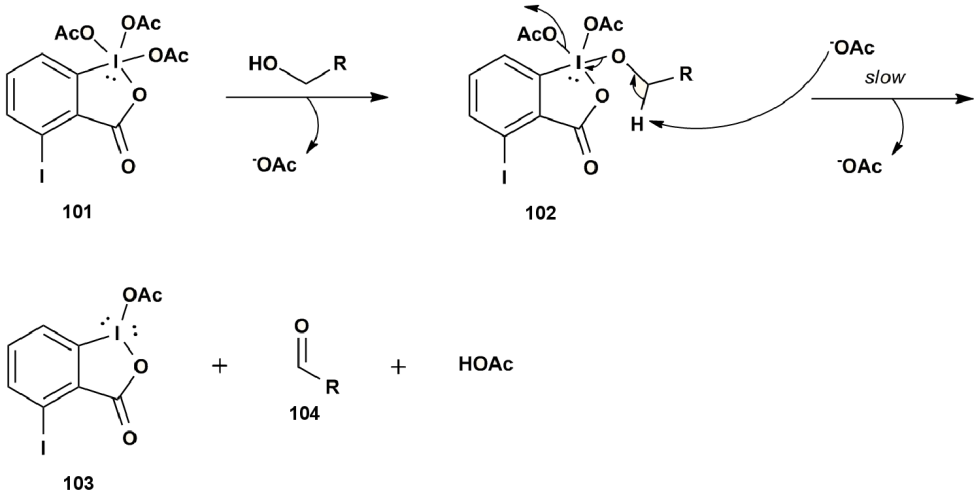

Scheme 2.9 DMP oxidation mechanism

In the presence of water, complexation of the alcohol is accompanied by ligand exchange of an additional acetate for a hydroxyl group (Scheme 2.10). The electron-donating OH ligand weakens the I-OAc bond such that $^{-}$OAc leaves faster than it otherwise would.

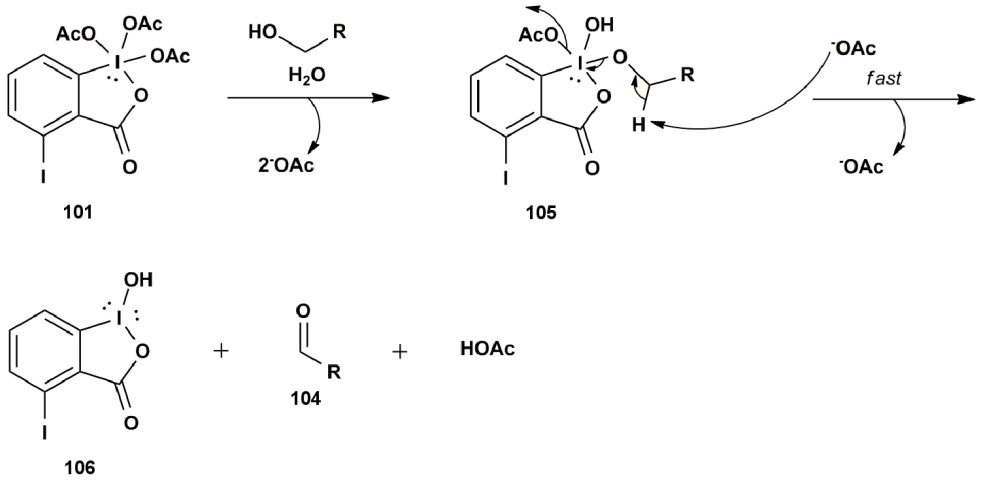

Scheme 2.10 DMP oxidation mechanism in the presence of water

The starting material **100** was therefore dissolved in wet dichloromethane to which DMP was added portion-wise at 0°C over an hour. The reaction was monitored by TLC and the formation of the aldehyde easily detected with a 2,4-dinitrophenylhydrazine (DNPH) stain. The reaction went to completion overnight and was subsequently quenched with a saturated sodium thiosulfate/sodium bicarbonate solution to remove the byproducts of iodinane and acetic acid. Following workup and column chromatography, the product **94** was obtained as a yellow oil in an excellent yield of 95%.

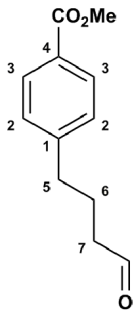

The oxidation was clearly evident by two main changes observed in the ^{1}H NMR spectrum. These were the appearance of the far downfield singlet at 9.77pm due to the aldehyde proton and the disappearance of the triplet for the former CH_2OH group at 3.66ppm. In addition, the H7 protons of the CH_2 group were observed to shift downfield due to the deshielding effect of the neighboring carbonyl functionality. The ^{13}C NMR spectrum correlated well with this data with the appearance of a new signal at 201.9ppm, accounting for the carbonyl group of the aldehyde, and the disappearance of the CH$_2$OH signal. Moreover, the intense absorption in the IR spectrum at 1715cm^{-1} was consistent with the presence of the aldehyde group.

2.4.4 Synthesis of methyl 4-(3-bromo-4-oxobutyl)benzoate 95

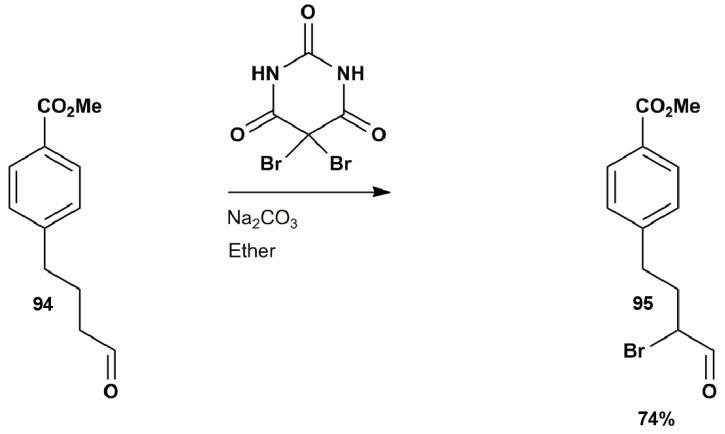

Having successfully circumvented the problems associated with the incomplete Heck reaction at the beginning of our synthesis, we were now in a position to test the α-bromination of the aldehyde and subsequent cyclo-condensation with 2,4-diamino-6-hydroxypyrimidine to afford the pemetrexed precursor **62**. The yield of the aromatic aldehyde **94** over three steps was 60%, making our synthetic route feasible despite the addition of two steps. Addition of 5,5-dibromobarbituric acid (DBBA) and sodium carbonate to a solution of starting material **94** in diethyl ether effected conversion to the α-bromoaldehyde **95** as reported by Barnett *et al.*[99]. The formation of the brominated aldehyde could be indirectly detected with the concurrent conversion of DBBA to barbituric acid which, as the reaction progressed was observed as a spot on the baseline of the TLC plate. After 64 hr at room temperature, the reaction mixture was filtered, conveniently removing the crystalline byproduct of barbituric acid. Excess DBBA was removed by washing the solution with a saturated sodium thiosulfate solution. After workup and purification by column chromatography, the product **95** was afforded as an orange oil in a good yield of 74%. Another method for bromination was investigated in which liquid bromine was used, however although this too selectively brominated at the α position, it was abandoned due to the significantly lower yield of product.

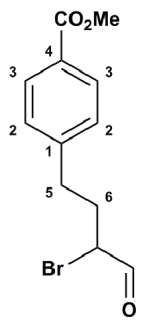

The ^{1}H NMR spectroscopic data for the starting material **94** and brominated product **95** were remarkably different. A triplet at 4.18ppm integrating for a single proton clearly indicated the successful α-bromination of the aldehyde **94**. Moreover, the slight upfield shift of the signal for the aldehyde proton demonstrated the shielding effect of the bromine atom at this position. The two triplets and multiplet accounting for the precursor's CH_2 groups were condensed into two multiplets suggesting several instances of coupling along the aliphatic chain of the compound. In the ^{13}C NMR spectrum, a new signal at 54.3ppm indicated bromination at C7. This was confirmed by the upfield shift of the signal for the carbonyl group upon bromi-

nation.

2.4.5 Synthesis of the pemetrexed ester 96

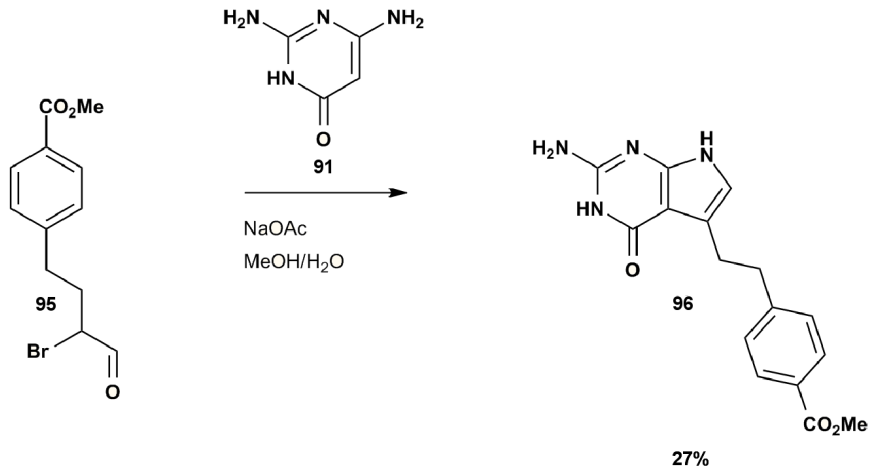

The brominated product was immediately taken into the next step, cyclocondensation with 2,4-diamino-6-hydroxypyrimidine to form the pemetrexed ester **96**. The brominated aldehyde **95**, in a methanol/water solution, was reacted with commercially available, 2,4-diamino-6-hydroxypyrimidine in the presence of sodium acetate at 45°C. TLC analysis after 18 hr indicated complete conversion to a single product which crashed out of solution and was subsequently filtered and recrystallised to afford the ester derivative **96** as a blue solid in a yield of 27%. This was much lower than the reported yield of 67%[99]. Attempts to improve the yield included repeating the experiment at 45°C over 5 min as reported by Eli Lilly and *Co.*[110]. However, these attempts failed to improve the yield and the synthesis was continued into the final step.

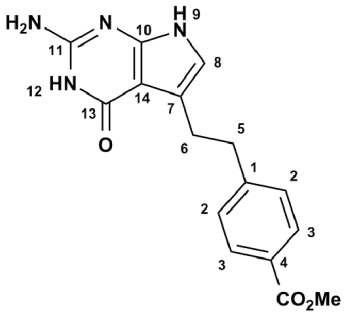

In the ^{1}H NMR spectrum of the product, the absense of the aldehyde proton at 9.47ppm and the α-CH proton at 4.18ppm, together with the appearance of four new signals accounting for two NH groups, one NH_2 group and a signal for H8 of the aromatic pyrrole, attested to the formation of the desired ester product **96**. This was confirmed by addition of D_2O which resulted in disappearance of the NH and NH_2 signals due to exchange with deuterium. The ^{13}C NMR spectrum confirmed successful cyclocondensation with the disappearance of the aldehyde carbonyl and CHBr groups, and appearance of several new aromatic peaks accounting for the newly formed pyrrole and pyrimidine rings. The mass spectrum was as expected with a significant increase in mass (313.1299amu) matching the calculated value of 313.1278amu for the parent ion **96**.

2.4.6 Synthesis of the pemetrexed precursor 62

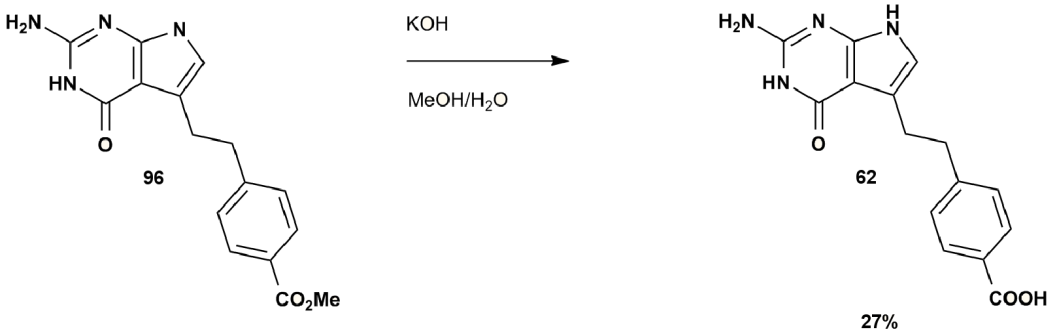

All that remained in preparation of the target molecule **62** was basic hydrolysis of the carboxylic ester **96**. This was achieved at room temperature using potassium hydroxide in an aqueous methanol solution. As the reaction progressed, the solution turned from blue to gray and the R_f value decreased slightly on formation of the more polar carboxylic acid. After 2 hr, TLC indicated complete conversion to the acid derivative **62**. Traces of starting material **96** were removed by an acid/base extraction leaving behind the hydrolysed product **62** which, after filtration, was obtained in a 27% yield. The yield was once again significantly lower than that reported (91%) by Barnett *et al.* Low yields possibly resulted from the comparably smaller scale used (approximately 50 times smaller than that reported by Barnett) making isolation of the desired product **62** difficult.

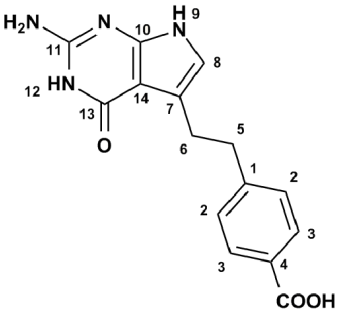

The ^{1}H NMR spectrum for the final product **62** was similar to that of its precursor **96**. Differences, including the presence of a broad O*H* singlet at 3.52ppm and the absence of the methyl peak, confirmed the formation of the desired product. Similarly, the methyl signal at 36.3ppm was no longer present in the ^{13}C NMR spectrum providing further evidence for the reaction's success.

We had thus successfully completed the synthesis of the unglutamated precursor of pemetrexed from the commercially available 4-iodobenzoic acid methyl ester in six steps and an overall yield of 3.2%. We therefore proceeded to the synthesis of analogues of this compound, some of which lack a terminal carboxylic acid. In the section to follow we will describe a variation of the synthesis described above towards these analogues of the pemetrexed precursor.

2.5 Planned approach towards analogues of the pemetrexed precursor

We chose to introduce structural variety into the phenyl moiety of the pemetrexed compound as highlighted in Fig. 2.1. Some of the analogues we planned to synthesise lack a terminal carboxylic acid and as such cannot be glutamated *in situ* by enzymes of the malarial parasite, thereby potentially serving as a useful comparison to those compounds which can, i.e. the precursors of pemetrexed and methotrexate. In addition, such derivatives could potentially exhibit antimalarial activity in their own right and in this respect would be tested *in vitro* for general antimalarial activity in a whole cell, *P. falciparum*, biological screen.

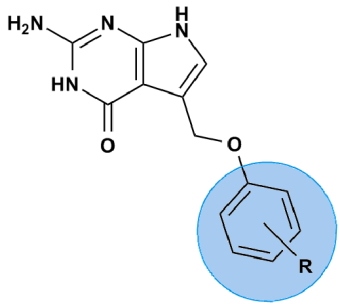

Fig. 2.1

Similarly to the pemetrexed precursor, the target molecule **107** could be disconnected to afford the commercially available 2,4 diamino-6-pyrimidone **91** and an α-haloaldehyde **108** (Scheme 2.11).

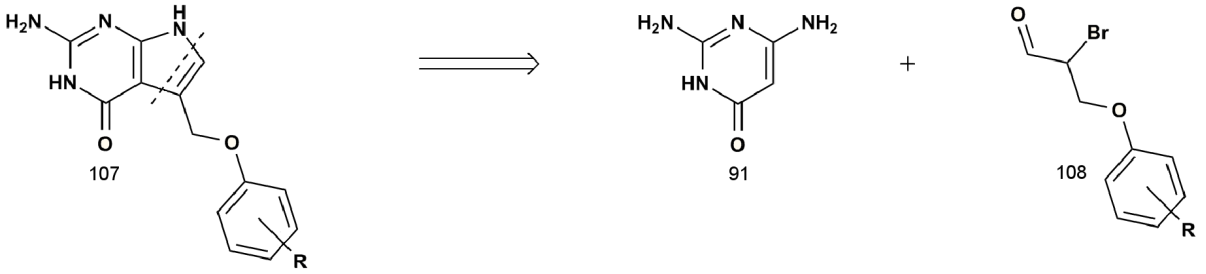

Scheme 2.11

We investigated three approaches for the synthesis of pemetrexed analogue **107**, with differences occurring in the proposed route towards the aromatic aldehyde intermediate **111**. In the first approach, we envisaged the desired pemetrexed analogues **107a-e** would be synthesised in four steps as shown in Scheme 2.12. Starting from the appropriately substituted phenol **109a-e**,

we would form the phenoxypropanol compounds **110a-e** by reaction with commercially available 3-bromopropan-1-ol under basic conditions. Oxidation of the the alcohol group to the aldehyde would afford compounds **111a-e**. With the aromatic aldehyde in hand, the remaining two steps towards pemetrexed derivatives **107a-e**, α-bromination and cyclocondensation, would be achieved in a similar manner to that described for the pemetrexed precursor **62** above.

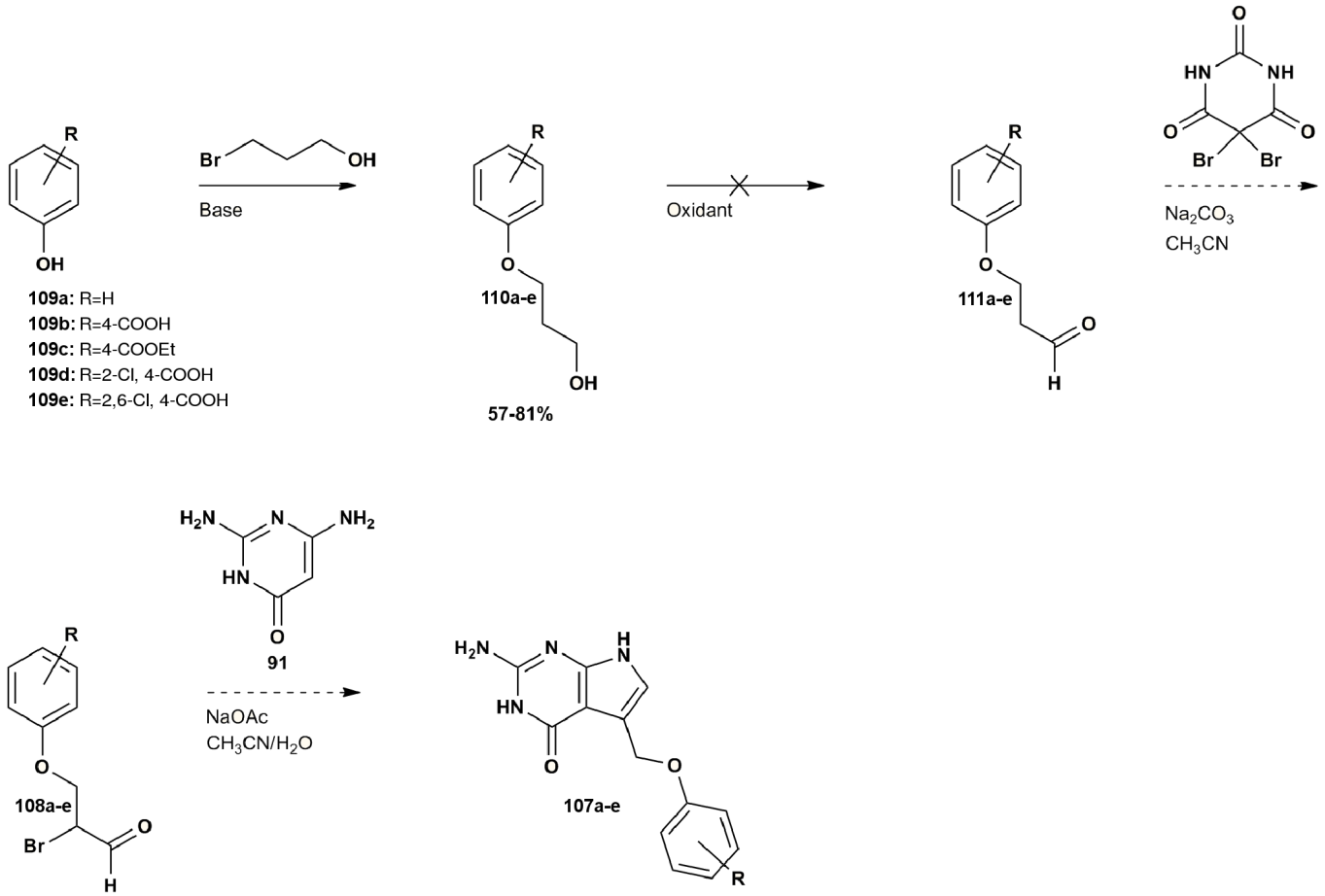

Scheme 2.12

The first step in the proposed synthesis worked relatively well with the desired phenoxypropanol compounds being obtained in yields of 57-81%. Different experimental conditions were used including sodium hydroxide in water, potassium hydroxide in ethanol and potassium carbonate in acetonitrile and acetone respectively. A Finkelstein reaction in which potassium iodide was stirred with 3-bromopropanol prior to reaction with compounds **109a-e** was found to improve yields with the unsubstituted phenolic analogue **109a** affording the best results. Analogues containing a *p*-COOH group (compounds **109b**, **109d** and **109e**) were obtained in comparably lower yields, possibly due to complications involving reaction with the carboxylic acid group as opposed to the phenolic group. With the phenoxypropanol compounds, **110a** and **110b**, in hand we attempted to oxidise the alcohol group to the aldehyde. Unfortunately all oxidising

agents tested, including PCC, oxalyl chloride (Swern oxidation) and DMP, failed to yield the desired products, **111a** and **111b**. At this point, we abandoned the proposed route and considered an alternative approach.

In the second approach shown in Scheme 2.13, we opted to form aromatic aldehydes **111a-c** by first synthesising Weinreb amides **116a-c** which could then be reduced to the desired compounds **111a-c**, thereby avoiding oxidative conditions. Compounds **116a-c** would be synthesised in two steps namely, reaction of starting materials **109a-c** with 3-bromopropanoic acid under basic conditions to afford the phenoxypropanoic acid compounds **112a-c**, which would in turn be converted to Weinreb amides **116a-c**. Unfortunately, difficulties with the synthetic route were encountered in the first step which resulted in very low yields of 3-18%. A Finkelstein reaction with potassium iodide was again employed, but in this case did not improve the yield of the reaction.

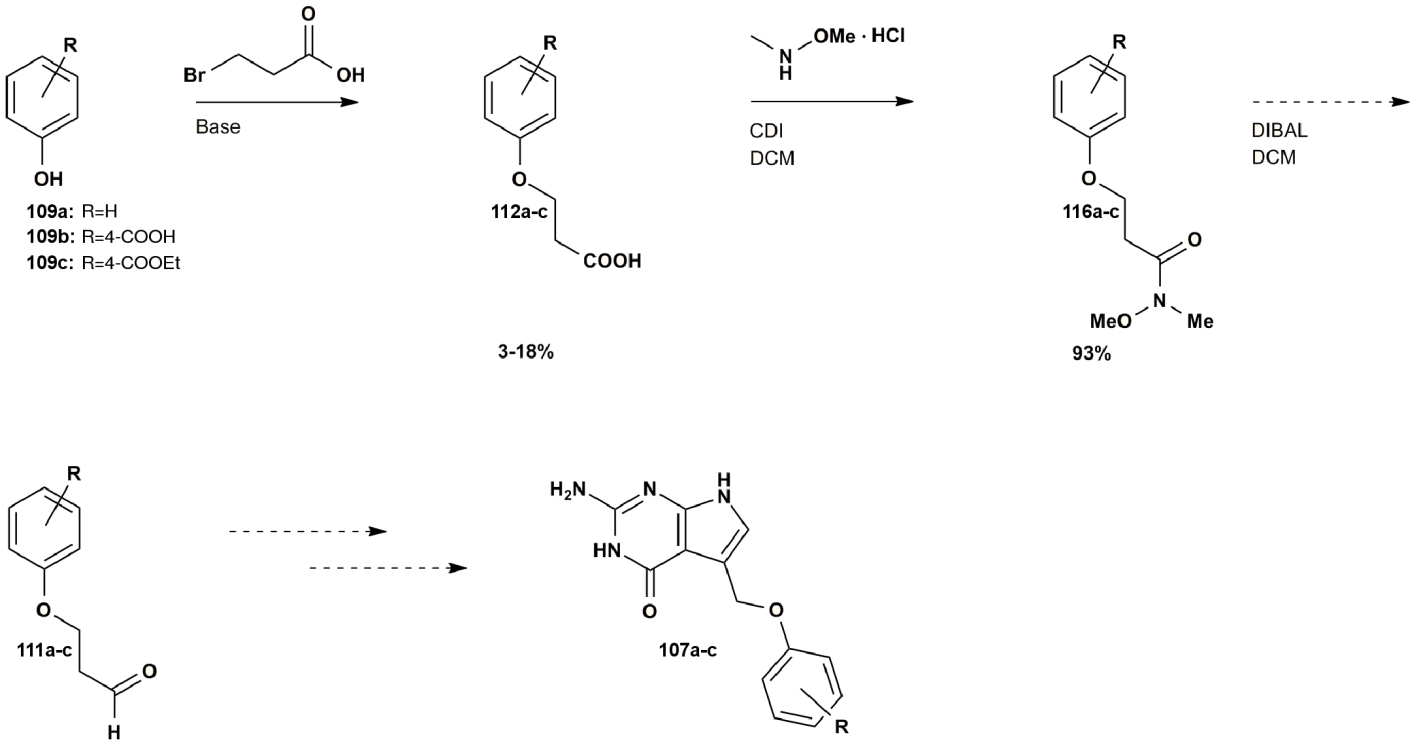

Scheme 2.13

We therefore decided to first convert the 3-bromopropanoic acid reagent to the Weinreb amide **114** before reacting it with the starting materials **109a-c**. Initially, this too resulted in low yields of 8-25%. This was overcome by first forming the acid chloride of 3-bromopropanoic acid before reaction with *N,O*-dimethylhydroxylamine in dichloromethane using pyrimidine to afford compound **114** in an overall yield of 55%. Unfortunately, when reacted with starting

materials **109a-c** (Scheme 2.14), the desired products **116a-c** were not formed, with phenolic starting materials **109a-c** being recovered in large quantities. Different experimental conditions were attempted, including potassium hydroxide/potassium iodide in ethanol, potassium carbonate/potassium iodide in acetone and sodium hydride/potassium iodide in THF, but these too failed to afford compounds **116a-c**.

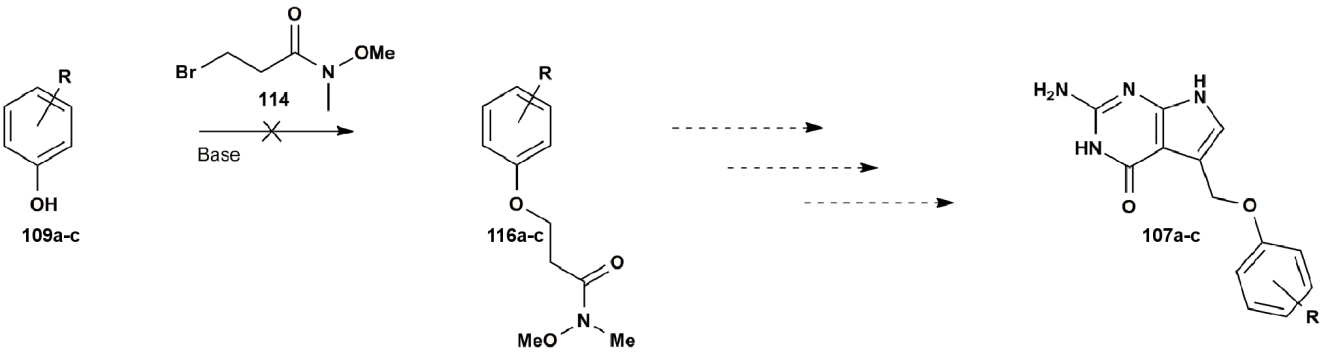

Scheme 2.14

We therefore considered a third approach in which aromatic aldehydes **111a-e** would be synthesised in four steps as shown in Scheme 2.15. Starting from the appropriately substituted phenol **109a-e**, we would form the phenoxypropanenitrile compounds **115a-e** by a Michael addition reaction with acrylonitrile in the presence of an appropriate base. Hydrolysis of the nitrile group to a carboxylic acid would yield the corresponding phenoxypropanoic acids **112a-e**. This would be followed by the formation of Weinreb amides **116a-e** which, as in the second approach, would be subsequently reduced to compounds **111a-e** leaving two steps remaining towards the synthesis of final products **107a-e**.

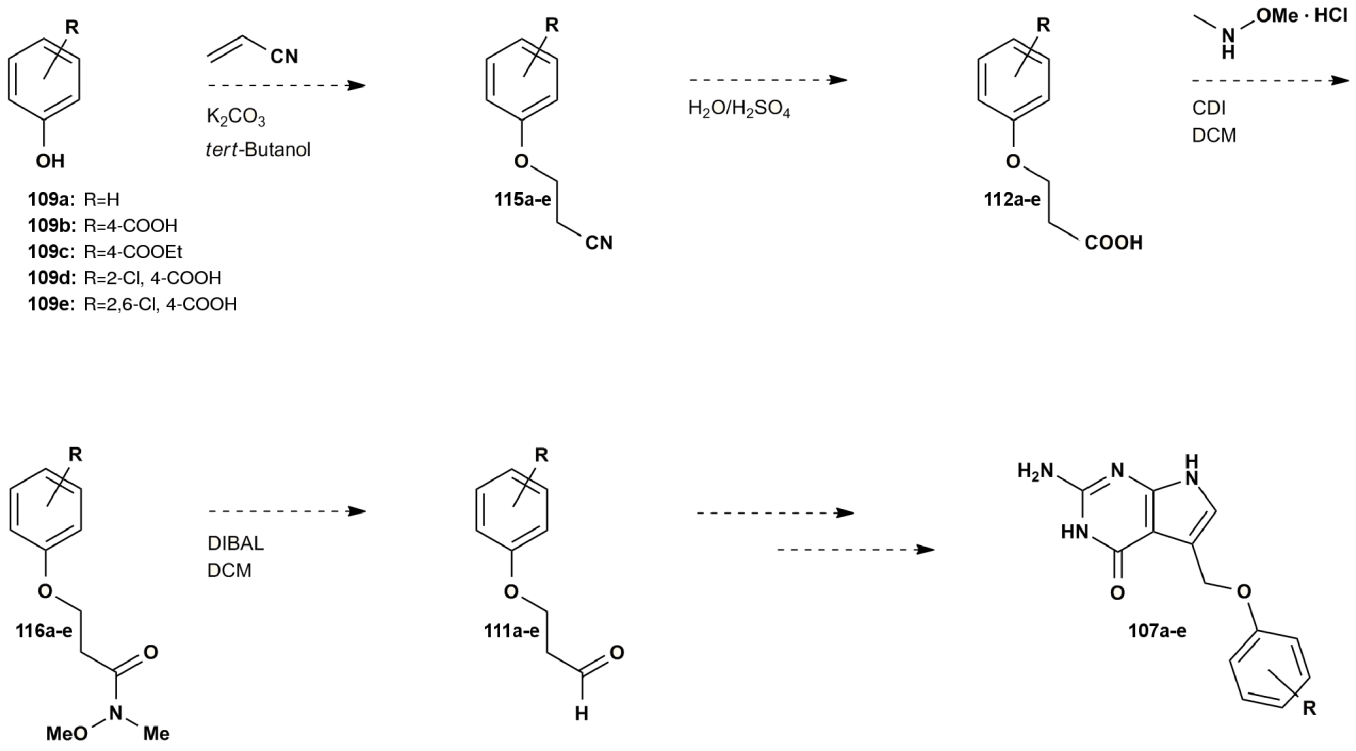

Scheme 2.15

2.6 Synthesis towards analogues of the pemetrexed precursor

2.6.1 Synthesis of 3-phenoxypropanenitrile 115a

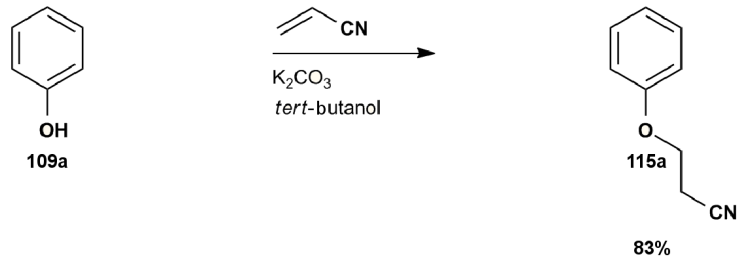

We began our synthesis with the most structurally simple derivative **109a**. The synthesis was commenced with a Michael addition of phenol **109a** to acrylonitrile. The literature is replete with examples of oxa-Michael addition reactions using numerous bases, Lewis acids and phase-transfer catalysts to promote the reaction[111], [112], [113], [114]. We followed the procedure reported by Zhong *et al.*[115] who optimised the reaction conditions so as to achieve high yields. Their method also has a convenient procedure for purification of the product. In this respect, phenol was treated with acrylonitrile in the presence of potassium carbonate and *tert*-butanol and refluxed overnight. TLC analysis indicated that a new product had formed, although a

large amount of starting material was still present. The reaction was left to stir for an additional night to ensure it went to completion. Following a workup, the product was purified by column chromatography and identified as the phenoxypropanenitrile **115a**, obtained as a a white solid in a pleasing yield of 83%.

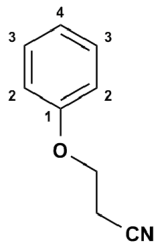

The product **115a** gave rise to a relatively uncomplicated ^{1}H NMR spectrum. Three signals appeared in the aromatic region, as expected. The doublet and triplet at 6.90ppm and 7.00ppm, owing to protons H2 and H4 respectively, were as a result of coupling to protons H3. The J values of 7.8Hz and 7.4Hz for these observed signals was as expected for *ortho* coupling. Protons H3 in turn could be assigned by default to the remaining *ortho* coupled, doublet of doublets in this region. Two triplets further upfield, each integrating for two protons, verified the addition of the alkyl chain and thus the formation of the desired product. The ^{13}C NMR spectrum contained seven signals accounting for four aromatic carbons, one CN group and two CH$_2$ groups. A medium absorption band in the IR spectrum at 2251cm^{-1} confirmed the presence of the nitrile group and the recorded melting point of 59°C corresponded well with the literature value of 59-60°C[116].

2.6.2 Synthesis of 3-phenoxypropanoic acid 112a

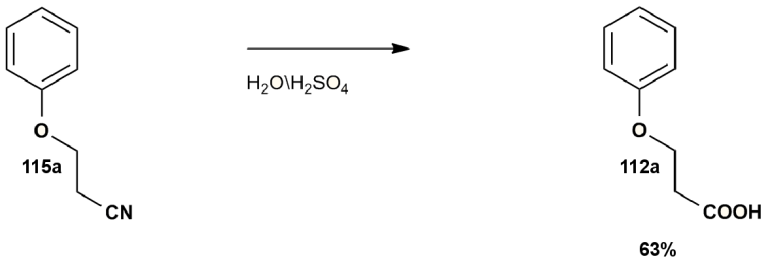

The terminal nitrile group was then completely hydrolysed under acidic conditions to the corresponding carboxylic acid. To this end, the starting material **115a** was dissolved in an aqueous, sulfuric acid solution and heated to reflux. The formation of the phenoxypropanoic acid product **112a** was immediately detected on TLC as a rapidly darkening spot on the baseline; an observation complemented by the color change of the reaction from yellow to clear. Interestingly, no intermediate carboxamide was observed and after 2 hr the reaction appeared to go to completion. The reaction mixture was cooled to room temperature and refrigerated to allow for the product to crystallise under acidic conditions. A white solid crystallised out of solution on standing and, after filtration, traces of the starting material removed by an acid-base extraction. In this way the phenoxypropanoic acid **112a** was recovered as a white, needle-like, crystalline solid in a reasonable yield of 63%. Although our recorded melting point was lower

than the literature value by 2°C, the spectroscopic data matched well with the results reported by Weiske and coworkers[117], reassuring us that the desired product had indeed been synthesised. Other methods for hydrolysis were tested including using an aqueous hydrochloric acid solution in methanol at 45-50°C, however, this resulted in a far lower yield of product (8%) and was subsequently abandoned.

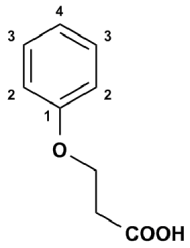

The ^{1}H NMR spectrum was almost identical to that of the starting material **115a**. Slight differences arose in the observed chemical shifts, with the signal for proton H4 and H2 condensing into one multiplet and the signals for the two CH_2 groups occurring further downfield due to the deshielding effect of the neighboring carboxylic acid group. In addition, a broad singlet at 9.71ppm, integrating for one proton, suggested the presence of an OH group. The ^{13}C NMR spectrum was more elucidating with the disappearance of the CN group signal at 117.2ppm. This was replaced by a signal at 177.4ppm owing to the terminal carbonyl group. The chemical shift for the former CH$_2$CN group had also changed, the deshielding effect of the newly formed carboxylic acid shifting it noticeably downfield. The transformation was also observed in the IR spectrum, where the medium CN peak was replaced by a broad absorption at 2639cm^{-1} for the OH group.

2.6.3 Synthesis of *N*-methoxy-*N*-methyl-3-phenoxypropanamide 116a

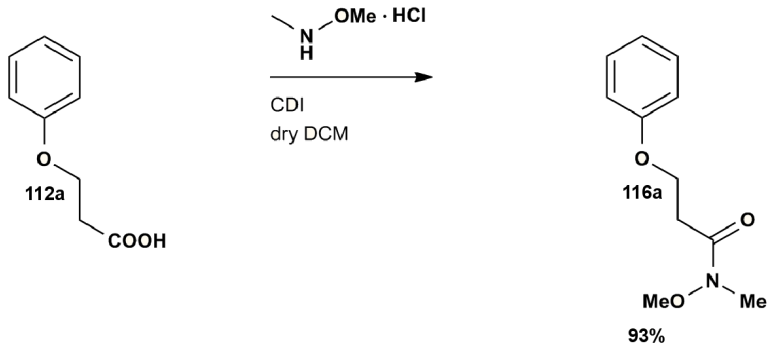

En route to the desired aromatic aldehyde **111a**, the terminal carboxylic acid was subjected to a transacylation reaction. The starting material **112a** was dissolved in dry dichloromethane to which 1,1-carbonyl diimidazole was added. The formation of the amide intermediate was made evident by the presence of bubbles indicating the release of carbon dioxide. By contrast, the imidazole byproduct was not detected. On reaction with N,O-dimethylhydroxylamine, the Weinreb amide **116a** that formed was observed at a slightly lower R_f value by TLC than that of the starting material **112a**. The reaction went to completion overnight and, after workup and purification by column chromatography, the Weinreb amide product **116a** was recovered

as a yellow oil in an excellent yield of 93%.

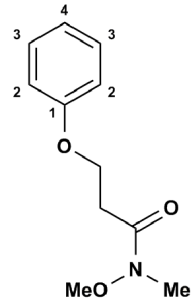

The success of the transacylation reaction was clearly evident in the ^{1}H NMR spectrum with the appearance of two prominent singlets at 3.64ppm and 3.14ppm accounting for the methoxy and methyl groups of the amide functionality. In conjuction with this, the previously observed broad hydroxy singlet associated with the carboxylic acid in the ^{1}H NMR spectrum of the precursor was no longer present. The remainder of the spectrum was similar to that of the phenoxypropanoic acid starting material **112a**, although all the signals, with the exception of the CH_2CO group, had shifted slightly upfield. The accompanying changes in the ^{13}C NMR spectrum included two additional signals at 61.4ppm and 31.9ppm due to the subtituents of the amide functionality. The OH peak in the IR spectrum was no longer present indicating successful conversion to the Weinreb amide.

2.6.4 Synthesis of 3-phenoxypropanal 111a

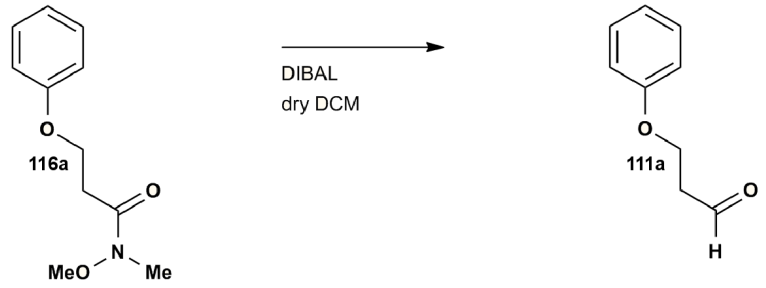

With the stable Weinreb amide **116a** in hand, we proceeded to form the free aldehyde **111a** by reduction of the amide with diisobutylaluminium hydride (DIBAL). The starting material **116a** was dissolved in dry dichloromethane and the reaction flask purged of any air which might otherwise have reacted with the DIBAL. The reducing agent was then carefully introduced into the reaction flask at -78°C and reaction progress monitored by TLC. Complete conversion of the Weinreb amide to the desired free aldehyde was observed after 3.7 hr and the reaction mixture consequently quenched with a saturated, aqueous potassium hydrogen sulfate solution. Alternative methods for quenching DIBAL, including addition of hydrochloric acid (1.35M) or a saturated, aqueous ammonium chloride solution both proved to be undesirable, with the product **111a** decomposing on workup. The aromatic aldehyde was also found to be sensitive to silica and thus, after filtration and workup, was not further purified by column chromatography. This was in contrast to the previously synthesised aromatic aldehyde **94**, which withstood oxidising experimental conditions followed by workup with a saturated sodium thiosulfate/sodium bicarbonate solution and purification by chromatography. Differ-

ences in stability could be explained by a retro-Michael or β elimination reaction occurring in the case of the phenoxypropanal compound **111a**. As shown in Scheme 2.16, this would afford propenal **118** and phenol **109a**. In comparison, the 4-oxobutyl moiety of aromatic aldehyde **94** could not undergo such a transformation allowing it to tolerate harsher experimental conditions.

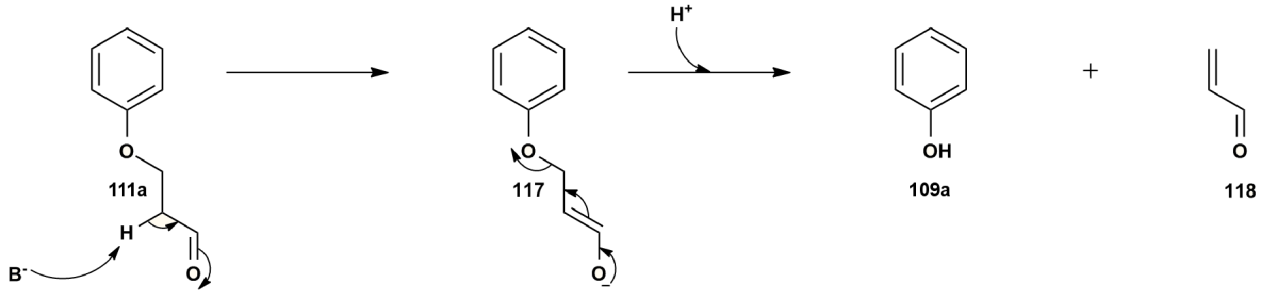

Scheme 2.16

Fortunately, the reaction progressed without the formation of any byproducts and, after quenching unreacted DIBAL during workup, the free aldehyde **111a** was recovered in a quantitative yield as a relatively clean, yellow oil, with only traces of starting material appearing in the ^{1}H and ^{13}C NMR spectra.

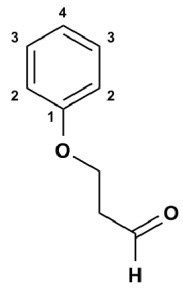

In the ^{1}H NMR spectrum, the presence of a singlet at 9.85ppm, integrating for a single proton, attested to the formation of the free aldehyde **111a**. The remainder of the spectrum resembled that of the precursor with a high degree of overlap occurring between the signals of the starting material and product. In the ^{13}C NMR spectrum, the formation of the desired product over that of the precursor was more obvious. The carbonyl group was observed to shift downfield by 29ppm on removal of the electron donating amide functionality. In addition, the signals for the methyl and methoxy groups could no longer be detected, simplifying the upfield region of the spectrum.

At this point, having completed the first four steps of our synthetic route in an overall yield of 49%, we were ready to attempt the α-bromination of the aromatic aldehyde **111a** and subsequent cyclocondensation reaction leading to the formation of the final pemetrexed precursor derivative **107a**. The experimental conditions would be based on those reported by Barnett *et al.*[99] which had proved successful in the synthesis of the pemetrexed precursor **62**.

2.6.5 Attempted synthesis of Pemetrexed derivative 107a

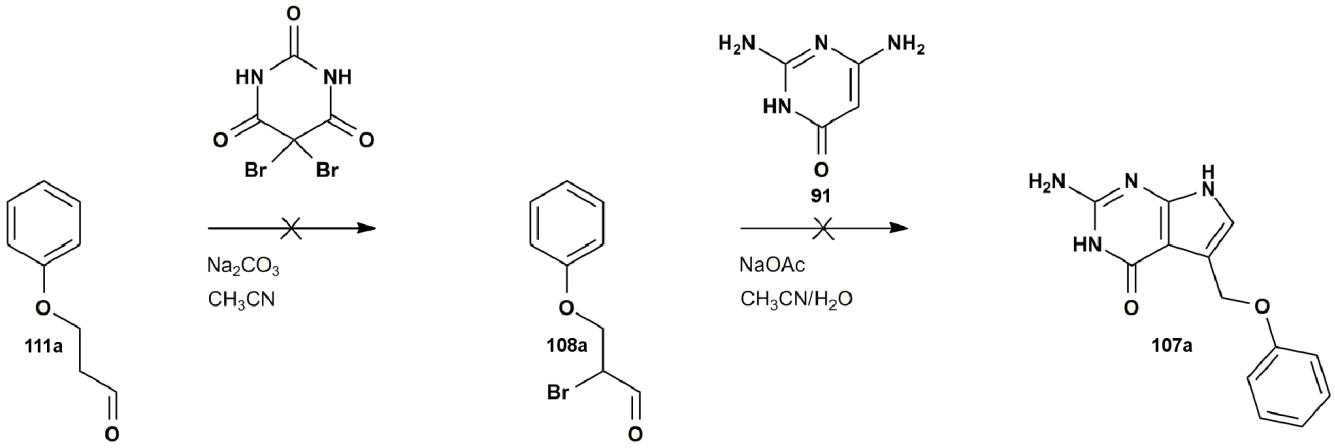

The last two steps in our synthetic route towards the pemetrexed derivative **107a** were performed *in situ*. The methodology we had used previously for selective bromination of an aldehyde at the α position (using DBBA in diethyl ether in the presence of sodium carbonate) had to be adjusted due to the poor solubility of the starting material **111a** in diethyl ether. Therefore, the phenoxypropanal compound was dissolved in dry acetonitrile to which sodium carbonate and DBBA were added. The reaction was once again monitored by the simultaneous formation of barbituric acid which, as expected, appeared as a darkening spot on the baseline of the TLC plate. After 30 min, no DBBA could be detected and we assumed that the brominating reagent had been used to form the desired 2-bromo-phenoxypropanal product **108a**. We anticipated that the brominated aldehyde could be just as unstable as its precursor **111a**. Thus, additional workups and purification procedures were avoided and, after filtering off the barbituric acid, the reaction mixture was carried directly into the next step. Sodium acetate and 2,4-diamino-6-hydroxypyrimidine dissolved in water were therefore added to the reaction mixture containing the brominated starting material **108a** in acetonitrile. The reaction mixture was heated to 45°C and monitored by TLC. After 18 hr, no starting materials could be detected and, much to our delight, a pink solid had formed which was subsequently filtered off.

Indeed, both starting materials appeared to be absent in the crude ^{1}H NMR spectrum, which no longer contained a singlet at 9.85ppm owing to the former C*H*O group of the free aldehyde **111a**. Peaks at 6.70ppm and 6.18ppm, which would otherwise account for the amine groups of starting material **91** were also not detected. These observations, together with the appearance of a broad signal at 10.62-11.03ppm, possibly owing to the N*H* groups of the pyrrole and pyrimidine rings of desired product **107a**, suggested we may have formed the pemetrexed derivative. Although, the ^{13}C NMR spectrum also confirmed the absence of starting materials **91** and **111a**, it contained numerous peaks and could not confirm the formation of the final product. Attempts to purify the solid compound including recrystallisation from methanol and

water proved unsuccessful and the reaction was repeated using a DMSO/water solvent system however, these attempts also failed to yield the pemetrexed derivative **107a**.

The unsuccessful synthesis of the analogue of the pemetrexed precursor could be due to the failure of either the α-bromination or cyclocondensation reaction. The success of the α-bromination was not confirmed as the brominated aldehyde **108a** was never analysed due to concerns over stability. Indeed, the aldehyde **111a** may well have undergone a more thermodynamically favorable, retro-Michael reaction providing an explanation for the failure of both steps.

Having failed to obtain the most structurally simple pemetrexed analogue **107a**, we abandoned this strategy and, still being within the realm of antimalarial drug discovery, focused our efforts on an entirely new route towards the synthesis of novel DHFR inhibitors using chemical modifications of a hit compound generated from a previous study.

2.7 Planned approach towards novel DHFR inhibitors

Chemical modification has proved to be a crucial strategy in addressing the problem of parasitic resistance. It has resulted in the improvement of existing drugs' antimalarial activity as well as the development of novel antimalarial compounds[53], [74], [75], [76]. More recently, this approach has been used in conjuction with published crystallographic data pertaining to both the wildtype and mutant forms of the PfDHFR-TS enzyme in complex with various inhibitors. This has helped to direct antimalarial research by aiding in the design of novel compounds which fit well within the active site of even resistant PfDHFR-TS strains, possessing multiple mutations.

The use of structural information to direct chemical modification is exemplified by work conducted by Rousseau and coworkers who used crystallographic data to aid the design of a library of flexible, cycloguanil analogues, structurally based on the well-known potent cycloguanil derivative, WR99210 (Fig. 2.2) [62], [80].

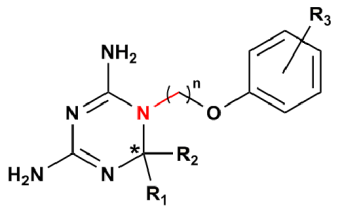

n = 1-4
R_1-R_3 = Me, Ph, H

Fig. 2.2

Rousseau changed the functionality around both the stereogenic centre and substituted phenol ring of WR99210 in addition to varying the length of the flexible chain linking the 1,2-dihydro-1,3,5-triazine-4,6-diamine heterocycle and substituted phenyl ring. Compounds bearing a 4-atom flexible tether such as **60** were found to be particularly potent, exhibiting activity in the nanomolar range. Although these results were very promising the synthesis of these dihydrotriazine compounds was problematic, resulting in low yields and isomeric mixtures. This project therefore aimed to further chemically modify the hit compound **60** generated from this study so as to prepare a series of novel compounds of simpler structure, that may be easier to synthesise. In this vein, we were interested in synthesising pyrimidine equivalents of the hit compound **60**.

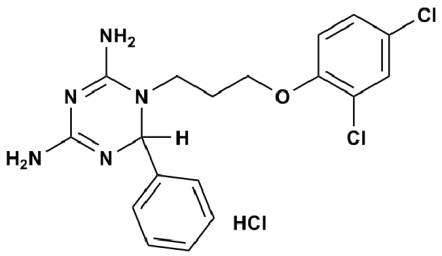

60

Having significantly simplified the structural complexity of the dihydrotriazine functionality, we proceeded to seek ways in which to synthesise our targeted series of pyrimidine analogues (Fig. 2.3).

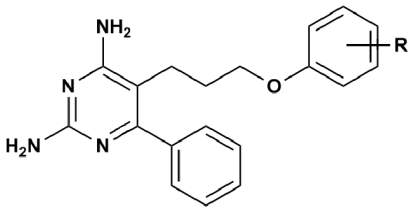

Fig. 2.3

A retrosynthesis of the target molecule **119** (Scheme 2.17) suggests it can be disconnected to guanidine **120** and an α-cyano ketone compound **121**.

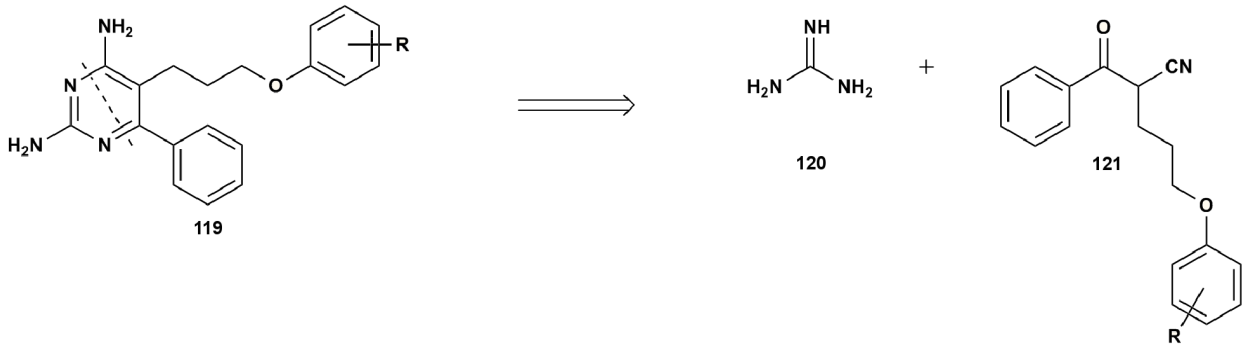

Scheme 2.17

The proposed synthetic route is shown in Scheme 2.18. The required substituted phenols **122a-d** are commercially available and, in the presence of potassium carbonate, would be alkylated with 1,4-dibromobutane to form the corresponding bromoethers **123a-d**. Functional group interconversion of the bromide to the nitrile **124a-d** would be achieved using potassium cyanide in a water/ethanol solution. The ethyl ester, ethyl benzoate, would then be added in the presence of a base to furnish the desired α-cyano ketone compounds **125a-d**. The preparation

of the enol ethers **126a-d**, using an acid catalyst in the form of triethylorthoformate, would facilitate the formation of the pyrimidine products **65a-d** by reaction with guanidine.

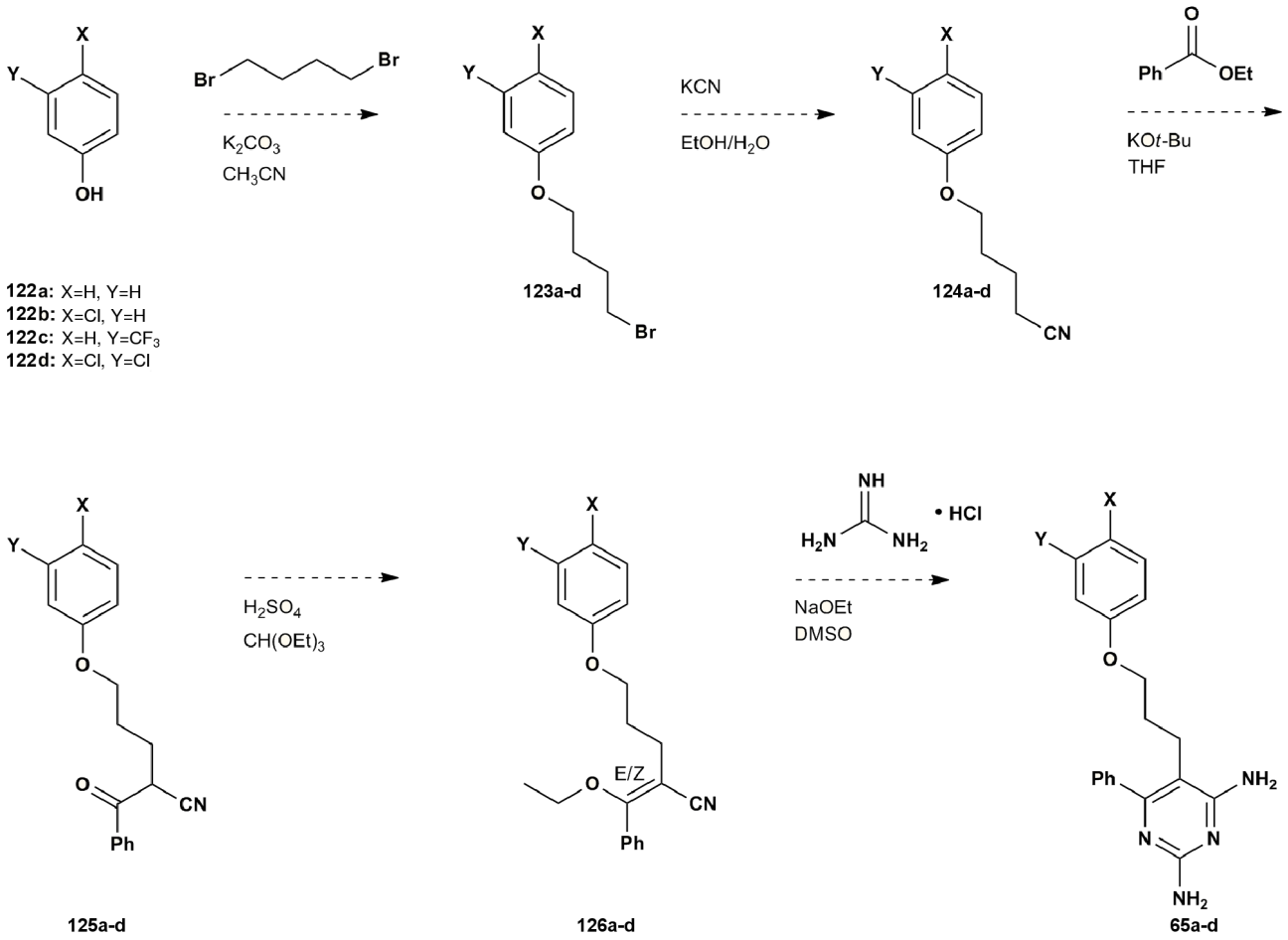

Scheme 2.18

Many structurally similar pyrimidines have been successfully synthesised including the well known antifolate, pyrimethamine[45]. However, this methodology has not been applied to the synthesis of the proposed analogues before. As such, we decided to initially test the methodology outlined above on the known compound 5,6-diphenylpyrimidine-2,4-diamine **69** under the same reaction conditions. The synthesis of this compound has been reported[118] and as such its synthesis would serve as an effective control for testing the experimental conditions in our proposed synthetic route.

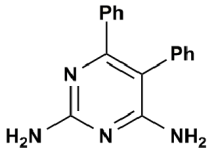

69

Using a retrosynthetic approach, the pyrimidine ring can once again be disconnected to guanidine **120** and an α-cyano ketone **127** (Scheme 2.19).

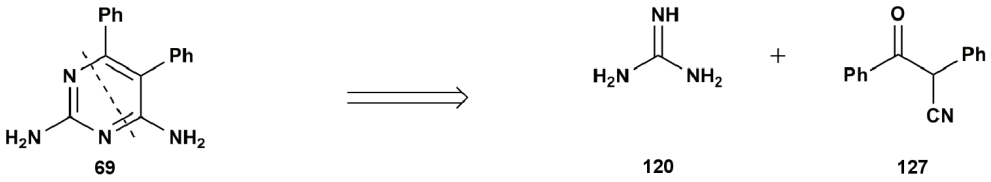

Scheme 2.19

The 2,4-diamino pyrimidine analogue **69** would thus be synthesised in three steps, using the methodology outlined in Scheme 2.20. Starting from commercially available 2-phenylacetonitrile **128**, 3-oxo-2,3-diphenylpropanenitrile **127** would be obtained by nucleophilic addition of the starting material to ethyl benzoate in the presence of potassium *tert*-butoxide. This would be followed by the formation of the enol ether intermediate **129**, once again formed by an acid catalysed reaction in the presence of triethylorthoformate. Finally, we believed the addition of guanidine would furnish the desired 5,6-diphenylpyrimidine-2,4-diamine **69**.

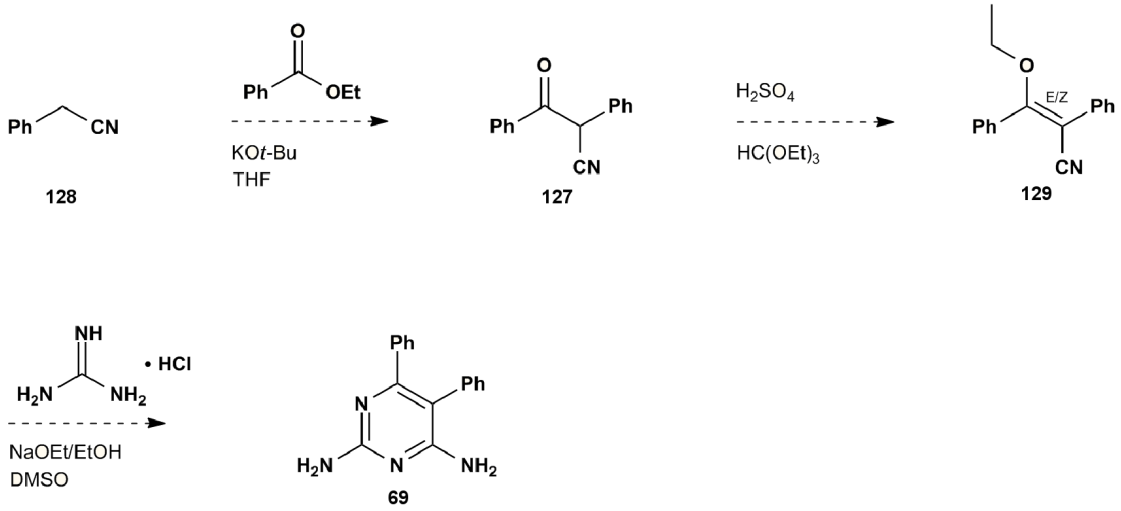

Scheme 2.20

2.7.1 Synthesis of 5,6-diphenylpyrimidine-2,4-diamine 69

2.7.1.1 Synthesis of 3-oxo-2,3-diphenylpropanenitrile 127

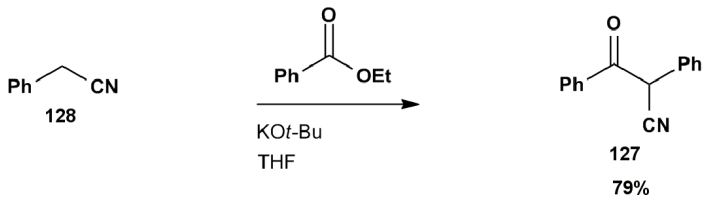

The α-cyano ketone **127** was assembled within the first step of the control study. Deprotonation at the α position of commercially available 2-phenylacetonitrile **128** by potassium *tert*-butoxide, allowed for the subsequent nucleophilic addition of the starting material to ethyl benzoate. To this end, all three reagents were dissolved in THF and reaction progress monitored by TLC. The more polar product was detected as a rapidly forming spot with a significantly lower R_f value. Complete conversion to the α-cyano ketone was observed after 30 min and the reaction quenched with a saturated ammonium chloride solution. Following workup and purification by column chromatography, the product **127** was acquired as an orange solid in a yield of 79%. Although the melting point was 7°C above the reported value[119], the NMR and mass spectroscopic data fitted well for the desired compound and confirmed the formation of the product.

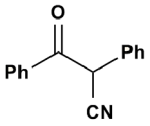

In the ^{1}H NMR spectrum, the presence of a singlet integrating for a single proton at 5.65ppm, attested to the successful nucleophilic addition at the α position. In the aromatic region, a series of multiplets accounted for the protons of the two phenyl substituents. The ^{13}C NMR spectrum contained eleven signals due to the eleven non-equivalent carbons present in the compound. The most distinct of these accounted for the carbonyl group and *C*H functionality, each appearing at the upper and lower extremes of the spectrum respectively. Furthermore, in the IR spectrum, stretching bands for both the C=O and CN functional groups were observed.

2.7.1.2 Synthesis of *E*/*Z*-3-ethoxy-2,3-diphenylacrylonitrile 129

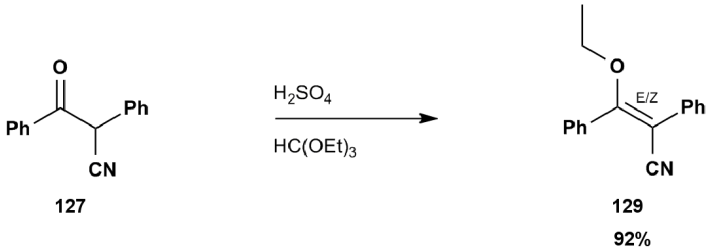

In order to ensure the success of the ring closure, and with it the formation of the pyrimidine moiety, the ethyl enol ether intermediate was intially synthesised. The transformation was achieved using triethylorthoformate and an acid catalyst. Despite heating the reaction mixture to 100°C, the reaction progressed slowly. After 108 hr at this temperature, TLC indicated that only traces of starting material remained. The reaction mixture was thus cooled and, after purification by column chromatography, the product **129** was obtained as a yellow oil in an excellent yield of 92%.

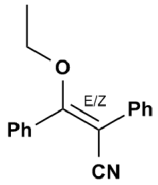

The formation of both the *E* and *Z* isomers was evident in the ^{1}H NMR spectrum which contained marginally overlapped signals at 3.91ppm and 1.27-1.34ppm owing to the OCH_2 and CH_3 groups respectively. The ratio of the two isomers was calculated to be 1:4 although, due to the high degree of overlap, we were unable to determine which isomer made up the majority of the mixture. In the ^{13}C NMR spectrum the presence of geometric isomers was indicated by the doubling of peaks due to the slightly different environments of the aromatic phenyl and OCH_2 groups in the *E* and *Z* isomers. The replacement of the signals for the C=O and *C*H groups with those of the ethyl and alkene functionalities confirmed the conversion of the α-cyano ketone to the enol ether product. In the IR spectrum, the stretching band for the C=O group had disappeared as expected on formation of the enol ether.

2.7.1.3 Synthesis of 5,6-diphenylpyrimidine-2,4-diamine 69

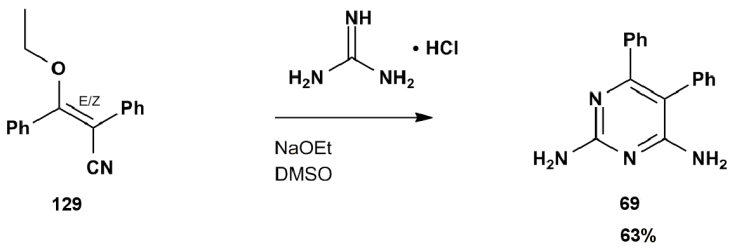

With the enol ether intermediate **129** in hand, we were in a position to test the final step of the control study. Firstly, guanidine hydrochloride was neutralised with a sodium ethoxide solution to afford the free base. Complete neutralisation was ensured by adjustment of the pH of the solution to approximately 7. In this way, overly basic conditions were effectively avoided. The excess ethanol was then removed by evaporation *in vacuo*, and the free base combined with the starting material in dry DMSO. The reaction mixture was heated to 85°C and monitored by TLC. Interestingly, both the *E* and *Z* isomers of the enol ether appeared to react, as both spots were observed to fade with the simultaneous formation of a much darker spot on the baseline. After 4.5 hr, no more starting material was detected by TLC. Subsequent work up and recrystallisation from dichloromethane afforded the product as a white powder in a reasonable yield of 63%.

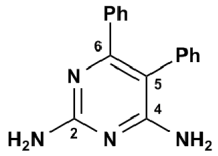

The ^{1}H NMR spectrum was significantly different to its enol ether precursor. The consumption of both geometric isomers rendered the aromatic region significantly simpler, with a condensed multiplet integrating for ten protons appearing at 7.06-7.30ppm. The presence of singlets at 6.07ppm and 5.70ppm accounted for the amine substituents. Interestingly, the singlet at 5.70ppm was particularly broad, possibly due to interaction of the C2-NH_2 group with neighboring nitrogen atoms of the pyrimidine ring. In the ^{13}C NMR spectrum, the addition of four signals at 162.7ppm, 162.3ppm, 161.9ppm and, most significantly, 106.5ppm testified to the formation of the pyrimidine ring. Stretching bands at 3481cm^{-1} and 3442cm^{-1} in the IR spectrum were consistent with the presence of the NH_2 groups.

The successful synthesis of 5,6-diphenylpyrimidine-2,4-diamine **69** from commercially available 2-phenylacetonitrile **128** in three steps and an overall yield of 46% reassured us as to the feasibility of the experimental methodology. In the section to follow we will describe the application of this route to the synthesis of our targeted series of flexible pyrimidine analogues.

2.7.2 Synthesis of novel DHFR inhibitors: 5-(3-phenoxypropyl)-6-phenylpyrimidine-2,4-diamine 65b and its analogues 65a, 65c and 65d

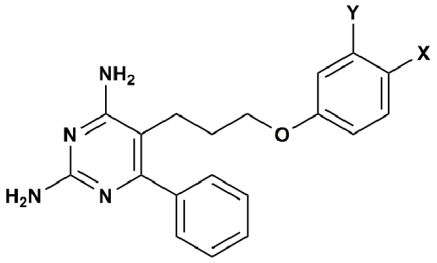

65a: X=H, Y=H
65b: X=Cl, Y=H
65c: X=H, Y=CF_3
65d: X=Cl, Y=Cl

The synthesis of the novel 4-chlorosubstituted analogue **65b** was conducted concurrently with the synthesis of precursors to the analogues **65a**, **65c** and **65d**. The first two steps of our synthesis were based on those previously reported[62],[120] whereas the experimental conditions for the last three steps stemmed directly from the results of the control study in which 5,6-diphenylpyrimidine-2,4-diamine **69** was successfully synthesised.

2.7.2.1 Synthesis of 1-(4-bromobutoxy)-4-chlorobenzene 123b

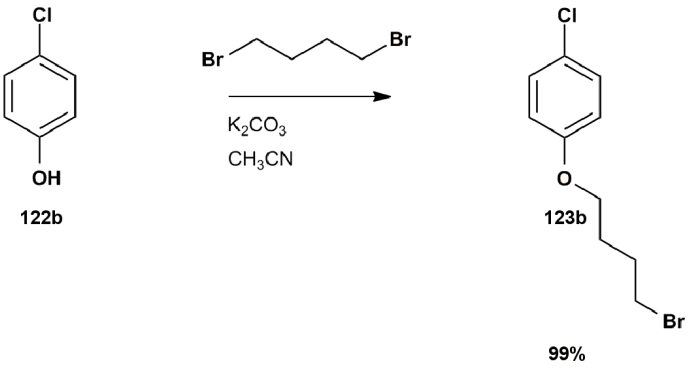

Starting from commercially available 4-chlorophenol, the bromoether **123b** was synthesised by alkylation of the hydroxyl group under basic conditions. As described by Gravestock *et al.*, an excess of the dibromoalkane reagent was necessary to prevent the phenol reacting twice with the symmetrical alkane[62]. Thus, the starting material was combined with three molar equivalents of dibromobutane in acetonitrile. Potassium carbonate was added and the reaction mixture stirred under reflux under an argon atmosphere. The product formed as a single spot on TLC,

absent of any aromatic impurities. The slightly increased R_f value suggested the addition of a hydrophobic, alkyl group. Distillation of the excess 1,4-dibromobutane followed by purification by column chromatography afforded the alkylated product **123b** as a low-melting, white solid in an almost quantitative yield of 99%.

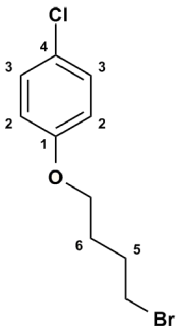

Apart from the aromatic signals, the ^{1}H NMR spectrum contained three signals owing to the CH_2 groups of the alkyl functionality. Two triplets in the middle of the spectrum were assigned to the OCH_2 and CH_2Br groups. The third signal, a multiplet at 2.10-1.87ppm integrating for four protons accounted for the remaining two CH_2 groups. The ^{13}C NMR spectrum was equally convincing. Four downfield signals accounted for six aromatic carbons, two being equivalent. The carbons of the alkyl functionality appeared further upfield as four conspicuous peaks.

The analogues, **123a**, **123c** and **123d** were prepared in a similar manner. The ^{1}H and ^{13}C NMR spectra closely resembled that for compound **123b**, described above. Differences were observed in the aromatic region in which *mono*, *di* and *tri*-substituted ring structures allowed for multiple instances of *ortho* and *meta* coupling. This was particularly evident for the *tri*-substituted compound **123d** whose H5 proton gave rise to a doublet of doublets, with J values of 8.9Hz and 2.9Hz, due to both *ortho* and *meta* coupling with neighboring protons H6 and H3. The ^{13}C NMR spectra for these compounds contained no less than six peaks in the aromatic region, accounting for the six nonequivalent carbons of the phenolic functionality.

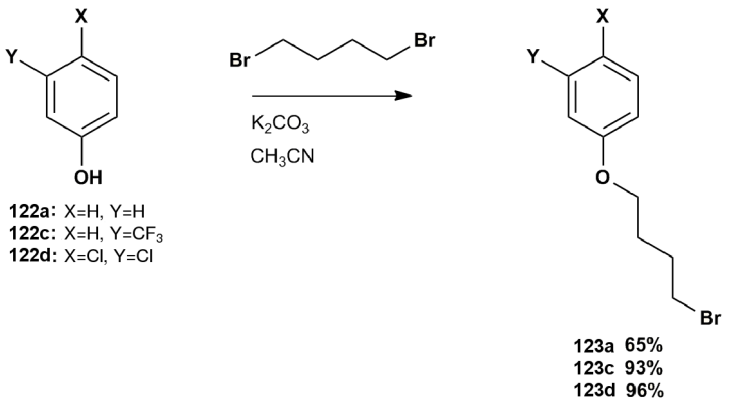

122a: X=H, Y=H
122c: X=H, Y=CF_3
122d: X=Cl, Y=Cl

123a 65%
123c 93%
123d 96%

2.7.2.2 Synthesis of 5-(4-chlorophenoxy)pentanenitrile 124b

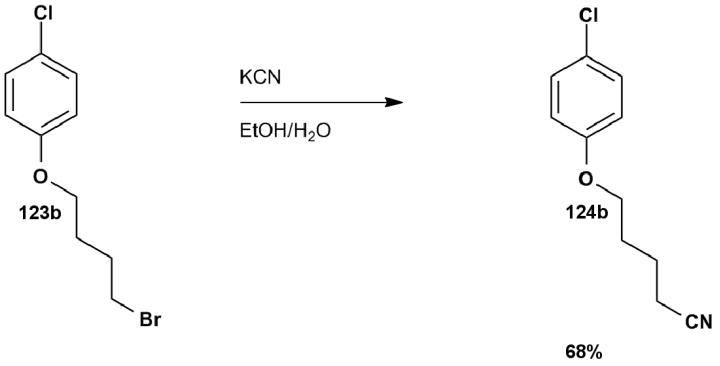

Conversion of the bromide to the nitrile was easily achieved with potassium cyanide in an ethanol/water solution. To this end, the 1-(4-bromobutoxy)-4-chlorobenzene **123b** was dissolved in an ethanol/water solution and treated with potassium cyanide. The reaction mixture was stirred and heated under reflux under an argon atmosphere. After stirring overnight, only traces of the starting remained. Following work up, these were removed by silica gel column chromatography, leaving the product **124b** as a low-melting, white solid in a yield of 68%.

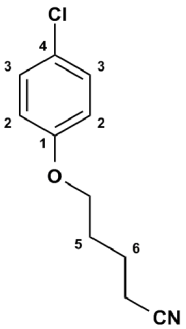

The ^{1}H NMR spectrum of the product closely resembled that of it bromoether precursor. In fact, only the CH_2 group adjacent to the site of functional group interconversion was affected. It was observed to shift further upfield, clearly illustrating the deshielding effects of the former bromine group. In the ^{13}C NMR spectrum, the appearance of a new peak at 119.4ppm owing to the CN group attested to the success of the reaction. The replacement of bromine was also reflected in the IR spectrum in which a stretching band for the CN group had appeared at 2239cm^{-1}.

The same observations were made for analogues **124a**, **124c** and **124d** which were isolated in similar yields of 71-74%. In addition, the melting points of the 5-phenoxypentanenitrile compounds were all found to be very low (25-29°C), owing to their structural similarity.

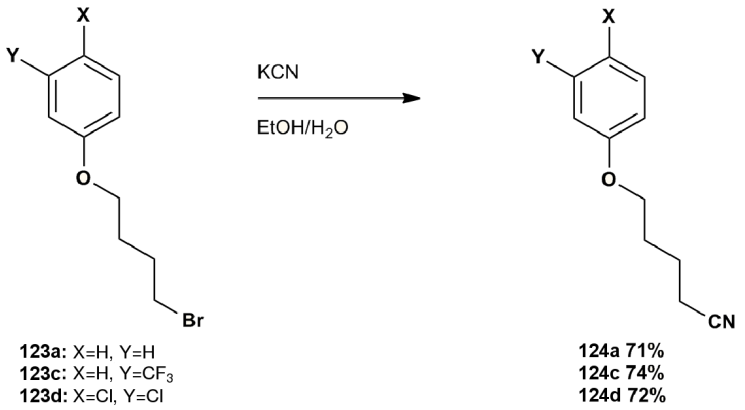

123a: X=H, Y=H
123c: X=H, Y=CF_3
123d: X=Cl, Y=Cl

124a 71%
124c 74%
124d 72%

2.7.2.3 Synthesis of 2-benzoyl-5-(4-chlorophenoxy)pentanenitrile 125b

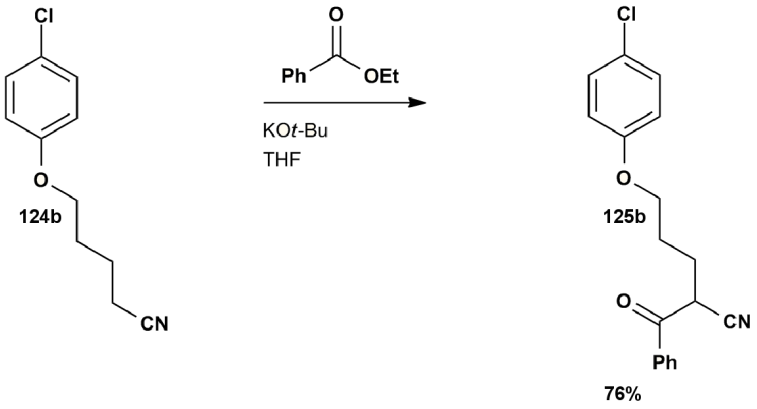

76%

Having successfully formed the pentanenitrile derivative **124b**, we continued with the third step of the synthesis of the α-cyano ketone compound. The starting material **124b** was dissolved in THF to which potassium *tert*-butoxide and ethyl benzoate were added. The reaction mixture was left to stir overnight under an argon atmosphere. Reaction progress was difficult to monitor by TLC owing to the similar R_f values of both starting material and product. The use of staining techniques (potassium permanganate stain) was required in order to differentiate between the two compounds. Unlike the starting material, the α-cyano ketone product stained yellow on contact with the oxidising agent, indicating that another compound had in fact formed. Following isolation and purification by chromatography, the product was obtained as a pale, yellow powder in a good yield of 76%.

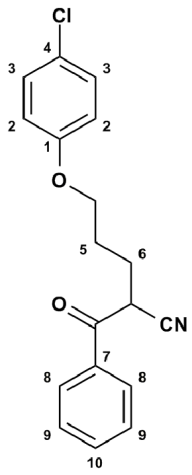

The addition of the benzoyl moiety *alpha* to the cyano group was clearly observed in the ^{1}H NMR spectrum which contained an additional three signals in the aromatic region showing *ortho* coupling due to the addition of the phenyl group. Happily, the appearance of a doublet of doublets, integrating for a single proton, at 4.48ppm coincided with the disappearance of the triplet accounting for the former CH_2CN group at 2.44ppm. In the ^{13}C NMR spectrum, the appearance of a signal at 190.4ppm due to the carbonyl group, together with four new peaks in the aromatic region confirmed the formation of the desired product **125b**. The presence of the carbonyl group was also observed in the IR spectrum which contained a stretching band at 1695cm^{-1}. The mass spectrum showed a significant increase in mass, corresponding well with the expected mass for product **125b**.

This was in line with the data for the other three analogues which all contained additional signals in their ^{1}H and ^{13}C NMR spectra. The yield for the trifluoromethyl substituted compound **125c** was comparably lower (13%) than the other analogues due to difficulties in separating the starting material from the desired product. After failed attempts at column chromatography, the product **125c** was isolated by recrystallisation from ethanol. Although successful, the majority of the desired compound remained in solution, resulting in a lower yield. Another observed discrepancy amongst the collection of 2-benzoyl-5-(4-chlorophenoxy)pentanenitrile compounds was the melting point of compound **125b** which was found to be remarkably higher (126-127°C) than compounds **125a**, **125c** and **125d**, which all melted within a range of 45-59°C.

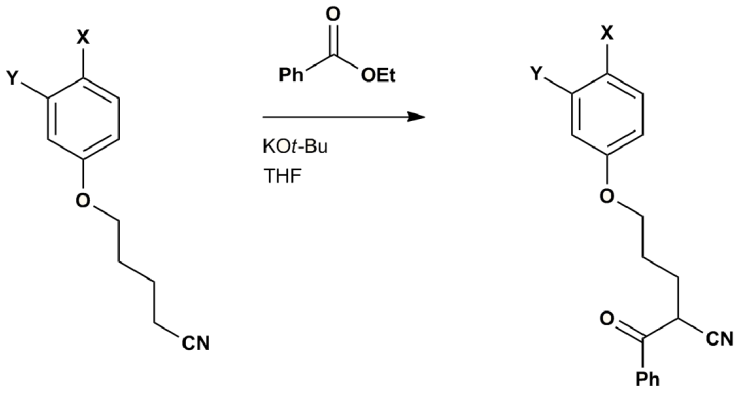

124a: X=H, Y=H
124c: X=H, Y=CF_3
124d: X=Cl, Y=Cl

125a 89%
125c 13%
125d 99%

We had thus successfully completed the first three steps of the synthesis of a novel series of flexible pyrimidine analogues in overall yields of 41%, 51%, 9% and 68% for analogues **125a-d**

respectively. All that remained in the synthesis of these pyrimidine analogues was the enol ether formation, and the final ring closing reaction. In the model study, the experimental time for enol ether formation was surprisingly long (108 hr). This was unexpected given that the α-hydrogen of the structurally rigid starting material **127** is positioned directly adjacent to an aromatic system. We imagined that, on deprotonation, the neighboring phenyl ring would allow for rapid stabilisation of the resulting anion, favoring the formation of the double bond, and with it a conjugated and thus more thermodynamically stable system. However, although successful, high temperatures and long experimental times were required for product formation. In the case of our more flexible antifolates, the α-hydrogen is separated from the electron rich phenyl ring by a comparably longer 4-atom chain. We thus expected enol ether formation, and the subsequent ring closing reaction, to be considerably more challenging.

2.7.2.4 Synthesis of *Z* -5-(4-chlorophenoxy)-2-(ethoxy(phenyl)methylene)pentanenitrile 126b

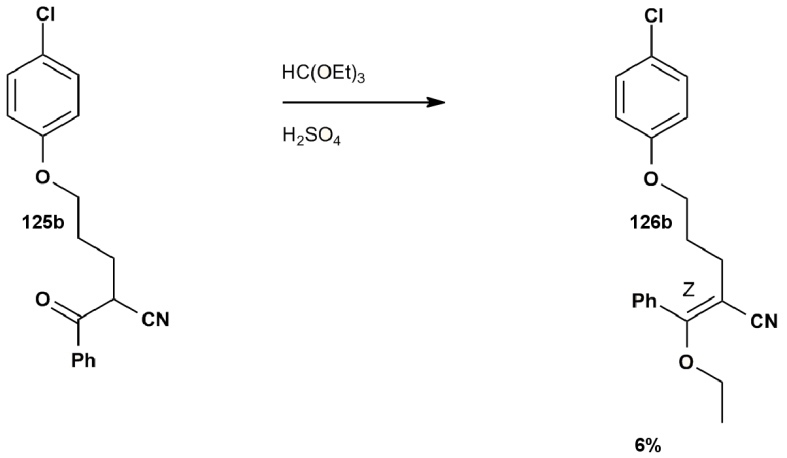

Enol ether formation of our flexible series of compounds was initially tested on the α-cyano ketone compound **125b**. Many examples for forming enol ether compounds from their corresponding keto-analogues can be found in the literature[118], [121], [122], [123], with the majority of these using the methylating agent diazomethane. However, given the explosive nature of this reagent[124], we hoped to avoid using diazomethane as the synthesis had to be suitable for potential application to large-scale preparation of compounds for biological testing. We therefore decided to use alternative methodology which, with the aid of a Dean Stark apparatus, uses triethylorthoformate and an acid catalyst to ensure transformation to the desired product. This proved effective in the control study in which the desired enol ether **129** was obtained as a mixture of the *E* and *Z* isomers in an excellent yield of 92%. To this end, the starting material **125b** was dissolved in triethylorthoformate and the reaction flask connected to a Dean Stark apparatus. After adding a few drops of sulfuric acid, the reaction mixture was heated to

100°C and monitored with the aid of TLC. Although the appearance of a higher running spot indicated the formation of the desired product **126b**, the presence of staring material, even after 36 hr, was also observed. In fact, over longer periods of 108 to 324 hr, it appeared as if more starting material was present, suggesting that an alternative product with an R_f value identical to that of the starting material, was being formed. Indeed, when the experimental conditions of the control study were replicated exactly, the product **126b** was isolated after 108 hr in a very low yield of 1%, with an alternative product being formed as the major product. The NMR spectroscopic data for this compound was peculiar. In the ^{1}H NMR spectrum only two signals were observed: a quartet and, further upfield, a triplet possibly due to the presence of both OCH_2 and CH_3 groups. This data correlated well with the ^{13}C NMR spectrum which contained signals at 69.4ppm and 14.6ppm, indicative of an ethoxy group, however more experimental data would be required to conclusively determine the structure of this compound which, together with its mechanism of formation, remains unclear.

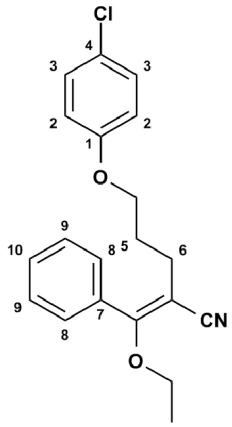

Although the desired product **126b** was isolated in very low yields, we were able to characterise it. Interestingly, in the ^{1}H NMR spectrum, only the *Z* isomer appeared to have formed. The three signals accounting for the phenyl functionality condensed into a singlet integrating for all five protons, thereby significantly simplifying the aromatic region of the spectrum. The loss of the signal owing to the former CHCN group together with the appearance of a quartet at 3.68ppm and a triplet at 1.16ppm due to the addition of the ethoxy group, confirmed that the desired enol ether intermediate **126b** had been obtained. This was supported by the ^{13}C NMR spectroscopic data in which the signal accounting for the former carbonyl group had been replaced with two new peaks at 168.2ppm and 94.9ppm, owing to the newly formed alkene. Furthermore, the IR spectrum no longer contained a band at 1695cm^{-1} for the C=O group, suggesting the reaction had worked.

In order to increase the yield of the desired product, the experimental time was decreased to 36 hr. This increased the yield of the desired enol ether to 6%, with the by-product still accounting for over 80% of the reaction mixture. Alternative acid catalysts and solvent systems were also investigated, however these caused difficulties of their own. For example, when the reaction was conducted using *para*-toluene sulfonic acid (PTSA) in both toluene and xylene, a *para*-substituted compound **130**, due to reaction of PTSA with triethylorthoformate, formed in addition to the product **126b** and unidentified byproduct. We also attempted to use the polymeric ion-exchange resin, Amberlyst 15, but no reaction was observed to occur in this case. Finally, the reaction was performed using triflic acid and nitroethane in ethanol. Although the yield was slightly improved (13%), it was once again considered too low to be of any practical

value.

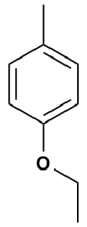

130

At this point, given the difficulties encountered in forming the desired product **126b**, we decided to break away from the experimental conditions outlined in the control study and follow the more well-known methodology for enol ether formation using diazomethane. Although inappropriate for use on an industrial scale, we thought that diazomethane, which requires no acid catalyst or other reagent, would provide us with a comparably cleaner route towards the enol ether with potentially higher yields.

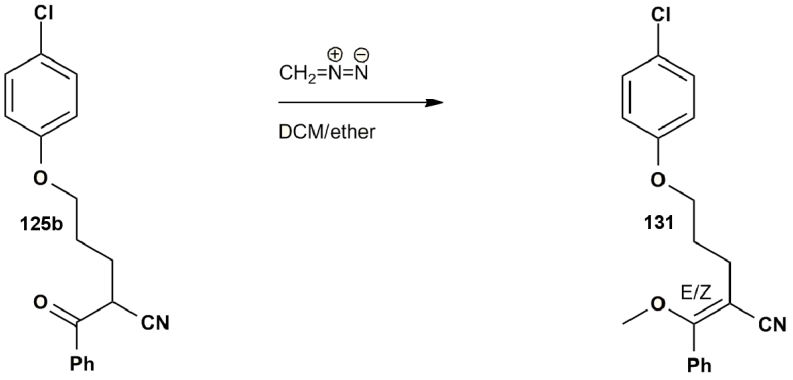

The reaction was conducted by treating diazald with potassium hydroxide in a diethyl ether/carbitol solution at 70-75°C. The hydrolysis of the *N*-methyl nitrosamide led to the formation of diazomethane, which was co-distilled with diethyl ether into the reaction flask containing the starting material **125b** dissolved in dichloromethane. Unlike previous attempts, the reaction went to completion overnight and, after removing the solvent *in vacuo*, the intermediate product **131** was obtained as a yellow oil in quantitative yields. No further purification was done and compound **131** was carried directly into the final step.

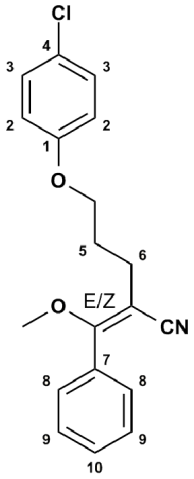

As predicted, the ^{1}H NMR spectrum of the enol ether was very clean with the presence of only minor impurities. As in the case of the control study, both *E* and *Z* isomers had formed, this time in a ratio of 1:0.7. The appearance of two singlets at 3.48ppm and 3.44ppm owing to the methoxy groups indicated successful conversion of the keto group to the enol ether. Similarly, in the ^{13}C NMR spectrum, the different chemical environments of each isomer was evident by the doubling up of peaks. As in the case of product **126b**, the IR spectrum no longer contained a band at $1695cm^{-1}$ for the C=O group.

The 3,4-dichloro analogue **132** was obtained in equally high yields. Apart from the aromatic region, the ^{1}H and ^{13}C NMR spectroscopic data was similar to that reported for product **131**. In addition, similar observations to those described above were made in the IR spectrum.

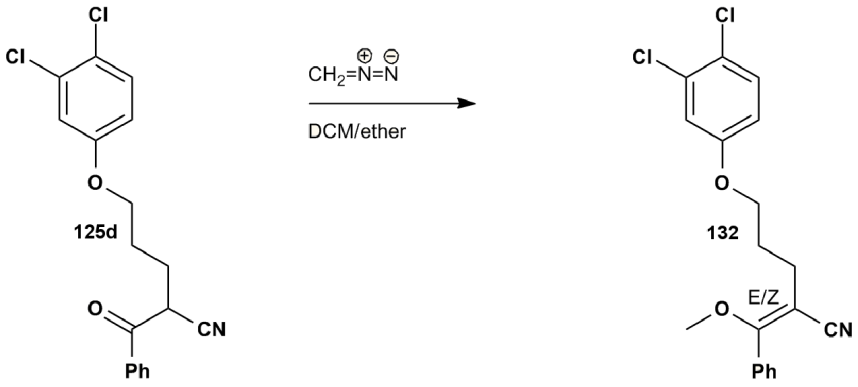

2.7.2.5 Synthesis of 5-(3-(4-chlorophenoxy)propyl)-6-phenylpyrimidine-2,4-diamine 65b

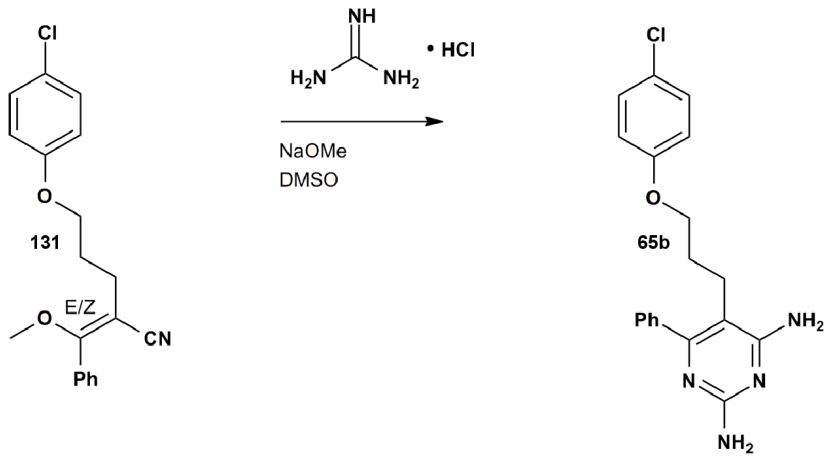

The success of the diazomethane reaction, which resulted in high yields of relatively clean enol ether intermediate **131**, allowed us to continue with the last step of the synthesis. Following the experimental conditions set out by the control study, the starting material **131** was dissolved in DMSO and combined with free guanidine, obtained by neutralisation of its hydrochloride salt with sodium ethoxide. The reaction mixture was heated to 100°C and monitored by TLC. After 108 hr, no starting material could be detected by TLC. The reaction mixture was then cooled and purified by column chromatography to afford the product as a creamy solid in a low yield of 9%. The reaction conditions were not optimised to improve the yield of the reaction at this stage.

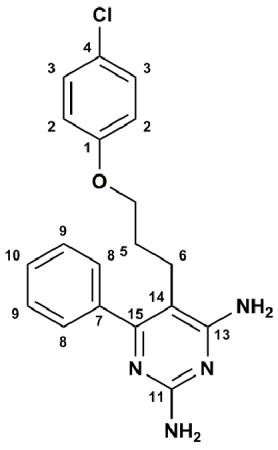

The consumption of both E and Z enol ether isomers rendered the ^{1}H NMR spectrum significantly simpler to that of its intermediate precursor **131**. The appearance of two broad singlets at 6.31ppm and 5.77ppm, assigned to the amine groups, was most striking and was the first indication that the reaction had worked. The ^{13}C NMR spectrum confirmed this with the appearance of three new signals at 163.7ppm, 163.4ppm and 160.9ppm together with a signal at 103.0ppm indicating the formation of the pyrimidine ring. The remainder of the spectrum contained similarities to the starting material **131**, however the disappearance of peaks owing to the former CN, alkene and methoxy groups left us in no doubt that we had in fact formed the desired product **65b**. This was also indicated in the IR spectrum which contained two new bands at 3335cm^{-1} and 3140cm^{-1} due to presence of the N-H groups.

This brought us to the end of our synthesis for the purposes of this MSc project. We had thus successfuly completed the synthesis of the novel DHFR inhibitor **65b** in five steps and an overall yield of 5%. At this stage, due to time constraints, the other analogues **65a**, **65c** and **65d** were not carried through to the final step of the synthesis and will be considered for future work.

2.8 Antimalarial testing results

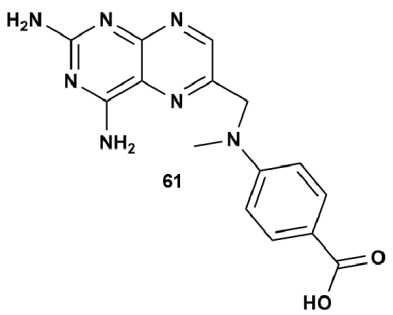

61

IC_{50} (μM): **2.478**

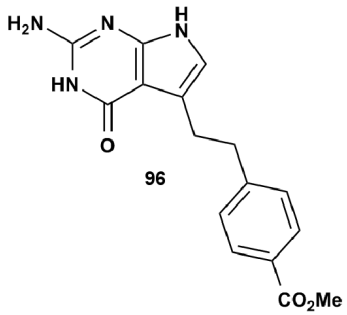

96

Average growth at 40μM: **88%**

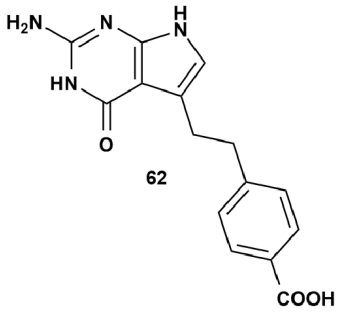

62

Average growth at 40μM: **107%**

Synthesised precursors of methotrexate **61** together with precursors of pemetrexed, **96** and **62**, were tested *in vitro* for biological activity. The compounds were tested in a whole cell *P. falciparum* screen against a cycloguanil resistant/CQ sensitive Gambian FCR-3 strain by Professor Robyn van Zyl in the WITS Department of Pharmacy and Pharmacology [125]. Both the ester and acid pemetrexed precursors were found to be inactive against the malarial parasite, with an average growth of 88% and 107% respectively, even at high concentrations of 40μM. By contrast, the methotrexate precursor **61** was found to exhibit an IC_{50} value of 2.478 μM against the cycloguanil resistant/CQ sensitive Gambian FCR-3 strain. The antimalarial activity exhibited in this case could result from glutamation of compound **61** by the enzymes of the parasite's *de novo* pathway, forming the active methotrexate drug *in situ*. Alternatively, the methotrexate precursor could exhibit general antimalarial activity in its own right against the DHFR enzyme. The assay would therefore have to be repeated such that the parasite is incubated with compound **61** for a longer period of time. Assessment by MS analysis could then determine if methotrexate is formed *in situ* by the parasite.

Chapter 3

Conclusions and Future work

3.1 Project summary

In conclusion, we have successfully synthesised potential antimalarial antifolates using two approaches. In the first instance, we used existing drugs for the treatment of other diseases in the search for new antimalarial compounds. Precursors of the chemotherapeutic drugs methotrexate and pemetrexed were successfully synthesised and some initial biological assessment of the compounds done. The second approach made use of chemical modification of a hit compound, (1-(3-(2,4-dichlorophenoxy)propyl)-6-phenyl-1,6-dihydro-1,3,5-triazine-2,4-diamine hydrochloride). This led to the synthesis of the novel, flexible pyrimidine analogue **65b**, with progress being made towards completing the synthesis of analogues **65a**, **65c** and **65d**.

The methotrexate precursor **61** was synthesised in seven steps (Scheme 3.1) by reported methods[91], [97]. Starting from commercially available guanidine hydrochloride **72** and malononitrile, 2,4,6-triaminopyrimidine **73** was formed under basic conditions. Nitrosation at the C5 position followed by reduction of the nitroso group afforded the tetraaminopyrimidine **75**. The central pteridine moiety was then introduced by condensation with dihydroxyacetone under oxidising conditions. Due to the formation of alternative 6-methyl and 7-substituted products, the 2,4-diamino-6-(hydroxymethyl)pteridine hydrochloride salt **76** was partially purified by conversion to its hydrobromide equivalent **77**. Finally, bromination followed by reaction with 4-(methylamino)benzoic acid furnished the desired methotrexate precursor **61** in seven steps and an overall yield of 2.2%.

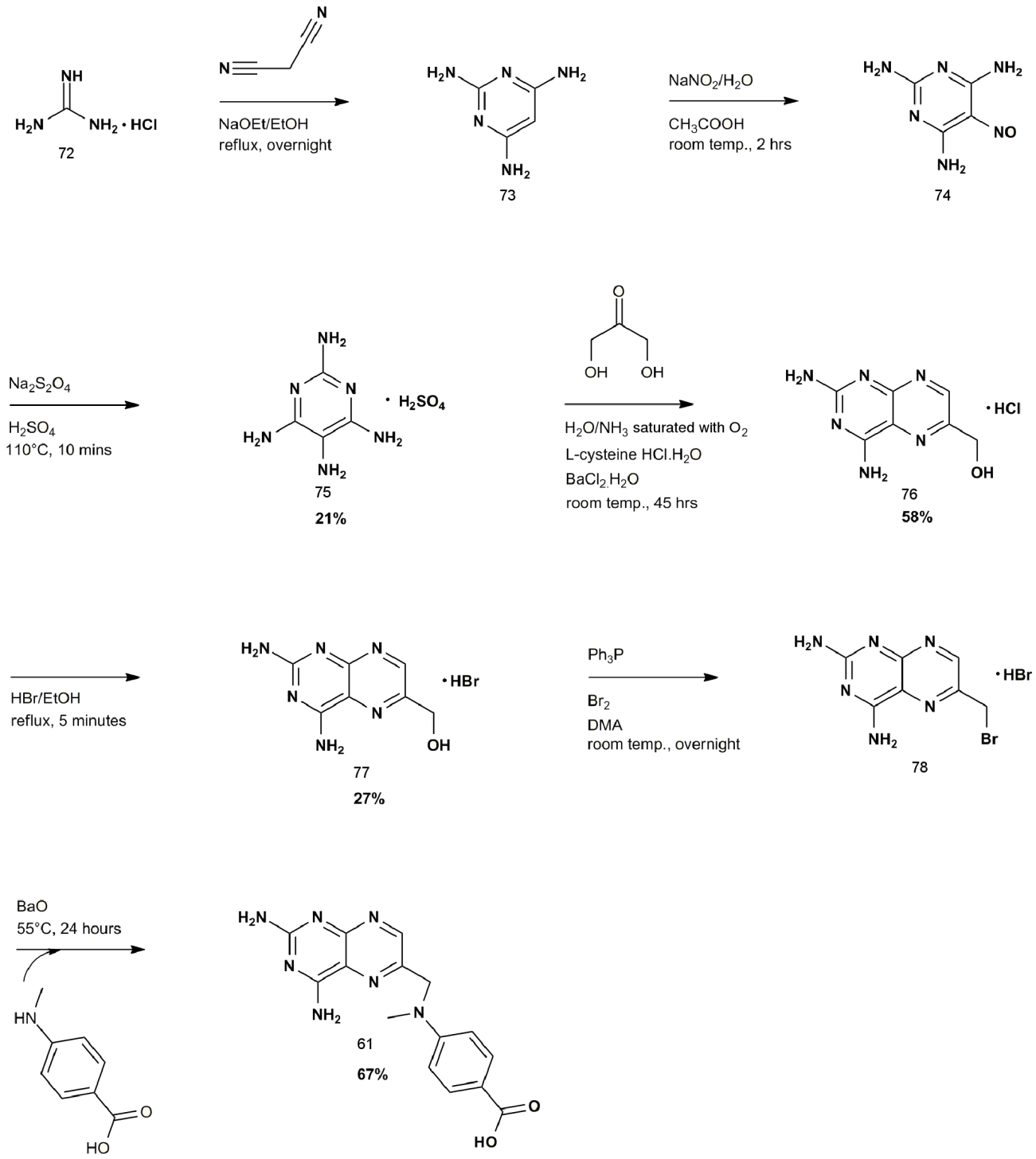

Scheme 3.1

Similarly, the pemetrexed precursor **62** was synthesised in six steps (Scheme 3.2) using previously reported methodology[99]. The synthesis commenced with the coupling of 4-iodobenzoic methyl ester **93** to 3-buten-1-ol using a palladium-catalysed Heck reaction. This resulted in the formation of the aromatic alkene **98** over the desired product **94**, such that the synthesis

had to be extended by an additional two steps. To this end, hydrogenation of the double bond followed by oxidation of the alcohol functionality afforded product **94**. With the aromatic aldehyde in hand, the pemetrexed ester **96** was derived from selective bromination at the α position followed by cyclocondensation with commercially available 2-amino-4-pyrimidone **91**. Ester hydrolysis of compound **96** afforded the final pemetrexed precursor **62** in six steps and an overall yield of 3.2%.

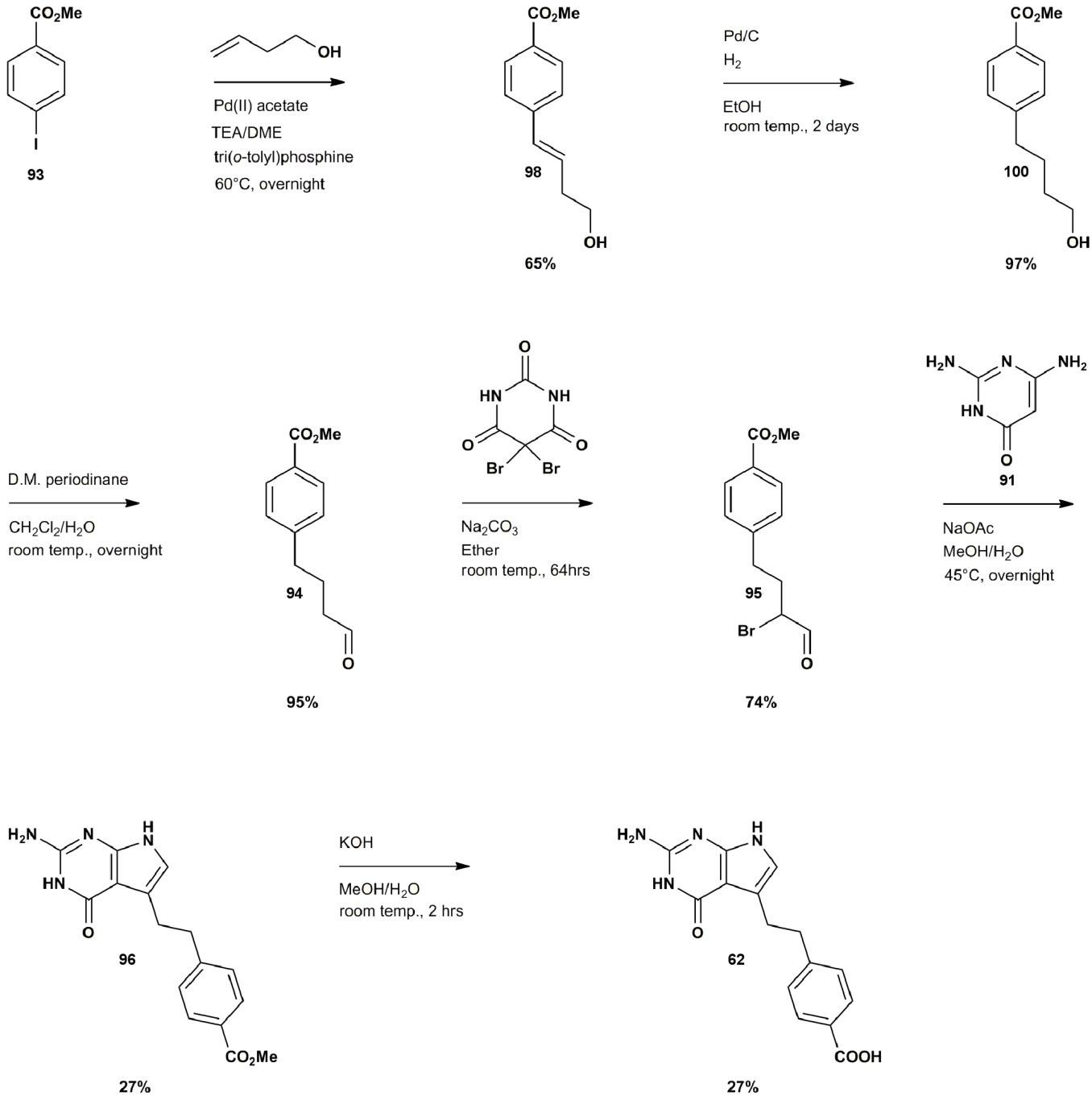

Scheme 3.2

The successful synthesis of the pemetrexed precursor **62** led us to attempt the synthesis of its derivatives, starting with the most structurally simple compound **107a**. As shown in Scheme 3.3, a Michael addition of phenol **109a** to acrylonitrile afforded the phenoxypropanenitrile **115a**. Hydrolysis of the terminal nitrile group to its corresponding carboxylic acid followed by formation of the Weinreb amide yielded product **116a**. The Weinreb amide functionality was subsequently reduced to the free aldehyde, affording product **111a** over four steps in an overall yield of 49%. Unfortunately, this compound proved to be very unstable, decomposing on further reaction. Thus, the synthesis of analogues of the pemetrexed precursor remains incomplete and, due to synthetic difficulties, had to be abandoned.

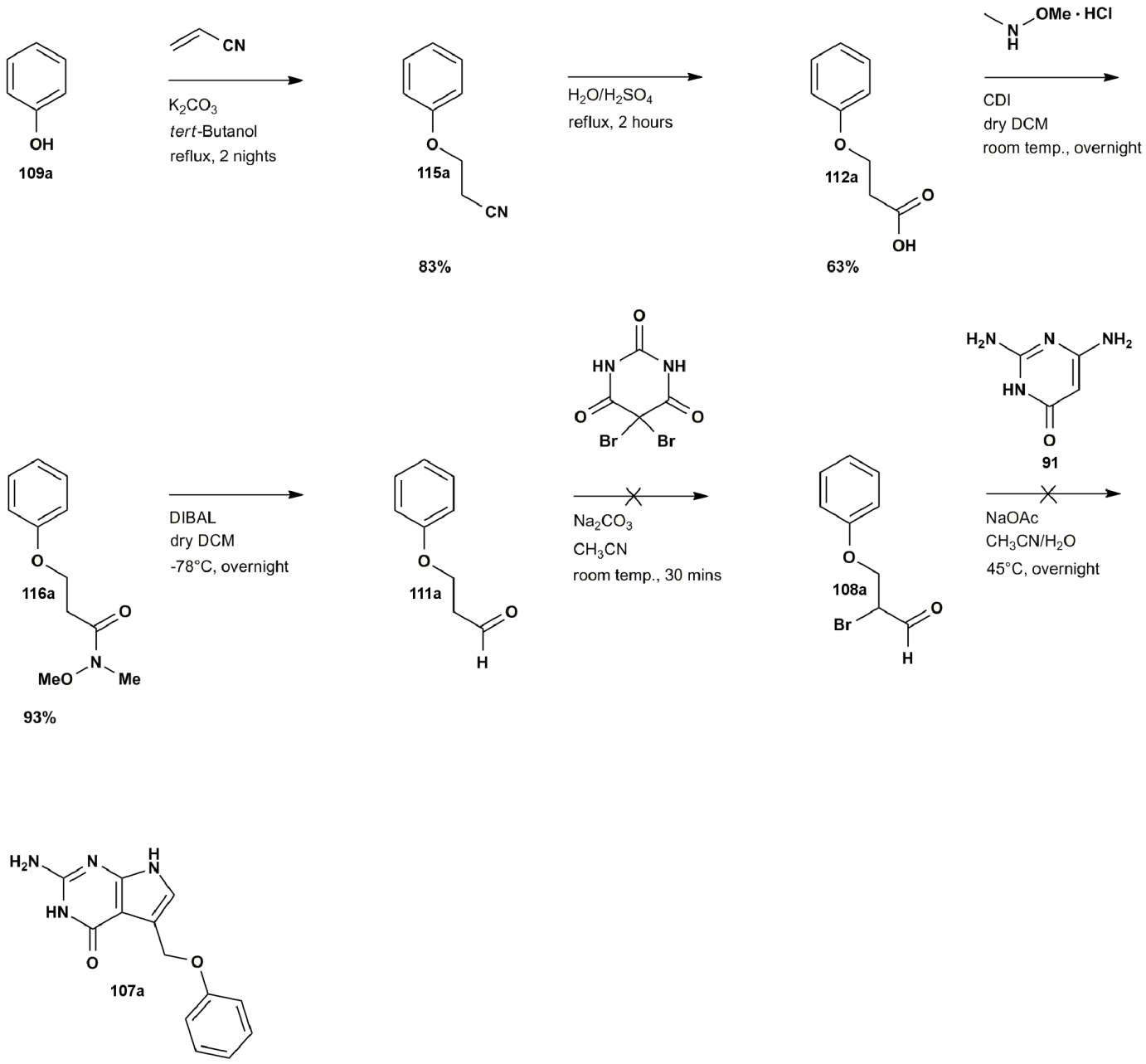

Scheme 3.3

At this point, we changed course so as to pursue the synthesis of other antifolates namely, a series of flexible pyrimidine analogues **65a-d**. Given the novel nature of these compounds, the viability of the last three steps of our proposed synthetic route was initially tested on the synthesis of the more rigid, pyrimethamine analogue **69**. This was achieved over three steps using the methodology set out by Russell and Hitchings[118]. As shown in Scheme 3.4, starting from commericially available 2-phenylacetonitrile **128**, the α-cyano ketone **127** was obtained by nucleophilic addition of the starting material to ethyl benzoate in the presence of a base. Formation of the enol ether intermediate **129** using triethylorthoformate and an acid catalyst, followed by the addition of guanidine, furnished the desired 5,6-diphenylpyrimidine-2,4-diamine

product **69** in three steps and an overall yield of 46%.

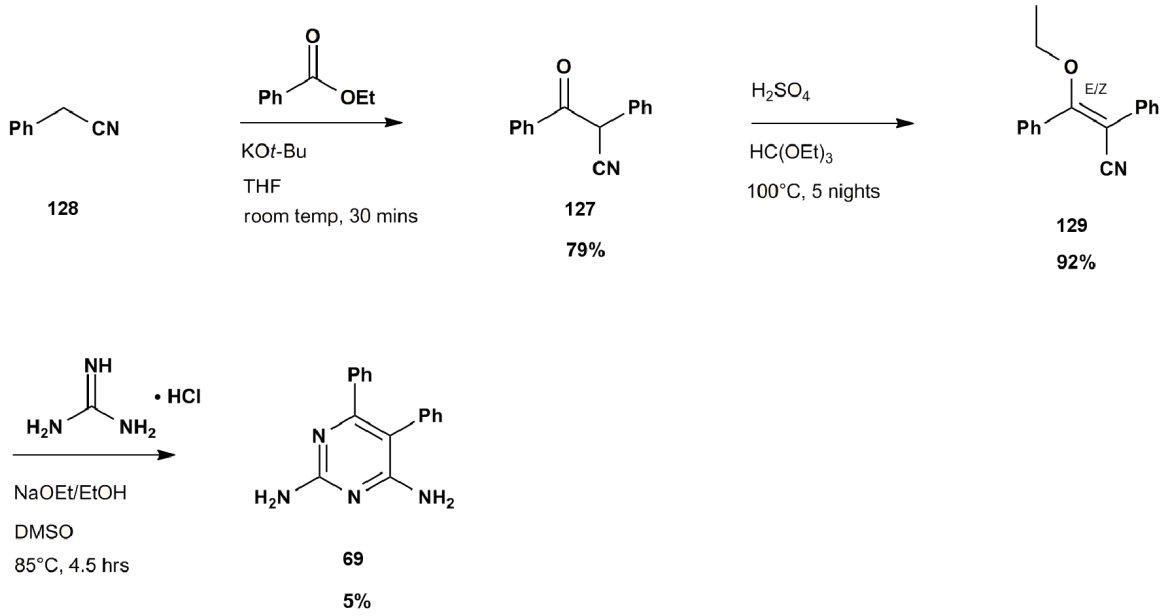

Scheme 3.4

Having successfully completed the control study, we proceeded with the synthesis of the targeted series of novel DHFR inhibitors **65a-d**. Using previously reported methods[62], the bromoether of each analogue **123a-d** was successfully synthesised by alkylation of the appropriately substituted phenol with 1,4-dibromobutane. Functional group interconversion of the bromide to the nitrile group was achieved using potassium cyanide in a water/ethanol solution as described by Starkulla *et al.*[120]. Mimicking the experimental conditions set out in the control study, ethyl benzoate was then added at the α-cyano position under basic conditions. In this way, α-cyano ketone compounds **125a-d** were afforded over three steps in overall yields of 41%, 51%, 9% and 68% respectively. Enol ether formation was tested on compound **125b** using the conditions employed in the control study (using triethylorthoformate and an acid catalyst). Unfortunately, this resulted in the formation of alternative compounds with the desired product **126b** forming in a low yield. The experimental conditions outlined in the control study were therefore discarded in lieu of the more widely used method for enol ether formation using diazomethane. The methylating agent ensured that enol ether intermediates **131** and **132** were obtained in high yields allowing for an attempt to be made at the assembly of our target compound **65**. With compound **131** in hand, the pyrimidine ring was formed upon reaction with guanidine in DMSO, forming analogue **65b** in five steps and an overall yield of 5%. In this way, we had proved the viability of the synthetic route towards the targeted series of flexible, pyrimidine analogues.

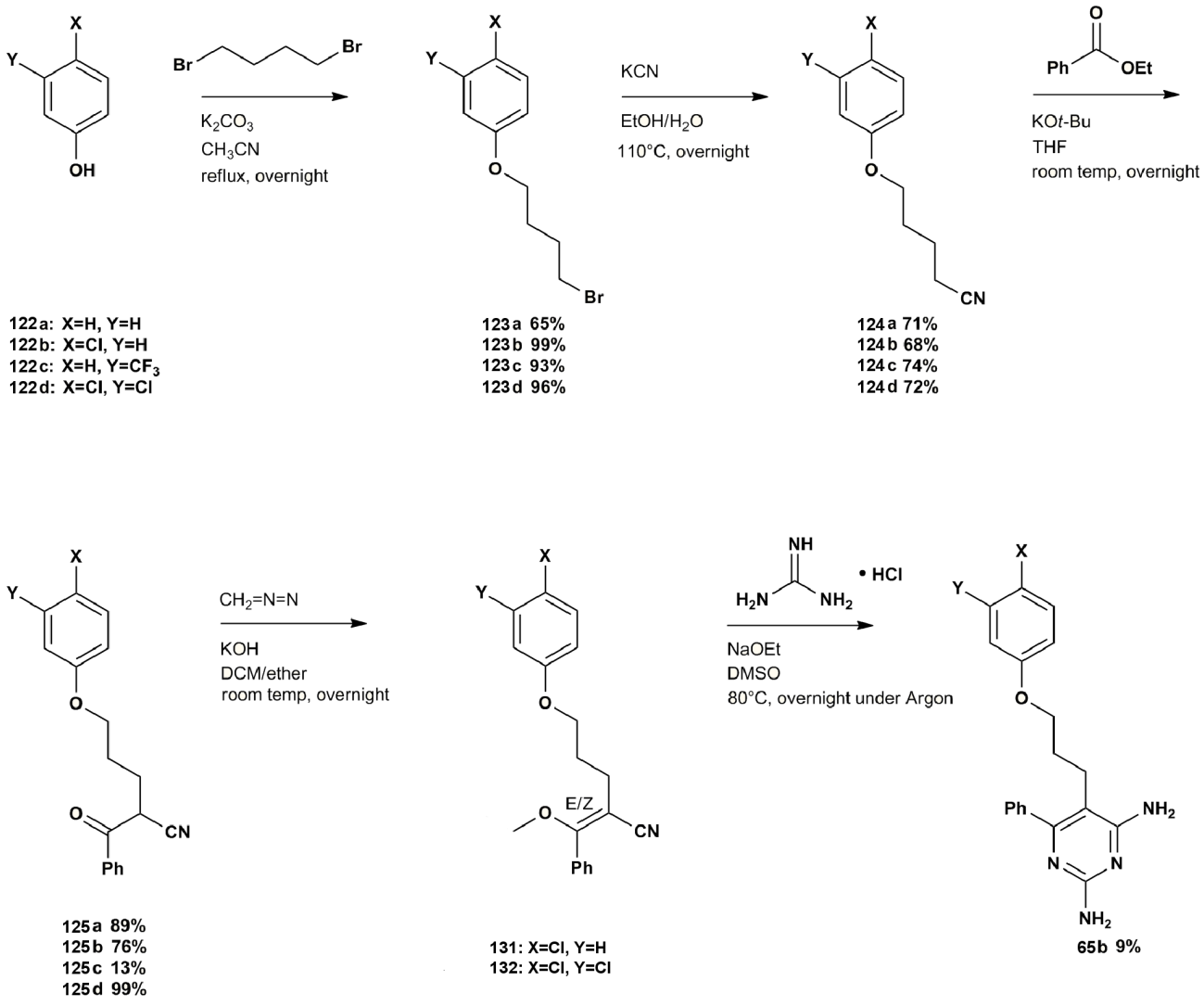

Antimalarial testing was conducted *in vitro* on both the methotrexate precursor **61** and pemetrexed precursors, **96** and **62** in a whole cell *P. falciparum* screen. The methotrexate precursor **61** was found to exhibit an IC_{50} value of 2.478μM against a cycloguanil resistant/CQ sensitive Gambian FCR-3 strain warranting further investigation of the potential conversion of this compound to methotrexate *in situ*. The pemetrexed precursors, **96** and **62** on the other hand, showed no antimalarial activity whatsoever.

3.2 Future work

Further *in vitro* studies would be required to determine the mechanism by which compound **61** exerts its antimalarial activity. That is, whether the methotrexate precursor undergoes glutamation by the enzymes of the parasite's *de novo* pathway to form the active methotrexate

drug *in situ* or whether compound **61** exhibits general antimalarial activity against the DHFR enzyme in its own right still needs to be determined. Incubation of the parasite with **61** for a longer period of time, followed by a HPLC-MS analysis of the assay sample may shed some light on this. The results of these initial biological studies will determine the nature of future studies involving the synthesis of second and third generation analogues.

The synthesis of derivatives of the pemetrexed acid precursor **107a-e** remains to be completed. Failure of the last two steps towards analogue **107a** was probably due to the unstable nature of the aromatic aldehyde **111a** formed in the fourth step. This intermediate could undergo a retro-Michael reaction providing a possible explanation for its instability. This would prevent formation of the desired brominated compound **108a** and hence final product **107a**. The synthetic route towards these compounds would therefore have to be redesigned so as to prevent the retro-Michael conversion from occurring, possibly by lengthening the hydrocarbon chain by one CH_2 group. This will afford longer chain analogues of pemetrexed (Fig. 3.1).

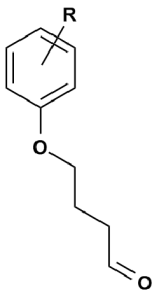

Fig. 3.1

The synthesis of flexible pyrimidine analogues **65a**, **65c** and **65d** also remains to be completed. In this case the synthetic route used to successfully synthesise compound **65b** could be employed. Other structurally similar compounds such as those shown in Fig. 3.2 could also be synthesised in order to test the steric constraints within the DHFR-TS active site. This series of compounds is also based on the original hit compound **60** and thus could also potentially exhibit antimalarial activity. This could potentially lead to the identification of new antifolates with potent antimalarial activity which could be further tested in *in vivo* studies.

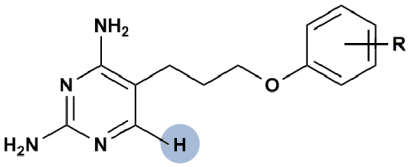

Fig. 3.2

Chapter 4

Experimental Procedures

4.1 General Procedures

4.1.1 Purification of solvents and reagents

Solvents used for reactions were dried over an appropriate drying agent and then distilled under nitrogen gas. Tetrahydrofuran and diethyl ether were distilled over sodium wire using benzophenone as an indicator. Toluene was distilled from sodium metal lumps. Dichloromethane and acetonitrile were distilled from calcium hydride. Reagents were obtained from commercial sources and used without further purification or purified by standard procedures outlined by Perrin *et al.*[126]. The solvents used for chromatographic purposes were distilled prior to use by means of conventional procedures.

4.1.2 Chromatography

Purification of compounds by column chromatography was achieved using Macherey-Nagel silica gel 60 (particle size 0.063mm to 0.200mm) as the adsorbent. Silica gel of particle size 0.040mm and 0.070mm was used for flash chromatography. Mixtures of ethyl acetate and hexane were used as the mobile phase. The reported R_f values are for analytical thin layer chromatography (TLC) performed using aluminium- backed Macherey-Nagel Alugram Sil G/UV_{254} plates pre-coated 0.25mm silica gel 60. Adsorbed compounds were either viewed under UV light or by dipping into potassium permanganate ($KMnO_4$) or 2,4-Dinitrophenyl hydrazine (DNPH) staining solutions.

4.1.3 Spectroscopic and physical data

^{1}H NMR and ^{13}C NMR spectra were recorded on a Bruker AVANCE 300 spectrophotometer at 300.13MHz and 75.47MHz, respectively. Occasionally, a Bruker Ultrashield 500 Plus spectrophotometer was employed for ^{1}H (500.13MHz) and ^{13}C (125.76MHz) spectra. Spectra were recorded in deuterated chloroform ($CDCl_3$), dimethyl sulfoxide (DMSO) or trifluoroacetic acid (CF_3CO_2D). They were reported in parts per million relative to tetramethylsilane at 0.00ppm in ^{1}H NMR spectra and the deuterated signals at 77.23ppm for $CDCl_3$, 39.51ppm for DMSO and, 116.60ppm and 164.2ppm for CF_3CO_2D in ^{13}C NMR spectra. Coupling constants/ J values are given in Hertz (Hz).

Infra-red spectra were recorded on a Bruker Tensor-27 Fourier Transform spectrometer. Measurements were made by loading the sample directly onto a diamond cell. The signals are reported on the wavenumber scale (υ/cm^{-1}).

Melting points were measured using the X-4 Melting Point Apparatus with microscope and are uncorrected.

High resolution mass spectra were recorded at Stellenbosch University in either the El^+ or El^- mode on a Waters Synapt G2 mass spectrometer

4.1.4 Other general procedures

All reactions, unless otherwise stated, were carried out under Ar (g) and reaction vessels were dried prior to use, either in the oven or flame-dried whilst under vacuum. The term *in vacuo* refers to the removal of solvent using a rotary evaporator. Following purification of products, residual solvent was removed using a high vacuum pump (*ca.* 0.1mmHg) at ambient temperature.

4.2 Experimental work for the synthesis of the methotrexate precursor

4.2.1 Synthesis of 2,4,6-triaminopyrimidine 73 [92],[93]

Guanidine hydrochloride (10.3g, 104mmol, 1 eq.) and malononitrile (8.63g, 113mmol, 1.1 eq.) were placed within a 250ml, round-bottomed flask equipped with a teflon stirrer bar and condenser. A sodium ethoxide solution (100ml, 1.45M) was added and the mixture was refluxed

under argon overnight. After cooling, the reaction mixture was filtered and the filter cake washed with EtOH to afford **73** as a creamy, brown solid in a quantitative yield.

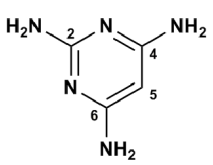

R_f (30% MeOH/EtOAc) 0.23. *mp*: 249-251°C. **^{1}H NMR** (300MHz, CF_3CO_2D): δH = 8.44 (2H, s, C2-NH_2); 7.20 (4H, br s, C4NH_2 and C6NH_2); 5.54 (1H, s, H5). **^{13}C NMR** (75MHz, $CDCl_3$): δC = 157.2 (C4 and C6); 152.7 (C2); 76.0 (C5). **IR** v_{max} (cm^{-1}): 3423, 3354 (N-H); 1614 (C=C); 1572 (C=N). **HRMS** (ESI): *m/z* 126.0774amu (*M+H*); calc. for $C_4H_8N_5$: 126.0778amu.

4.2.2 Synthesis of 2,4,5,6-tetraaminopyrimidine sulfate 75 [93]

The triaminopyrimidine **73** (15.6g, 125mmol, 1 eq.) was dissolved in glacial acetic acid (64ml) and an aqueous sodium nitrite solution was added (206ml, 1M) dropwise over 30 min resulting in the release of a brown gas. After 2 hr of stirring, a pink solid formed which was subsequently filtered off and washed with water. The partially air-dried 2,4,6-triamino-5-nitrosopyrimidine **74** (1.99g, 11.7mmol, 1 eq.) was then suspended in water (5ml) and, while stirring, sodium dithionite (2.03g, 11.7mmol, 2.1 eq.) was added portion-wise. Aqueous sulfuric acid (6ml, 0.5M) was then added dropwise forming a yellow suspension which was heated to 110°C. After 10 min, the reaction mixture became colourless and was cooled overnight. A yellow solid crashed out of solution on cooling and was filtered off and washed with ice-cold water. The crude product was recrystallised from methanol to afford **75** as a beige powder (0.58g, 21%).

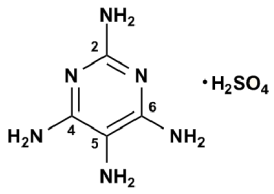

R_f (30% MeOH/EtOAc) 0.05. *mp*: >300°C. **IR** v_{max} (cm^{-1}): 3122 (N-H); 1642 (C=N); 1550 (C=C).

4.2.3 Synthesis of 2,4-diamino-6-(hydroxymethyl)pteridine hydrobromide 77 [97]

Tetraaminopyrimidine sulfate **75** (5.06g, 21.4mmol, 1 eq.) was added to a stirred solution of barium chloride dihydrate (4.85g, 19.9mmol, 1 eq.) in water (100ml) at 90°C. After 15 min, the reaction mixture was cooled and the resulting barium sulphate salt, filtered off. The filtrate was collected and placed within a 250ml, three-necked, round-bottomed flask together with L-cysteine hydrochloride monohydrate (3.80g, 21.2mmol, 1 eq.), ammonium chloride (54.8g, 935mmol), an ammonia solution (25% v/v, 3ml) and water (45ml). The reaction mixture was cooled to 5°C while stirring and saturated with oxygen *via* a glass tube inlet. Dihydroxyacetone (2.84g, 31.5mmol, 1.5 eq.) was then added in one portion. After 20 min, the cooling bath

was removed and the solution left to stir at room temperature for 45 hr. A steady stream of oxygen gas was bubbled through the reaction mixture over this period. The solution was then cooled overnight and the yellow precipitate that formed was filtered off and washed with water. The crude product was recrystallised from ethanol and water to afford the hydrochloride salt **76** in a 6.7:1 ratio as a yellow solid (2.84g, 58%). The mixture (4.72g, 20.6mmol, 1 eq.) was combined with ethanol (200ml) in a 500ml round-bottomed flask equipped with a stirrer bar and condenser. The reaction mixture was heated to 70-75°C and, while stirring, a hydrobromic acid solution (7ml, 48%) in ethanol (120ml) was added. The mixture was then refluxed for 5 min until all the solid had dissolved at which point, it was cooled and refrigerated overnight. The reaction mixture was filtered and the filter cake washed with ethanol to afford **77** as a yellow powder (1.52g, 27%).

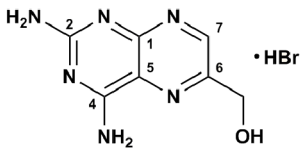

^{1}H NMR (500MHz, CF_3CO_2D): δH = 9.29 (1H, s, H7); 5.95 (2H, s, 6-CH_2OH). **^{13}C NMR** (75MHz, $CDCl_3$): δC = 158.8 (Ar-C); 157.6 (Ar-C); 152.9 (C7); 151.6 (Ar-C); 147.5 (Ar-C). 68.7 (CH_2).

4.2.4 Synthesis 4-(((2,4-diamino-6-pteridinyl)methyl)methylamino)benzoic acid 61 [127]

Bromine (4.99g, 31.2mmol, 4.0 eq.) was added dropwise to a stirred solution of triphenylphosphine (8.13g, 31.0mmol, 0.3 eq.) and dry DMA (40ml) at 0-5°C. Solid **77** (2.38g, 10.4mmol, 1 eq.) was then added in one portion and the reaction mixture was left to stir at room temperature overnight under an argon atmosphere. 4-(methylamino)benzoic acid (2.30g, 15.2mmol, 1 eq.) and barium oxide (1.62g, 10.6mmol, 1 eq.) were then added to the reaction mixture, which was stirred at 55°C for 24 hr. The reaction mixture was cooled and the yellow solid that formed was filtered off. The crude product was recrystallised from methanol/water to afford **61** as a dark yellow powder (2.85g, 67%).

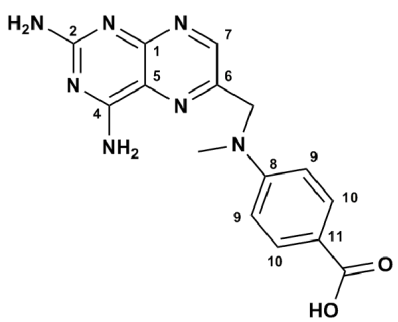

R_f (30% MeoH/EtOAc) 0.21. *mp*: 255°C. **^{1}H NMR** (500MHz, CF_3CO_2D): δH = 8.96 (1H, s, C7-H); 8.34 (2H, d, J = 7.8Hz, 2 x H10); 7.99 (2H, d, J = 7.8Hz, 2 x H9); 5.42 (2H, s, 6-CH_2N); 3.69 (3H, s, NCH_3). **^{13}C NMR** (75MHz, $CDCl_3$): δC = 172.3 (C=O); 158.2 (Ar-C); 153.4 (C7); 148.1 (Ar-C); 146.7 (Ar-C); 146.2 (Ar-C); 135.5 (2 x C10) 135.4 (Ar-C); 134.3 (C8); 124.6 (C11) 124.0 (2 x C9); 62.6 (CH_2); 49.2 (CH_3). **IR** v_{max} (cm^{-1}): 3328 (O-H); 3187 (N-H); 1652 (C=O); 1596 (C=C).

HRMS (ESI): *m/z* 326.1371amu (*M+H*); calc. for $C_{15}H_{16}N_7O_2$: 326.1379amu.

4.3 Experimental work for the synthesis of the pemetrexed precursor

4.3.1 Synthesis of *trans*-methyl 4-(4-hydroxybut-1-en-1-yl)benzoate 98 [106]

Palladium(II) acetate (428mg, 1.91mmol, 0.1 eq.) was added to a two-necked, round-bottomed flask fitted with a condenser and a dropping funnel to which starting material **93** (5.00g, 19.1mmol, 1 eq.) and tri(*o*-tolyl)phosphine (1.16g, 3.82mmol, 0.2 eq.), dissolved in a dimethoxymethane/tri solution (28ml, 2.6ml), were added. The reaction vessel was degassed and purged with argon. Argon was then bubbled into the dropping funnel by means of a Pasteur pipette and the solution was quickly added to the reaction flask. The red/brown mixture was heated to 60°C and the reaction mixture left to react for 18 hr under an argon atmosphere. The reaction mixture was then cooled to room temperature and the solvent evaporated *in vacuo*. The residue was partitioned between DCM (250ml) and water (250ml) and the aqueous layer re-extracted with additional DCM (2 x 250ml). The combined organic layers were dried ($MgSO_4$), filtered and the volatiles evaporated *in vacuo*. The residue was purified by column chromatography using 5-10% EtOAc/hexane to yield the *trans* isomer of **98** exclusively as a yellow solid (2.33g, 65%).

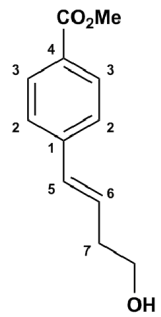

R_f (30% EtOAc/hexane) 0.25. *mp*: 50-51°C. **^{1}H NMR** (300MHz, $CDCl_3$): δH = 7.97 (2H, d, J = 8.4Hz, 2 x H3); 7.41 (2H, d, J = 8.4Hz, 2 x H2); 6.53 (1H, d, J = 16.2Hz, H5); 6.36 (1H, dt, J = 6.9Hz and 15.9Hz, H6); 3.91 (3H, s, OCH_3); 3.79 (2H, t, J = 6.3Hz, CH_2OH); 2.48-2.55 (2H, m, 2 x H7). **^{13}C NMR** (75MHz, $CDCl_3$): δC = 167.0 (C=O); 141.8 (C1); 131.8 (C5); 129.9 (2 x C3); 129.5 (C6); 128.7 (C4); 126.0 (2 x C2); 61.9 (CH_2OH); 52.1 (OCH_3); 36.5 (C7). **IR** υ_{max} (cm^{-1}): 3325 (-OH); 2956 (=C-H); 1719 (C=O); 1606 (C=C). **HRMS** (ESI): *m/z* 207.1027amu (*M+H*); calc. for $C_{12}H_{15}O_3$: 207.0978amu.

4.3.2 Synthesis of methyl 4-(4-hydroxybutyl)benzoate 100 [108]

The starting material **98** (500mg, 2.48mmol, 1 eq.) was dissolved in ethanol (175ml) in a two-necked round bottomed flask to which palladium on carbon (55mg, 0.1 eq.) was added. The reaction vessed was then degassed and purged with hydrogen gas and the reaction left to stir for 36 hr. Reaction progress was monitored using TLC. Once complete, the reaction mixture

was filtered through celite and the solvent evaporated *in vacuo*. The residue was purified by column chromatography using 10% EtOAc/hexane to yield **100** as a yellow oil (0.49g, 97%).

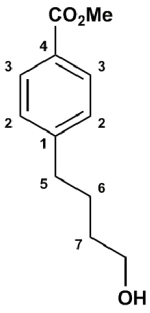

R_f (30% EtOAc/hexane) 0.31. **^{1}H NMR** (300MHz, $CDCl_3$): δH = 7.95 (2H, d, J = 8.4Hz, 2 x H3); 7.25 (2H, d, J = 8.4Hz, 2 x H2); 3.90 (3H, s, OCH_3); 3.66 (2H, t, J = 6.3Hz, CH_2OH); 2.70 (2H, t, J = 7.8Hz, 2 x H5); 1.50-1.80 (4H, m, 2 x H6 and 2 x H7). **^{13}C NMR** (75MHz, $CDCl_3$): δC = 167.2 (CO$_2$Me); 148.0 (C1); 129.7 (2 x C3); 128.5 (2 x C2); 127.8 (C4); 62.6 (CH$_2$OH); 52.0 (OCH$_3$); 35.7 (C5); 32.2 (C7); 27.3 (C6). **IR** v_{max} (cm^{-1}): 2936 (=C-H); 1717 (C=O); 1609 (C=C). **HRMS** (ESI): m/z 209.1170amu (M+H); calc. for $C_{12}H_{17}O_3$: 209.1178amu.

4.3.3 Synthesis of methyl 4-(4-oxobutyl)benzoate 94 [108]

The starting material **100** (1.66g, 7.97mmol, 1 eq.) was dissolved in wet dichloromethane (130ml), prepared by mixing water and dichloromethane in a separating funnel and collecting the organic phase. The reaction flask was placed within an ice-bath and the solution cooled down to 0°C. Dess-Martin periodinane (2.61g, 8.76mmol, 1.1 eq.) was added portion-wise while stirring, over an hour. The ice-bath was then removed and the solution left to react overnight under an argon atmosphere. During this time, a white suspension formed. The reaction mixture was quenched with a saturated $Na_2S_2O_3$/$NaHCO_3$ solution (100ml, 1:1) and the aqueous layer re-extracted with additional DCM (3 x 150ml). The combined organic layers were dried ($MgSO_4$), filtered and the volatiles evaporated *in vacuo*. The residue was purified by column chromatography using 10% EtOAc/hexane to yield **94** as a yellow oil (1.57 g, 95%).

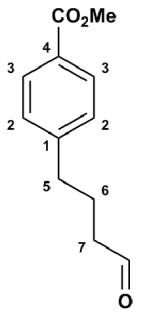

R_f (30% EtOAc/hexane) 0.46. **^{1}H NMR** (300MHz, $CDCl_3$): δH = 9.77 (1H, s, HC=O); 7.97 (2H, d, J = 8.1Hz, 2 x H3); 7.25 (2H, d, J = 8.1Hz, 2 x H2); 3.91 (3H, s, OCH_3); 2.71 (2H, t, J = 7.8Hz, 2 x H7); 2.47 (2H, t, J = 7.2Hz, 2 x H5); 1.93-2.03 (2H, m, 2 x H6). **^{13}C NMR** (75MHz, $CDCl_3$): δC = 201.9 (C=O); 167.1 (CO$_2$Me); 146.7 (C1); 129.9 (2 x C3); 128.5 (2 x C2); 126.9 (C4); 52.0 (OCH$_3$); 43.0 (C7); 35.0 (C5); 23.2 (C6). **IR** v_{max} (cm^{-1}): 2951 (=C-H); 1715 (C=O); 1610 (C=C). **HRMS** (ESI): m/z 207.1021amu (M+H); calc. for $C_{12}H_{15}O_3$: 207.0978amu.

4.3.4 Synthesis of methyl 4-(3-bromo-4-oxobutyl)benzoate 95 [99]

The aldehyde **111** (471mg, 2.28mmol, 1 eq.) was dissolved in dry diethyl ether (10ml). Sodium carbonate (315mg, 2.97mmol, 1.3 eq.) and 5,5-dibromobarbituric acid (326mg, 1.14mmol, 0.6 eq.) were added portionwise forming a white suspension which was left to stir for 64 hr at room temperature under an argon atmosphere. The barbituric acid byproduct that formed was filtered off and the reaction mixture quenched with a saturated sodium thiosulfate solution (10ml). The organic product was extracted with additional diethyl ether (3 x 15ml) and washed with an aqueous sodium carbonate (10ml) and brine solution (10ml) in succession. The combined organic extracts were dried ($MgSO_4$), filtered and the volatiles evaporated *in vacuo*. The residue was purified by column chromatography using 10% EtOAc/hexane to yield **95** as an orange oil (480mg, 74%).

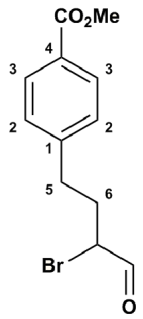

R_f (30% EtOAc/hexane) 0.63. **^{1}H NMR** (300MHz, $CDCl_3$): δH = 9.47 (1H, s, *H*C=O); 7.98 (2H, d, J = 8.1Hz, 2 x H3); 7.28 (2H, d, J = 7.8Hz, 2 x H2); 4.18 (1H, t, J = 6.0Hz, C*H*Br); 3.91 (3H, s, OCH_3); 2.66-3.07 (2H, m, 2 x H5); 2.16-2.44 (2H, m, 2 x H6). **^{13}C NMR** (75MHz, $CDCl_3$): δC = 192.4 (*H*C=O); 167.0 (*C*O_2Me); 145.1 (C1); 130.0 (2 x C3); 128.6 (2 x C2); 127.7 (C4); 54.3 (*C*HBr); 52.1 (O*C*H_3); 32.8 (C6); 32.7 (C5). **IR** υ_{max} (cm^{-1}): 2951 (=C-H); 1715 (C=O); 1610 (C=C). **HRMS** (ESI): m/z 285.0126amu (M+H); calc. for $C_{12}H_{14}BrO_3$: 285.0078amu.

4.3.5 Synthesis of the methyl 4-(2-(2-amino-4-oxo-4,7-dihydro-3H-pyrrolo(2,3-d)pyrimidin-5-yl)ethyl)benzoate 96 [99]

Sodium acetate (719mg, 8.76mmol, 3.0 eq.) and 2,4-diamino-6-hydroxypyrimidine (490mg, 3.89mmol, 1.3 eq.) were combined in a MeOH/H_2O solution (5ml, 1:4) under an argon atmosphere. The reaction mixture was heated up to 45°C and the brominated aldehyde **95** (833mg, 2.92mmol, 1 eq.) added dropwise over 20 min. After 18 hr, a solid blue precipitate was filtered off and recrystallised from methanol and water to afford **96** as a blue solid (249mg, 27%).

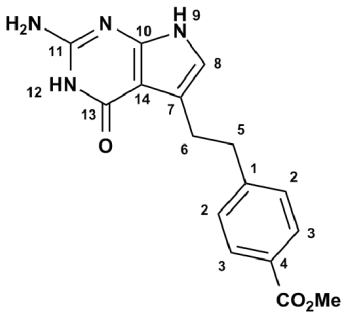

R_f (95% EtOAc/methanol) 0.84. *mp*: >250°C. **^{1}H NMR** (300MHz, DMSO): δH = 10.63 (1H, s, N*H*9); 10.20 (1H, s, N*H*12); 7.86 (2H, d, J = 7.8Hz, 2 x H3); 7.34 (2H, d, J = 8.1Hz, 2 x H2); 6.31 (1H, s, C*H*8); 6.04 (2H, s, NH_2); 3.82 (3H, s, OCH_3); 2.97-3.02 (2H, m, H5 x 2); 2.83-2.88 (2H, m, H6 x 2). **^{13}C NMR** (75MHz, DMSO): δC = 166.2 (*C*O_2Me); 159.3 (13C=O); 152.2 (C11); 151.3 (C10); 148.3 (C1); 129.1 (2 x C3); 128.7 (2 x C2); 127.0 (C4); 117.5

(C7); 113.4 (C8); 98.7 (C14); 51.9 (OCH_3); 36.2 (C5); 27.8 (C6). **IR** v_{max} (cm^{-1}): 3204 (NH); 1713 (CN); 1628 (C=O). **HRMS** (ESI): *m/z* 313.1299amu (*M+H*); calc. for $C_{16}H_{17}N_4O_3$: 313.1278amu.

4.3.6 Synthesis of the 4-(2-(2-amino-4-oxo-4,7-dihydro-3H-pyrrolo(2,3-d)pyrimidin-5-yl)ethyl)benzoic acid 62 [99]

The ester **96** (100mg, 0.32mmol, 1 eq.) was dissolved in a $MeOH/H_2O$ solution (4ml, 3:1) to which potassium hydroxide (18mg, 0.32mmol, 1 eq.) was added. The solution turned from blue to gray and after 2 hr, was transferred to a separating funnel and diluted with ethyl acetate (10ml) and water (10ml). After thorough mixing, the organic phase was separated and the aqueous phase further extracted with ethyl acetate (2 x 10ml). The aqueous phase was acidified to pH 1 with an aqueous HCl solution (10M) forming a blue precipitate which was filtered off to afford the final product **62** as a blue solid (25.5mg, 27%).

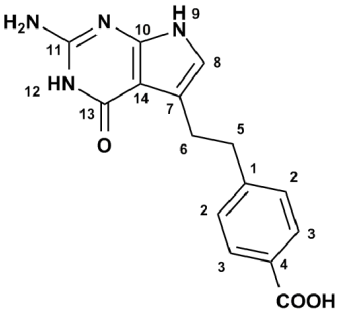

R_f (95% EtOAc/methanol) 0.59. *mp*: >250°C. **^{1}H NMR** (300MHz, DMSO): δH = 10.85 (1H, s, N*H*9); 10.60 (1H, s, N*H*12); 7.84 (2H, d, *J* = 8.1Hz, 2 x H3); 7.32 (2H, d, *J* = 8.1Hz, 2 x H2); 6.38 (1H, s, C*H*8); 3.52 (1H, br s, OH); 2.96-3.01 (2H, m, H5 x 2); 2.84-2.88 (2H, m, H6 x 2). **^{13}C NMR** (75MHz, DMSO): δC = 167.3 (CO_2H); 158.7 (13C=O); 151.7 (C10); 147.6 (C1); 139.1 (C11); 129.3 (2 x C3); 128.5 (2 x C2); 128.2 (C4); 118.0 (C7); 114.0 (C8); 98.8 (C14); 36.1 (C5); 27.6 (C6). **IR** v_{max} (cm^{-1}): 3130 (NH); 1669 (C=O). **HRMS** (ESI): *m/z* 299.1144amu (*M+H*); calc. for $C_{15}H_{16}N_4O_3$: 299.1178amu.

4.4 Experimental work towards analogues of the pemetrexed precursor

4.4.1 Synthesis of 3-phenoxypropanenitrile 115a [115]

Phenol **109a** (2.00g, 21.3mmol, 1 eq.), *tert*-butanol (0.2ml, 2.13mmol, 0.1 eq.), potassium carbonate (294mg, 2.13mmol, 0.1 eq.) and acrylonitrile (14ml, 213mmol, 10 eq.) were combined and the solution refluxed under an argon atmosphere. Reaction progress was monitored by TLC. When complete (36 hr), the reaction mixture was cooled to room temperature and the pH adjusted to 6-7 with aqueous phosphoric acid. The excess acrylonitrile was evaporated *in*

vacuo and the residue partitioned between ethyl acetate (30ml) and water (30ml). The aqueous layer was re-extracted with additional ethyl acetate (2 x 20ml) and the combined organic layers dried ($MgSO_4$), filtered and the volatiles evaporated *in vacuo*. The residue was purified by column chromatography using 30% EtOAc/hexane to yield **115a** as a fluffy, white solid (2.60g, 83%).

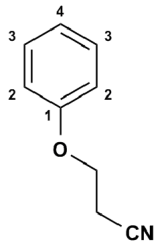

R_f (20% EtOAc/hexane) 0.40. *mp*: 59°C. **^{1}H NMR** (300MHz, $CDCl_3$): δH = 7.30 (2H, dd, J = 7.8Hz and 7.4Hz, 2 x H3); triplet J = 7.00 (1H, t, J = 7.4Hz, H4); 6.90 (2H, d, J = 7.8Hz, 2 x H2); 4.18 (2H, t, J = 6.5Hz, OCH_2); 2.81 (2H, t, J = 6.5Hz, CH_2CN). **^{13}C NMR** (75MHz, $CDCl_3$): δC = 157.7 (C1); 129.7 (2 x C3); 121.8 (C4); 117.2 (*C*N); 114.7 (2 x C2); 62.6 (O*C*H_2); 18.6 (*C*H_2CN). **IR** υ_{max} (cm^{-1}): 2934 (=C-H); 2251 (C-N); 1598, 1587 (C=C). **HRMS** (ESI): *m/z* 148.0768amu (*M+H*); calc. for $C_9H_{10}NO$: 148.0778amu.

4.4.2 Synthesis of 3-phenoxypropanoic acid 112a [128]

The starting material **115a** (2.00g, 13.6mmol, 1 eq.) was added to a stirred H_2SO_4/H_2O solution (30ml, 1:1) and heated to reflux. On heating, the reaction mixture turned from yellow to clear and after 2 hr, was cooled to room temperature. After refrigerating overnight, a pale yellow solid crashed out of solution and was filtered off and washed with hexane. The filtered solid was redissolved in ethyl acetate (40ml) and the pH adjusted to 10 with potassium hydroxide. Water (30ml) was added and traces of unreacted starting material **115a** extracted with ethyl acetate (2 x 30ml). The combined aqueous layers were acidified with H_2SO_4 to pH 1 and re-extracted with additional ethyl acetate (3 x 25ml). The combined organic layers were dried ($MgSO_4$), filtered and the volatiles evaporated *in vacuo* to afford **112a** as a white, needle-like, crystalline solid (1.42g, 63%).

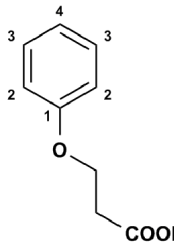

R_f (100% EtOAc) 0.89. *mp*: 93°C. **^{1}H NMR** (300MHz, $CDCl_3$): δH = 9.71 (1H, br s, O*H*); 7.28 (2H, dd, J = 8.8Hz, J = 7.4Hz, 2 x H3); 6.97 (1H, t, J = 7.4Hz, H4); 6.91 (2H, d, J = 8.8Hz, 2 x H2); 4.25 (2H, t, J = 6.3Hz, OCH_2); 2.85 (2H, t, J = 6.3Hz, CH_2COOH). **^{13}C NMR** (75MHz, $CDCl_3$): δC = 177.4 (C=O); 158.4 (C1); 129.5 (2 x C3); 121.2 (C4); 114.7 (2 x C2); 63.0 (O*C*H_2); 34.5 (*C*H_2COOH). **IR** υ_{max} (cm^{-1}): 2891 (=C-H); 2639 (OH); 1701 (C=O); 1601, 1586 (C=C). **HRMS** (ESI): *m/z* 165.0544amu (*M-H*); calc. for $C_9H_9O_3$: 167.0678amu.

4.4.3 Synthesis of *N*-methoxy-*N*-methyl-3-phenoxypropanamide 116a

The starting material **112a** (2.49g, 15.0mmol, 1 eq.) was dissolved in dry dichloromethane (75ml) to which 1,1-carbonyl diimidazole (2.91g, 17.9mmol, 1.2 eq.) was added. After 20 min, *N*,*O*-dimethylhydroxylamine hydrochloride (1.75g, 17.9mmol, 1.2 eq.) was added in one portion and the reaction mixture stirred overnight at room temperature under an argon atmosphere. The reaction mixture was transferred to a separating funnel and washed with both saturated ammonium chloride (40ml) and ammonium hydrogen carbonate (40ml) solutions and the organic product extracted with DCM (3 x 40ml). The extracts were dried over anhydrous $MgSO_4$, and the solvent removed *in vacuo*. The residue was purified by column chromatography (20% EtOAc/hexane) to yield **116a** as a pale, yellow oil (3.13g, 93%).

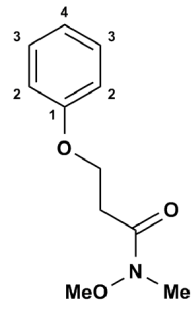

R_f (30% EtOAc/hexane) 0.38. **^{1}H NMR** (300MHz, $CDCl_3$): δH = 7.19 (2H, t, J = 8.6Hz, 2 x H3); 6.83-6.88 (3H, m, 2 x H2, H4); 4.22 (2H, t, J = 6.7Hz, OCH_2); 3.64 (3H, s, OCH_3); 3.14 (3H, s, NCH_3); 2.86 (2H, t, J = 6.7Hz, CH_2CO). **^{13}C NMR** (75MHz, $CDCl_3$): δC = 171.6 (C=O); 158.6 (C1); 129.4 (2 x C3); 120.9 (C4); 114.6 (2 x C2); 63.5 (OCH_2); 61.4 (OCH_3); 31.9 (NCH_3); 29.7 (CH_2CO). **IR** υ_{max} (cm^{-1}): 2936 (=C-H); 1657 (C=O); 1599, 1587 (C=C). **HRMS** (ESI): m/z 210.1132amu ($M+H$); calc. for $C_{11}H_{16}NO_3$: 210.1178amu.

4.4.4 Synthesis of 3-phenoxypropanal 111a [129]

The Weinreb amide **116a** (300mg, 1.43mmol, 1 eq.) was dissolved in dry dichloromethane (21ml) in a two-necked, round-bottomed flask and cooled to -78°C under an Argon atmosphere. Diisobutylaluminium hydride in dichloromethane (1.9ml, 1.0M, 1.86mmol, 1.3 eq.) was added dropwise over 10 min. The reaction mixture was stirred for 3.7 hr before being warmed to 0°C, quenched with a saturated, aqueous $KHSO_4$ solution (20ml) and filtered. The product was extracted from the filtrate with DCM (3 x 30ml), dried over anhydrous Na_2SO_4 and the solvent removed *in vacuo*. The product **111a** was not purified further but recovered quantitatively as a yellow oil (3.13g) in a 1:0.2 ratio of product to starting material.

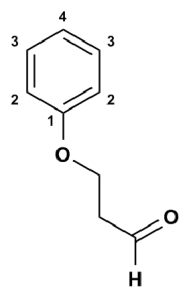

R_f (50% EtOAc/hexane) 0.81. **^{1}H NMR** (300MHz, $CDCl_3$): δH = 9.85 (1H, s, CHO); 7.27 (2H, dd, J = 7.8Hz, J = 7.4Hz, 2 x H3); 7.00 (1H, t, J = 7.4Hz, H4); 6.90 (2H, d, J = 7.8Hz, 2 x H2) 4.30 (2H, t, J = 6.2Hz, OCH_2); 2.89 (2H, td, J = 6.3Hz, 1.5Hz, CH_2CO). **^{13}C NMR** (75MHz, $CDCl_3$): δC = 200.3 (C=O); 158.4 (C1); 129.5 (2 x C3); 121.2 (C4); 114.6 (2 x C2); 61.6 (OCH_2); 43.3 (CH_2CO). **IR** υ_{max} (cm^{-1}): 2935 (=C-H); 1720 (C=O); 1599 (C=C).

4.4.5 Attempted synthesis of 2-amino-5-(phenoxymethyl)-3H-pyrrolo[2,3-d]pyrimidin-4(7H)-one 107a

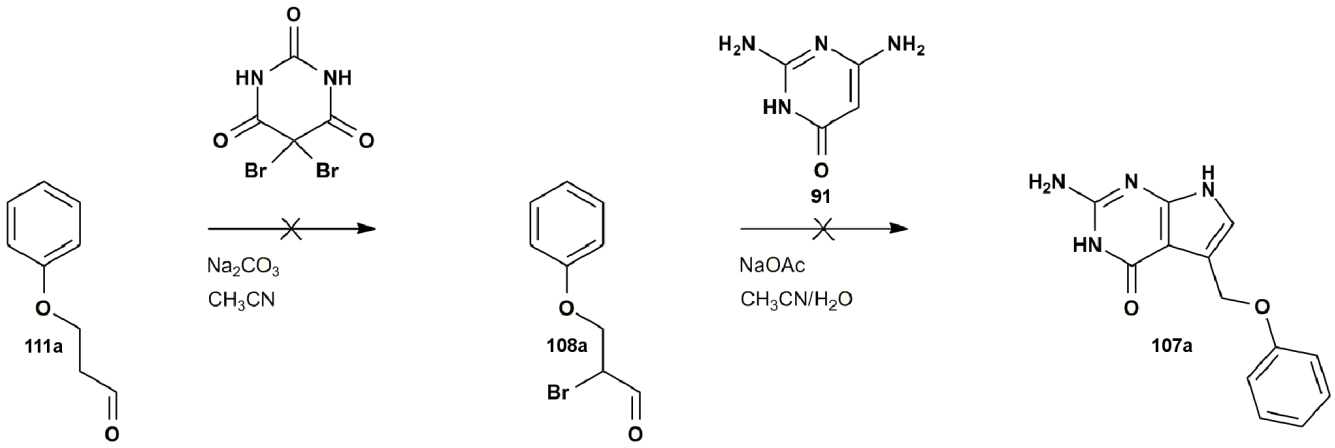

The aldehyde **111a** (839mg, 5.59mmol, 1 eq.) was dissolved in dry acetonitrile (11ml). Sodium carbonate (770mg, 7.26mmol, 1.3 eq.) and 5,5-dibromobarbituric acid (799mg, 2.79mmol, 0.5 eq.) were added portionwise forming a white suspension. The reaction mixture was stirred under an argon atmosphere and reaction progress monitored by TLC (30% EtOAc/hexane). After 30 min, the barbituric acid byproduct that formed was filtered off and 2-bromo-3-phenoxypropanal **108a** carried directly into the next step without isolation. Sodium acetate (513mg, 6.26mmol, 1.1 eq.) and 2,4-diamino-6-hydroxypyrimidine (691mg, 5.48mmol, 1 eq.) in water (11ml) were then added to the reaction mixture which was heated up to 45°C. After 18 hr under an argon atmosphere, a solid pink precipitate (1.40g) was isolated, but this was not the desired product **107a**.

4.5 Experimental work for the synthesis of 5,6-diphenyl pyrimidine-2,4-diamine 69

4.5.1 Synthesis of 3-oxo-2,3-diphenylpropanenitrile 127 [130]

To a mixture of 2-phenylacetonitrile **128** (5.0ml, 42.7mmol, 1 eq.) dissolved in THF (297ml) was added potassium *tert*-butoxide (14.4g, 128mmol, 3 eq.) and ethyl benzoate (24.5ml, 171mmol, 4 eq.), turning the solution from clear to brown. The reaction mixture was stirred under an argon atmosphere and reaction progress monitored by TLC (20% EtOAc/hexane). When complete (30 min), the reaction mixture was quenched with a saturated ammonium chloride solution

(150ml) and the THF evaporated *in vacuo*. The aqueous layer was extracted with ethyl acetate (3 x 100ml) and the combined organic layers dried ($MgSO_4$), filtered and the volatiles evaporated *in vacuo*. The residue was purified by column chromatography (5% EtOAc/hexane) to yield **24** as an orange solid (7.43g, 79%).

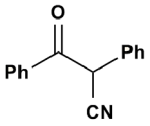

R_f (20% EtOAc/hexane) 0.36. *mp*: 88°C. **^{1}H NMR** (300MHz, $CDCl_3$): δH = 7.94 (2H, d, J = 7.3Hz, 2 x Ar-H); 7.57 (1H, t, J = 7.4Hz, Ar-H); 7.30-7.46 (7H, m, 7 x Ar-H); 5.65 (1H, s, CH). **^{13}C NMR** (75MHz, $CDCl_3$): 189.0 (C=O); 134.5 (Ar-C); 133.6 (Ar-C); 130.4 (Ar-C); 129.6 (Ar-C); 129.3 (Ar-C); 129.1 (Ar-C); 129.0 (Ar-C); 128.3 (Ar-C); 116.7 (CN); 46.6 (CH). **IR** υ_{max} (cm^{-1}): 3150 (=C-H); 2205 (C-N); 1738 (C=O); 1613 (C=C). **HRMS** (ESI): m/z 222.0921amu (M+H); calc. for $C_{15}H_{12}NO$: 222.0878amu.

4.5.2 Synthesis of *E*/*Z*-3-ethoxy-2,3-diphenylacrylonitrile 129 [131],[132]

The starting material **127** (0.50g, 2.54mmol, 1 eq.) was dissolved in triethylorthoformate (8.0ml, 48.2mmol, 19 eq.) to which a few drops of sulfuric acid were added. The reaction flask was connected to a Dean-Stark apparatus and heated at 100°C over 108 hr. The reaction mixture was then cooled and purified by column chromatography (10% EtOAc/hexane) to yield **129** as a yellow oil (0.58g, 92%).

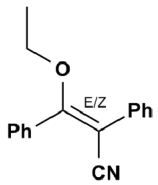

R_f (20% EtOAc/hexane) 0.58. **^{1}H NMR** (300MHz, $CDCl_3$) E isomer: δH = 7.80 (2H, d, J = 7.3Hz, 2 x Ar-H); 7.05-7.58 (8H, m, 8 x Ar-H); 3.91 (2H, q, J = 7.1Hz, CH_2); 1.27 (3H, t, J = 7.1Hz, CH_3). Z isomer: δH = 7.05-7.58 (8H, m, 10 x Ar-H); 3.91 (2H, q, J = 7.1Hz, CH_2); 1.34 (3H, t, J = 7.1Hz, CH_3). **^{13}C NMR** (75MHz, $CDCl_3$): E isomer 168.3 (C=COCH$_2$); 132.7 (Ar-C); 132.2 (Ar-C); 130.7 (Ar-C); 129.6 (Ar-C); 128.7 (Ar-C); 127.7 (Ar-C); 120.0 (CN); 96.1 (C=CCN); 67.6 (OCH$_2$); 15.3 (OCH$_3$). Z isomer 168.1 (C=COCH$_2$); 132.4 (Ar-C); 131.4 (Ar-C); 130.4 (Ar-C); 129.3 (Ar-C); 128.3 (Ar-C); 127.4 (Ar-C); 120.0 (CN); 96.7 (C=CCN); 66.9 (OCH$_2$); 15.3 (OCH$_3$). **IR** υ_{max} (cm^{-1}): 2995 (=C-H); 2204 (C-N); 1588 (C=C). **HRMS** (ESI): m/z 250.1242amu (M+H); calc. for $C_{17}H_{16}NO$: 250.1278amu.

4.5.3 Synthesis of 5,6-diphenylpyrimidine-2,4-diamine 69 [118]

Guanidine hydrochloride salt (245mg, 4.15mmol, 1.7 eq.) was dissolved in a solution of sodium ethoxide (2.5ml, 4.64mmol, 1.9 eq.) in ethanol to afford the free base. The pH of the solution was adjusted, using guanidine hydrochloride and sodium ethoxide, to approximately 7. The

sodium chloride salt formed was filtered off and the excess ethanol removed by evaporation *in vacuo*. The starting material **129** (582mg, 2.44mmol, 1 eq.), dissolved in dry DMSO (5ml), was then added dropwise and the reaction mixture heated to 85°C for 4.5 hr. The reaction mixture was then cooled and poured into a separating funnel containing DCM (15ml). The organic layer was successively washed with water (10ml) and brine (10ml), dried ($MgSO_4$), filtered and the volatiles evaporated in vacuo. Recrystallisation of the crude solid from DCM afforded **129** as a white powder (367mg, 63%).

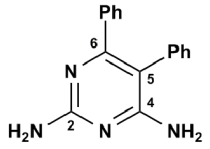

R_f (20% EtOAc/hexane) 0.63. *mp*: 241°C. **^{1}H NMR** (300MHz, DMSO): δH = 7.06-7.30 (10H, m, 10 x Ar-H); 6.07 (2H, s, C4NH_2); 5.70 (2H, br s, C2-NH_2). **^{13}C NMR** (75MHz, DMSO): 162.7 (C6); 162.3 (C2); 161.9 (C4); 139.6 (Ar-C); 136.1 (Ar-C); 131.0 (Ar-C); 129.0 (Ar-C); 128.6 (Ar-C); 127.5 (Ar-C); 127.1 (Ar-C); 126.7 (Ar-C); 106.5 (C5). **IR** υ_{max} (cm^{-1}): 3481 (N-H); 3442 (N-H); 1631 (C=N); 1541 (C=C).

4.6 General procedure for the synthesis of (4-bromobutoxy) benzene 123a and its analogues 123c-d

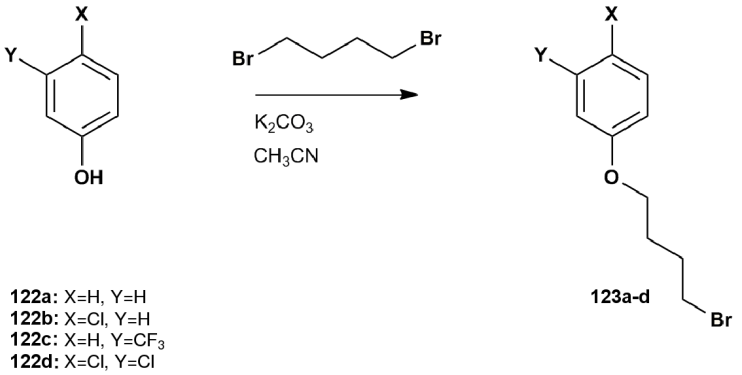

To a mixture of **122a-d** (1 eq.) and 1,4-dibromobutane (3 eq.) dissolved in dry acetonitrile was added potassium carbonate (1.5 eq.). The resulting heterogeneous mixture was stirred and heated under reflux under an argon atmosphere. Reaction progress was monitored by TLC. When complete (3 hr-overnight), the reaction mixture was cooled to room temperature and filtered through celite. The solvent was evaporated *in vacuo* and the residue partitioned between DCM and an aqueous NaOH solution (0.1M). The aqueous layer was re-extracted with additional DCM. The combined organic layers were dried ($MgSO_4$), filtered and the volatiles evaporated in vacuo. The resulting residue was then transferred to a distillation apparatus and the excess 1,4-dibromobutane distilled off, *in vacuo* (oil pump, 10 mmHg). The following products were isolated after purification by silica gel chromatography:

4.6.1 Synthesis of (4-bromobutoxy)benzene 123a [133]

Compound **122a** (5.00g, 53.0mmol), 1,4-dibromobutane (18.3ml), acetonitrile (320ml) and potassium carbonate (11.00g, 79.7mmol) afforded, after distillation and column chromatography using 20% EtOAc/hexane as eluent, **123a** (7.68g, 65%) as a white solid.

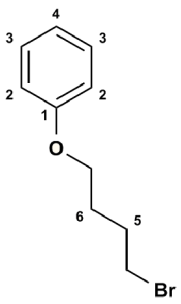

R_f (30% EtOAc/hexane) 0.89. *mp*: 38-39°C. **^{1}H NMR** (300MHz, $CDCl_3$): δH = 7.25-7.31 (2H, m, 2 x H2); 6.87-6.96 (3H, m, 2 x H3 and H4); 3.99 (2H, t, J = 6.0Hz, OCH_2); 3.49 (2H, t, J = 6.0Hz, CH_2Br); 1.88-2.13 (4H, m, 2 x H5 and 2 x H6). **^{13}C NMR** (75MHz, $CDCl_3$): δC = 158.8 (C1); 129.5 (2 x C3); 120.7 (C4); 114.4 (2 X C2); 66.7 (OCH$_2$); 33.5 (CH$_2$Br); 29.5 (C5); 27.9 (C6). **IR** v_{max} (cm^{-1}): 3041, 2956, 2930, 2871 (=C-H); 1599, 1583 (C=C).

4.6.2 Synthesis of 1-(4-bromobutoxy)-4-chlorobenzene 123b [134]

Compound **122b** (9.11g, 70.9mmol), 1,4-dibromobutane (24.5ml), acetonitrile (400ml) and potassium carbonate (14.7g, 106mmol) afforded, after distillation and column chromatography using 20% EtOAc/hexane as eluent, **123b** (18.47g, 99%) as a white solid.

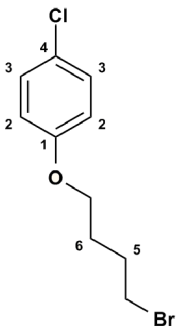

R_f (30% EtOAc/hexane) 0.89. *mp*: 28°C. **^{1}H NMR** (300MHz, $CDCl_3$): δH = 7.22 (2H, d, J = 9.0Hz, 2 x H3); 6.81 (2H, d, J = 9.0Hz, 2 x H2); 3.96 (2H, t, J = 5.9Hz, OCH_2); 3.48 (2H, t, J = 6.5Hz, CH_2Br); 1.87-2.10 (4H, m, 2 x H5 and 2 x H6). **^{13}C NMR** (75MHz, $CDCl_3$): δC = 157.5 (C1); 129.3 (2 x C3); 125.6 (C4); 115.7 (2 X C2); 67.2 (OCH$_2$); 33.3 (CH$_2$Br); 29.4 (C5); 27.8 (C6). **IR** v_{max} (cm^{-1}): 2957, 2921, 2878 (=C-H); 1593, 1578 (C=C).

4.6.3 Synthesis of 1-(4-bromobutoxy)-3-(trifluoromethyl)benzene 123c [134]

Compound **122c** (6.00g, 37.0mmol), 1,4-dibromobutane (12.8ml), acetonitrile (250ml) and potassium carbonate (7.67g, 55.5mmol) afforded after distillation, **123c** (10.26g, 93%) as a pale, yellow oil.

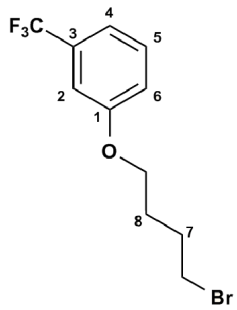

R_f (20% EtOAc/hexane) 0.78. **^{1}H NMR** (300MHz, $CDCl_3$): δH = 7.38 (1H, t, J = 9.0Hz, H5); 7.20 (1H, d, J = 6.0Hz, H4); 7.11 (1H, br s, H2); 7.06 (1H, d, J = 9.0Hz, H6); 4.02 (2H, t, J = 5.9Hz, OCH_2); 3.49 (2H, t, J = 6.5Hz, CH_2Br); 1.85-2.15 (4H, m, 2 x H7 and 2 x H8). **^{13}C NMR** (75MHz, $CDCl_3$): δC = 159.0 (C1); 131.9 (q, J_{CF} = 32.3Hz, C3) 130.0 (C5); 124.0 (q, J = 270Hz, CF$_3$); 118.0 (C6); 117.4 (C4); 111.2 (C2); 67.2 (OCH$_2$); 33.2(CH$_2$Br); 29.4 (C7); 27.8(C8). **IR** v_{max} (cm^{-1}): 2945 (=C-H); 1591 (C=C).

4.6.4 Synthesis of 4-(4-bromobutoxy)-1,2-dichlorobenzene 123d [135]

Compound **122d** (8.00g, 49.1mmol), 1,4-dibromobutane (17.0ml), acetonitrile (300ml) and potassium carbonate (10.2g, 74.0mmol) afforded after distillation, **123d** (14.1g, 96%) as a white solid.

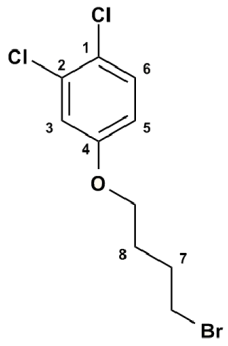

R_f (20% EtOAc/hexane) 0.80. *mp*: 24°C. **^{1}H NMR** (300MHz, $CDCl_3$): δH = 7.31 (1H, d, J = 8.9 Hz, H6); 6.98 (1H, d, J = 2.9 Hz, H3); 6.74 (1H, dd, J = 8.9Hz and 2.9 Hz, H5); 3.97 (2H, t, J = 6.0Hz, OCH_2); 3.49 (2H, t, J = 6.0Hz, CH_2Br); 1.86-2.13 (4H, m, 2 x H7 and 2 x H8). **^{13}C NMR** (75MHz, $CDCl_3$): δC = 157.9 (C4); 132.9 (C6); 130.7 (C2); 124.0 (C1); 116.3 (C5); 114.5 (C3); 67.5 (OCH$_2$); 33.2(CH$_2$Br); 29.3 (C7); 27.7(C8). **IR** v_{max} (cm^{-1}): 2950 (=C-H); 1592, 1565 (C=C).

4.7 General procedure for the synthesis of 5-phenoxy pentanenitrile 124a and its analogues 124c-d

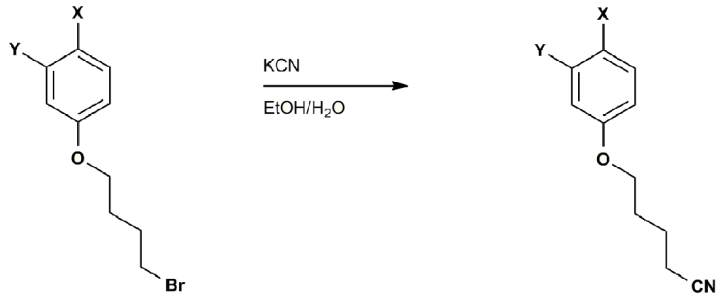

123 a: X=H, Y=H
123 b: X=Cl, Y=H
123 c: X=H, Y=CF_3
123 d: X=Cl, Y=Cl

124a-d

To a mixture of **123a-d** (1 eq.) dissolved in an ethanol/water solution (3:1) was added potassium cyanide (1.1 eq.). The resulting heterogeneous mixture was stirred and heated under reflux under an argon atmosphere overnight. Reaction progress was monitored by TLC (30% EtOAc/hexane). When complete (overnight), the reaction mixture was cooled to room temperature and the solvent evaporated *in vacuo*. The residue was partitioned between DCM and an aqueous NaOH solution (0.1M). The aqueous layer was re-extracted with additional DCM. The combined organic layers were dried (Na_2SO_4), filtered and the volatiles evaporated *in vacuo*. The residue was purified by silica gel chromatography. The following products were prepared by this method:

4.7.1 Synthesis of 5-phenoxypentanenitrile 124a [136]

Compound **123a** (7.57g, 34.2mmol), ethanol/water (3:1, 200ml) and potassium cyanide (2.45g, 34.2mmol) afforded after column chromatography using 5% EtOAc/hexane as eluent, **124a** (4.25g, 71%) as a white solid.

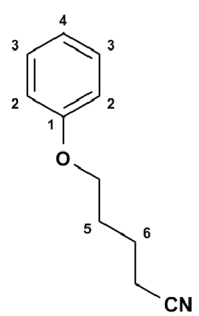

mp: 26-27°C. R_f (30% EtOAc/hexane) 0.68. **^{1}H NMR** (300MHz, $CDCl_3$): δH = 7.25-7.31 (2H, m, 2 x H3); 6.87-6.97 (3H, m, 2 x H2 and H4); 4.00 (2H, t, J = 5.6 Hz, OCH_2); 2.44 (2H, t, J = 6.8Hz, CH_2CN); 1.72-2.06 (4H, m, 2 x H5 and 2 x H6); **^{13}C NMR** (75MHz, $CDCl_3$): δC = 158.7 (C1); 129.5 (2 x C3); 120.9 (C4); 119.5 (*C*N); 114.4 (2 x C2); 66.5 (O*C*H_2); 28.2 (C5); 22.5 (C6); 17.0 (*C*H_2CN). **IR** v_{max} (cm^{-1}): 2959, 2937, 2876 (=C-H); 2241 (C≡N); 1602, 1585 (C=C). **HRMS** (ESI): *m/z* 176.1082 (*M+H*); calc. for $C_{11}H_{14}NO$: 176.1078amu.

4.7.2 Synthesis of 5-(4-chlorophenoxy)pentanenitrile 124b [137]

Compound **123b** (18.5g, 83.6mmol), ethanol/water (3:1, 300ml) and potassium cyanide (5.99g, 9.19mmol) afforded, after column chromatography using 5% EtOAc/hexane as eluent, **124b** (12.0g, 68%) as a white solid.

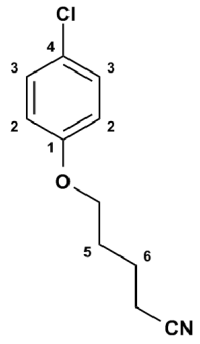

mp: 28-29°C. R_f (30% EtOAc/hexane) 0.67. **^{1}H NMR** (300MHz, $CDCl_3$): δH = 7.21 (2H, d, J = 9.0Hz, 2 x H3); 6.81 (2H, d, J = 9.0Hz, 2 x H2); 3.97 (2H, t, J = 5.6Hz, OCH_2); 2.44 (2H, t, J = 6.8Hz, CH_2CN); 1.78-2.01 (4H, m, 2 x H5 and 2 x H6). **^{13}C NMR** (75MHz, $CDCl_3$): δC = 157.3 (C1); 129.4 (2 x C3); 125.8 (C4); 119.4 (*C*N); 115.7 (2 x C2); 67.0 (O*C*H_2); 28.2 (C5); 22.4 (C6); 17.0 (*C*H_2CN). **IR** υ_{max} (cm^{-1}): 2959, 2937, 2876 (=C-H); 2239 (C≡N); 1595, 1578 (C=C). **HRMS** (ESI): *m/z* 210.0687 (*M+H*); calc. for $C_{11}H_{13}ClNO$: 210.0678amu.

4.7.3 Synthesis of 5-(3-(trifluoromethyl)phenoxy)pentanenitrile 124c

Compound **123c** (6.00g, 20.2mmol), ethanol/water (3:1, 200ml) and potassium cyanide (1.47g, 22.6mmol) afforded after column chromatography using 5% EtOAc/hexane as eluent, **124c** (3.66g, 74%) as a pale, yellow oil.

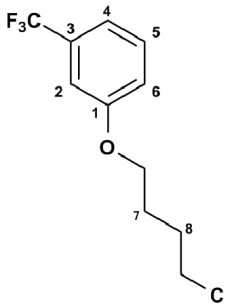

R_f (20% EtOAc/hexane) 0.43. **^{1}H NMR** (300MHz, $CDCl_3$): δH = 7.38 (1H, t, J = 9.0Hz, H5); 7.21 (1H, d, J = 6.0Hz, H4); 7.11 (1H, br s, H2); 7.06 (1H, dd, J = 3.0Hz and 9.0Hz, H6); 4.03 (2H, t, J = 5.9Hz, OCH_2); 2.45 (2H, t, J = 6.5Hz, CH_2CN); 1.80-2.02 (4H, m, 2 x H7 and 2 x H8). **^{13}C NMR** (75MHz, $CDCl_3$): δC = 158.9 (C1); 131.9 (q, J_{CF} = 32.3Hz, C3) 130.1 (C5); 125.8 (q, J_{CF} = 270Hz, *C*F_3); 122.2 (C6); 119.4 (*C*N); 118.0 (C4); 111.1 (C2); 67.0 (O*C*H_2); 28.1 (C7); 22.4 (C8); 17.0 (*C*H_2CN). **IR** υ_{max} (cm^{-1}): 2945 (C≡N); 2878 (=C-H); 1592 (C=C). **HRMS** (ESI): *m/z* 224.0888amu (*M+H-F*); calc. for $C_{12}H_{12}F_2NO$: 224.0916amu.

4.7.4 Synthesis of 5-(3,4dichlorophenoxy)pentanenitrile 124d

Compound **123d** (6.08g, 20.4mmol), ethanol/water (3:1, 200ml) and potassium cyanide (1.44g, 22.1mmol) afforded after column chromatography using 5% EtOAc/hexane as eluent, **124d** (3.59g, 72%) as a white solid.

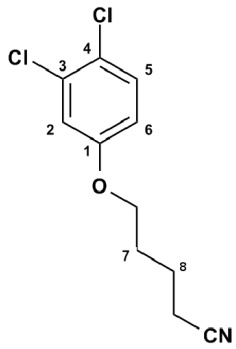

mp: 26°C. R_f (20% EtOAc/hexane) 0.36. **^{1}H NMR** (300MHz, $CDCl_3$): δH = 7.31 (1H, d, J = 8.9 Hz, H5); 6.97 (1H, d, J = 2.9 Hz, H2); 6.74 (1H, dd, J = 8.9 Hz and 2.9Hz, H6); 3.97 (2H, t, J = 5.6Hz, OCH_2); 2.44 (2H, t, J = 6.8Hz, CH_2CN); 1.81-1.99 (4H, m, 2 x H8 and 2 x H7). **^{13}C NMR** (75MHz, $CDCl_3$): δC = 157.8 (C1); 132.9 (C3); 130.7 (C5); 124.2 (C4); 119.3 (*C*N); 116.3 (C2); 114.5 (C6); 67.3 (O*C*H_2); 28.0(C7); 22.3 (C8); 17.0 (*C*H_2CN). **IR** v_{max} (cm^{-1}): 2944 (=C-H); 2246 (C≡N); 1592, 1566 (C=C). **HRMS** (ESI): m/z 244.0299amu (M+H); calc. for $C_{11}H_{12}Cl_2NO$: 244.0278amu.

4.8 General procedure for the synthesis of 2-benzoyl-5-phenoxypentanenitrile 125a and its analogues 125c-d

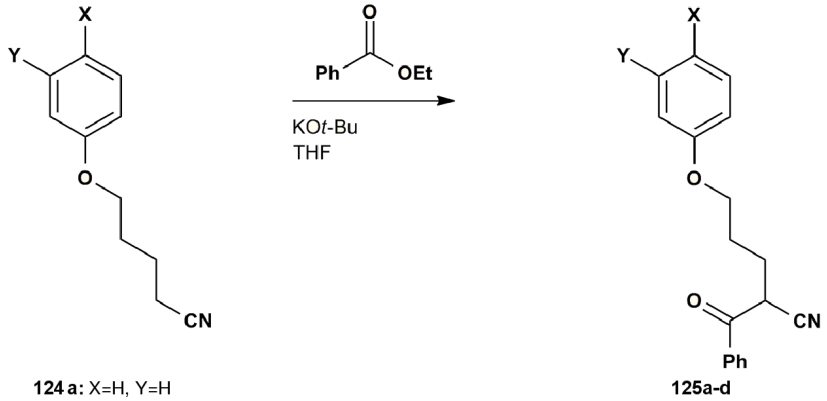

124 a: X=H, Y=H
124 b: X=Cl, Y=H
124 c: X=H, Y=CF_3
124 d: X=Cl, Y=Cl

125a-d

To a mixture of **124a-d** (1 eq.) dissolved in dry THF was added potassium *tert*-butoxide (3 eq.) and ethyl benzoate (4 eq.). The resulting heterogeneous mixture was stirred at room temperature, under an argon atmosphere overnight. Reaction progress was monitored by TLC (20% EtOAc/hexane). When complete, the reaction mixture was quenched with a saturated ammonium chloride solution and the THF evaporated *in vacuo*. The aqueous residue was washed twice with ethyl acetate and the organic layers were combined, dried ($MgSO_4$) and filtered. The volatiles were evaporated *in vacuo* and the residue was purified by silica gel chromatography. The following products were synthesised using this method:

4.8.1 Synthesis of 2-benzoyl-5-phenoxypentanenitrile 125a

Compound **124a** (500mg, 2.85mmol), THF (20ml), potassium *tert*-butoxide (961mg, 8.56mmol) and ethyl benzoate (1.64ml, 11.4mmol) afforded after column chromatography using 5% EtOAc/hexane as eluent, **125a** (729mg, 89%) as a creamy, white solid.

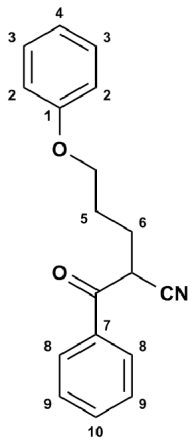

R_f (20% EtOAc/hexane) 0.50. *mp*: 45°C. **^{1}H NMR** (300MHz, $CDCl_3$): δH = 7.97 (2H, d, J = 12Hz, 2 x H8); 7.64 (1H, t, J = 12Hz, H10); 7.49 (2H, t, J = 12Hz, 2 x H9); 7.26 (2H, dd, J = 7.4Hz and 7.8Hz, 2 x H3); 6.95 (1H, t, J = 7.4Hz, H4); 6.85 (2H, d, J = 7.8Hz, 2 x H2); 4.52 (1H, dd, J = 6.0Hz and 6.0Hz, C*H*CN); 4.10 (2H, dd, J = 6.0Hz and 6.0Hz, OCH_2); 3.95-4.13 (4H, m, 2 x H5 and 2 x H6). **^{13}C NMR** (75MHz, $CDCl_3$): δC = 190.54 (C=O); 158.5 (C1); 134.5 (C10); 134.0 (C7); 129.5 (2 x ArC); 128.8 (2 x ArC); 128.2 (2 x ArC); 121.1 (C4); 117.2 (*C*N); 114.4 (2 x C2); 66.5 (O*C*H_2); 39.4 (*C*HCN); 26.9 (C6); 26.5 (C5). **IR** υ_{max} (cm^{-1}): 2963, 2941, 2889 (=C-H); 2237 (C≡N); 1702 (C=O); 1600, 1586 (C=C). **HRMS** (ESI): *m/z* 280.1338 (*M+H*); calc. for $C_{18}H_{18}NO_2$: 280.1378amu.

4.8.2 Synthesis of 2-benzoyl-5-(4-chlorophenoxy)pentanenitrile 125b

Compound **124b** (11.9g, 56.7mmol), THF (377ml), potassium *tert*-butoxide (19.1g, 170mmol) and ethyl benzoate (32.6ml, 227mmol) afforded, after column chromatography using 10% EtOAc/hexane as eluent, **125b** (13.0g, 76%) as a pale, yellow powder.

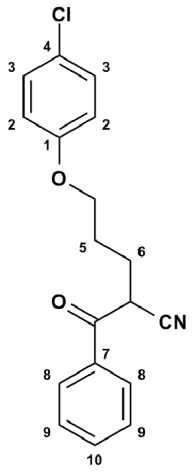

R_f (20% EtOAc/hexane) 0.41. *mp*: 126-127°C. **^{1}H NMR** (300MHz, $CDCl_3$): δH = 7.96 (2H, d, J = 7.2Hz, 2 x H8); 7.66 (1H, t, J = 7.2Hz, H10); 7.51 (2H, t, J = 7.2Hz, 2 x H9); 7.22 (2H, d, J = 9.0Hz, 2 x H3); 6.78 (2H, d, J = 9.0Hz, 2 x H2); 4.48 (1H, dd, J = 6.0Hz and 6.0Hz, C*H*CN); 4.01 (2H, dd, J = 6.0Hz and 6.0Hz, OCH_2); 2.00-2.36 (4H, m, 2 x H5 and 2 x H6). **^{13}C NMR** (75MHz, $CDCl_3$): δC = 190.4 (C=O); 157.1 (C1); 134.6 (C10); 134.0 (C7); 129.4 (2 x C3); 129.2 (2 x C8); 128.8 (2 x C9); 125.9 (C4); 117.1 (*C*N); 115.7 (2 x C2); 67.0 (O*C*H_2); 39.4 (*C*HCN); 26.7 (C6); 26.5 (C5). **IR** υ_{max} (cm^{-1}): 2970, 2946, 2877 (=C-H); 2241 (C≡N); 1695 (C=O); 1595, 1580 (C=C). **HRMS** (ESI): *m/z* 314.0948amu (*M+H*); calc. for $C_{18}H_{17}ClNO_2$: 314.0978amu.

4.8.3 Synthesis of 2-benzoyl-5-(3-(trifluoromethyl)phenoxy)pentanenitrile 125c

Compound **124c** (2.70g, 11.1mmol), THF (76ml), potassium *tert*-butoxide (3.74g, 33.3mmol) and ethyl benzoate (6.4ml, 44.5mmol) afforded after column chromatography using 10% EtOAc/hexane as eluent and recrystallisation from ethanol **125c** (512mg, 13%) as a white solid.

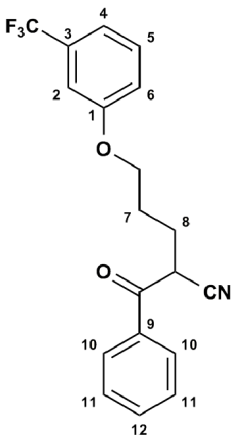

R_f (20% EtOAc/hexane) 0.43. *mp*: 56-59°C. **^{1}H NMR** (300MHz, $CDCl_3$): δH = 7.98 (2H, d, J = 7.2Hz, 2 x H10); 7.65 (1H, t, J = 7.5Hz, H12); 7.52 (2H, t, J = 7.8Hz, 2 x H11); 7.38 (1H, t, J = 9.0Hz, H5); 7.21 (1H, d, J = 6.0Hz, H4); 7.05 (1H, br s, H2); 7.02 (1H, d, J = 8.4Hz, H6) 4.49 (1H, dd, J = 6Hz and 6Hz, CHCN); 4.06-4.10 (2H, m, OCH_2); 2.03-2.39 (4H, m, 2 x H7 and 2 x H8). **^{13}C NMR** (75MHz, $CDCl_3$): δC = 190.3 (C=O) 158.6 (C1); 134.6 (C9); 134.0 (C12); 131.95 (q, J_{CF} = 32.3Hz, C3) 130.1 (C5); 129.2 (2 x C10); 128.8 (2 x C11); 123.9 (q, J_{CF} = 273Hz, CF_3); 117.8 (C6); 117.1 (C4); 111.3 (C2); 67.0 (OCH$_2$); 39.3 (CHCN); 26.7 (C8); 26.5 (C7). **IR** υ_{max} (cm^{-1}): 2931 (C≡N); 2869 (=C-H); 1692 (C=O); 1606 (C=C); 1448 (C-F). **HRMS** (ESI): m/z 348.1211amu (M+H); calc. for $C_{19}H_{17}F_3NO_2$: 348.1178amu.

4.8.4 Synthesis of 2-benzoyl-5-(3,4-dichlorophenoxy)pentanenitrile 125d

Compound **124d** (2.08g, 8.50mmol), THF (80ml), potassium *tert*-butoxide (2.86g, 25.5mmol) and ethyl benzoate (5.0ml, 3.48mmol) afforded, after column chromatography using 5% EtOAc/hexane as eluent, **125d** (2.82g, 99%) as a white solid.

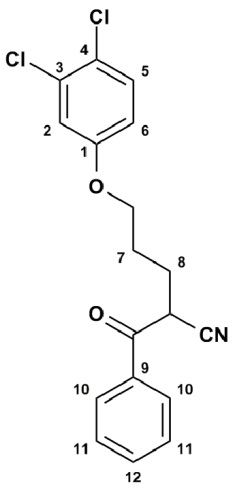

R_f (20% EtOAc/hexane) 0.31. *mp*: 46°C. **^{1}H NMR** (300MHz, $CDCl_3$): δH = 7.97 (2H, d, J = 6.1Hz, 2 x H10); 7.66 (1H, t, J = 7.2Hz, H12); 7.52 (2H, dd, J = 6.1Hz and 7.2Hz, 2 x H11); 7.26 (1H, s, H2); 7.23 (2H, d, J = 9.2Hz, H5); 6.77 (1H, d, J = 9.2Hz, H6); 4.48 (1H, dd, J = 5.7Hz, 5.9Hz, CHCN); 4.03 (2H, dd, J = 6.0Hz and 6.0Hz, OCH_2); 2.12-2.36 (4H, m, 2 x H7 and 2 xH8). **^{13}C NMR** (75MHz, $CDCl_3$): δC = 190.3 (C=O); 157.1 (C1); 134.6 (C12); 133.8 (C9); 129.5 (C5); 129.1 (C10); 128.8 (C11); 126.1 (C4); 117.4 (CN); 117.2 (C2); 115.7 (C6); 67.0 (OCH$_2$); 39.5 (CHCN); 26.7 (C8); 26.5 (C7). **IR** υ_{max} (cm^{-1}): 2939, 2893, 2869 (=C-H); 2236 (C≡N); 1694 (C=O).

4.9 General procedure for the synthesis of *E*/*Z*-5-(4-chlorophenoxy)-2-(methoxy(phenyl)methylene) pentanenitrile 131 and *E*/*Z*-5-(3,4-dichlorophenoxy)-2-(methoxy(phenyl)methylene) pentanenitrile 132

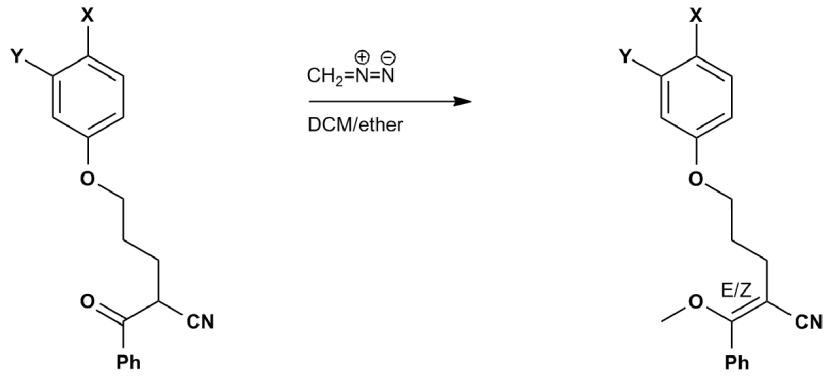

125b X=Cl, Y=H
125d X=Cl, Y=Cl

126e
126d

Aqueous potassium hydroxide solution (10.7M, 20.0 eq.), diethyl ether and carbitol were placed within a reaction flask to which a dropping funnel and a condenser were attached. Diazald (3 eq.), dissolved in diethyl ether, was placed within the dropping funnel and the apparatus lowered into a waterbath at 70-75°C. The Diazald solution was then slowly allowed to drip into the reaction flask. The resulting diazomethane was distilled (in diethyl ether) into a conical flask containing the starting material **125b** or **125d** dissolved in dry DCM. The dropping funnel was washed twice with additional diethyl ether and, after the distillation was complete, the reaction cooled and left to stir overnight. DCM was evaporated *in vacuo* and the isolated residue used without any further purification.

4.9.1 Synthesis of *E*/*Z*-5-(4-chlorophenoxy)-2-(methoxy(phenyl) methylene)pentanenitrile 131

Reaction of a potassium hydroxide solution (6ml, 10.7M, 20 eq.) in diethyl ether (10ml) and carbitol (3.5ml) with Diazald (2.00g, 9.34mmol) in diethyl ether (20ml) resulted in the generation of diazomethane. Reaction of the methylating agent in diethyl ether with the starting material **125b** (1.00g, 3.19mmol) in DCM (50ml) afforded **131** as a yellow oil in a quantitative yield.

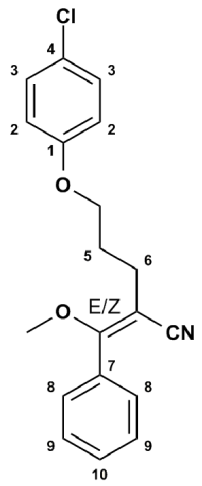

R_f (20% EtOAc/hexane) 0.51. **^{1}H NMR** (300MHz, $CDCl_3$): δH = *E* isomer: 7.39-7.47 (4H, m, 4 x Ar-H); 7.12-7.26 (3H, m, 3 x Ar-H); 6.85 (2H, d, J = 9.0Hz, 2 x H3); 4.03 (2H, t, J = 6.1Hz, OCH_2); 3.44 (3H, s, OCH_3); 2.57 (2H, t, J = 7.8Hz, 2 x H6); 2.02-2.11 (2H, m, 2 x H5). *Z* isomer: 7.39-7.47 (4H, m, 4 x Ar-H); 7.12-7.26 (3H, m, 3 x Ar-H); 6.67 (2H, d, J = 9.0Hz, 2 x H2); 3.85 (2H, t, J = 5.9Hz, OCH_2); 3.48 (3H, s, OCH_3); 2.24 (2H, t, J = 7.8Hz, 2 x H6); 1.92-2.00 (2H, m, 2 x H5). **^{13}C NMR** (75MHz, $CDCl_3$): δC = *E* isomer: 168.9 (C=*C*OCH$_2$); 157.6 (C1); 131.5 (C7); 130.5 (C10); 129.3 (C3); 128.9 (C8); 128.8 (C9); 125.5 (C4); 120.1 (*C*N); 115.8 (C2); 94.2 (C=*C*CN); 67.1 (O*C*H$_2$); 58.3 (O*C*H$_3$); 27.7 (C5); 23.8 (C6). *Z* isomer: 168.7 (C=*C*OCH$_2$); 157.3 (C1); 130.7 (C7); 130.3 (C10); 129.2 (C3); 128.8 (C8); 128.7 (C9); 125.5 (C4); 118.2 (*C*N); 115.7 (C2); 91.9 (C=*C*CN); 66.1 (O*C*H$_2$); 58.1 (O*C*H$_3$); 28.1 (C5); 25.0 (C6). **IR** υ_{max} (cm^{-1}): 2944, 2872, 2850 (=C-H); 2207 (C≡N); 1676 (C=C). **HRMS** (ESI): *m/z* 328.1107amu (*M+H*); calc. for $C_{19}H_{19}ClNO_2$: 328.6257amu.

4.9.2 Synthesis of *E/Z*-5-(3,4-dichlorophenoxy)-2-(methoxy(phenyl) methylene)pentanenitrile 132

Reaction of a potassium hydroxide solution (6ml, 10.7M, 20 eq.) in diethyl ether (10ml) and carbitol (3.5ml) with Diazald (1.85g, 8.64mmol) in diethyl ether (20ml) resulted in the generation of diazomethane. Reaction of the methylating agent in diethyl ether with the starting material **125b** (1.00g, 2.87mmol) in DCM (50ml) afforded **132** as a yellow oil in a quantitative yield.

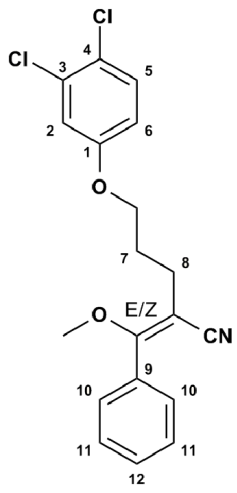

R_f (20% EtOAc/hexane) 0.62. **^{1}H NMR** (300MHz, $CDCl_3$): δH = *E* isomer: 7.17-7.47 (5H, m, 2 x H10, H12, 2 x H11); 7.00 (1H, dd, J = 2.9Hz, 2.9Hz, H2); 6.77 (1H, dd, J = 2.9Hz, 8.9Hz, H6); 6.59 (1H, dd, J = 8.9Hz, 8.9Hz, H5); 4.03 (2H, t, J = 6.1Hz, OCH_2); 3.47 (3H, s, OCH_3); 2.57 (2H, t, J = 7.1Hz, 2 x H8); 2.02-2.11 (2H, m, 2 x H7). *Z* isomer: 7.17-7.47 (5H, m, 2 x H10, H12, 2 x H11); 7.00 (1H, dd, J = 2.9Hz, 2.9Hz, H2); 6.77 (1H, dd, J = 2.9Hz, 8.9Hz, H6); 6.59 (1H, dd, J = 8.9Hz, 8.9Hz, H5); 3.84 (2H, t, J = 5.8Hz, OCH_2); 3.48 (3H, s, OCH_3); 2.24 (2H, t, J = 6.9Hz, 2 x H8); 1.93-2.00 (2H, m, 2 x H7). **^{13}C NMR** (75MHz, $CDCl_3$): δC = *E* isomer: 169.0 (C=*C*OCH$_2$); 158.1 (C1); 132.8 (C3); 131.5 (C9); 130.7 (C5); 130.5 (C12); 128.9 (C10); 128.8 (C11); 123.9 (C4); 120.1 (*C*N); 116.4 (C6); 114.6 (C2); 94.1 (C=*C*CN); 66.4 (O*C*H$_2$); 58.3 (O*C*H$_3$); 27.6 (C7); 23.8 (C8). *Z* isomer: 168.8 (C=*C*OCH$_2$); 157.7 (C1); 132.7 (C3); 130.7 (C9); 130.5 (C5); 130.3 (C12); 128.9 (C10); 128.7

(C11); 123.9 (C4); 118.1 (*C*N); 116.4 (C6); 114.3 (C2); 91.7 (C=*C*CN); 66.4 (O*C*H_2); 58.1 (O*C*H_3); 27.9 (C7); 24.9 (C8). **IR** v_{max} (cm^{-1}): 2942 (=C-H); 2208 (C≡N); 1694 (C=C). **HRMS** (ESI): *m/z* 362.0721amu (*M+H*); calc. for $C_{19}H_{18}Cl_2NO_2$: 361.0636amu.

4.10 Synthesis of *Z* -5-(4-chlorophenoxy)-2-(ethoxy(phenyl) methylene)pentanenitrile 126b

The starting material **125b** (800mg, 2.67mmol, 1 eq.) was dissolved in triethylorthoformate (8.0ml, 50.7mmool, 19 eq.) to which a few drops of sulfuric acid were added. The reaction flask was connected to a Dean-Stark apparatus and heated at 100°C over 36 hr. The reaction mixture was then cooled and purified by column chromatography (10% EtOAc/hexane) to yield **126b** as a yellow oil (0.054g, 6%).

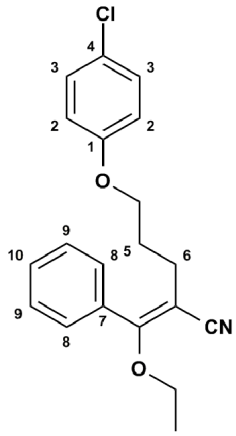

R_f (20% EtOAc/hexane) 0.60. **^{1}H NMR** (300MHz, $CDCl_3$): δH = 7.44 (5H, s, 5 x Ar-H); 7.23 (2H, d, J = 8.9Hz, 2 x H3); 6.84 (2H, d, J = 8.9Hz, 2 x H2); 4.01 (2H, t, J = 6.0Hz, OCH_2); 3.68 (2H, q, J = 7.0Hz, OCH_2CH_3); 2.59 (2H, t, J = 7.2Hz, 2 x H6); 2.03-2.12 (2H, m, 2 x H5); 1.16 (3H, t, J = 7.1Hz, OCH_2CH_3). **^{13}C NMR** (75MHz, $CDCl_3$): δC = 168.2 (C=*C*OCH_2); 157.6 (C1); 132.1 (C10); 130.4 (C7); 129.3 (2 X C3); 128.8 (2 x C8); 128.7 (2 x C9); 125.5 (C4); 120.2 (*C*N); 115.8 (2 x C2); 94.9 (C=*C*CN); 67.1 (O*C*H_2); 66.7 (O*C*H_2CH$_3$); 27.8 (C6); 24.0 (C5); 15.2 (OCH$_2$*C*H$_3$). **IR** v_{max} (cm^{-1}): 2981, 2929 (=C-H); 2209 (C≡N); 1726 (C=C).

4.11 Synthesis of 5-(3-(4-chlorophenoxy)propyl)-6-phenyl pyrimidine-2,4-diamine 65b

Guanidine hydrochloride salt (221mg, 2.33mmol, 1.7 eq.) was dissolved in a solution of sodium methoxide (9.7ml, 2.62mmol, 1.9 eq.) in methanol to afford the free base. The sodium chloride salt formed was filtered off and the excess methanol removed by evaporation *in vacuo*. The starting material **131** (500mg, 1.38mmol, 1 eq.), dissolved in dry DMSO (5ml), was then added dropwise and the reaction mixture heated to 100°C over 108 hr. The reaction mixture was then cooled, DMSO removed under vacuum and the residue purified by column chromatography to afford **65b** as a creamy solid (50mg, 9%).

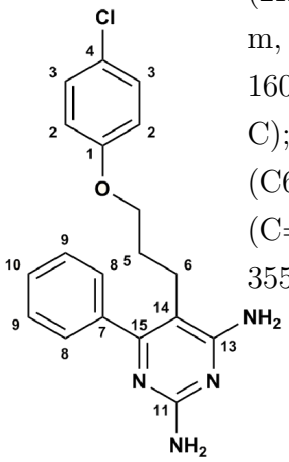

R_f (20% EtOAc/hexane) *mp*: 132°C. **^{1}H NMR** (300MHz, DMSO): δH = 7.34 (5H, s, 5 x Ar-H); 7.27 (2H, d, J = 9.0Hz, 2 x H3); 6.78 (2H, d, J = 9.0Hz, 2 x H2); 6.31 (2H, br s, C9NH_2); 5.77 (2H, br s, C7NH_2); 3.80 (2H, t, J = 6.0Hz, OCH_2); 2.41 (2H, t, J = 6.0Hz, 2 x H6); 1.75-1.80 (2H, m, 2 x H5); **^{13}C NMR** (75MHz, DMSO): δC = 163.7 (C15); 163.4 (C11); 160.9 (C13); 157.2 (C1); 140.0 (C7); 128.9 (2 x C3);128.3 (Ar-C);127.9 (Ar-C);127.4 (Ar-C);123.9 (C4); 116.1 (2 x C2); 103.0 (C14); 67.1 (OCH$_2$); 28.0 (C6); 21.6 (C5). **IR** v_{max} (cm^{-1}): 3335, 3140 (N-H); 2931 (=C-H); 2189 (C=N). **HRMS** (ESI): m/z 355.1328amu (M+H); calc. for $C_{19}H_{20}ClN_4O$: 355.6479amu.

Bibliography

[1] B. Greenwood and T. Mutabingwa, "Malaria in 2002," *Nature*, vol. 415, pp. 670–672, 2002.

[2] D. M. Melvin, "2704." Public Health Image Library (PHIL), Department of Health and Human Services, Centers for Disease Control and Prevention, 1973.

[3] A. Gregson and C. V. Plowe, "Mechanisms of Resistance of Malaria Parasites to Antifolates," *Pharmacol. Rev.*, vol. 57, pp. 117–145, 2005.

[4] B. M. Greenwood, K. Bojang, C. J. M. Whitty, and G. A. Targett, "Malaria," *Lancet*, vol. 365, no. 9469, pp. 1487–98, 2005.

[5] J. Sachs and P. Malaney, "The economic and social burden of malaria," *Nature*, vol. 415, pp. 680–685, 2002.

[6] W. H. Organisation, "World Malaria Report 2011," tech. rep., WHO, 2011.

[7] G. F. Killeen, U. Fillinger, I. Kiche, L. C. Gouagna, and B. G. J. Knols, "Eradication of *Anopheles gambiae* from Brazil: lessons for malaria control in Africa?," *Lancet*, vol. 2, pp. 618–627, 2002.

[8] C. Curtis and J. Lines, "Should DDT be Banned by International Treaty?," *Parasitol. Today*, vol. 16, pp. 119–121, 2000.

[9] R. Romi, M. Razaiarimanga, R. Raharimanga, E. Rakotondraibe, L. Ranaivo, V. Pietra, A. Raveloson, and G. Majori, "Impact of the malaria control campaign (1993-1998) in the highlands of Madagascar: parasitological and entomological data," *Am. J. Trop. Med. Hyg.*, vol. 66, pp. 2–6, 2002.

[10] C. Curtis, "Restoration of Malaria control in the Madagascar highlands by DDT spraying," *Am. J. Trop. Med. Hyg.*, vol. 66, p. 1, 2002.

[11] D. Connell, *Introduction to Ecotoxicology.* Wiley, 1999.

[12] K. Larson, "Bad blood," in *OnEarth: A Survival Guide for the Planet*, Natural Resources Defense Council, 2007.

[13] W. Rogan and A. Chen, "Health risks and benefits of bis(4-chlorophenyl)-1,1,1-trichloroethane (DDT)," *Lancet*, vol. 366, pp. 763–73, 2005.

[14] C. Lengeler, "Insecticide-treated bed nets and curtains for preventing malaria," *Cochrane Database Syst. Rev.*, vol. 2, p. Art. No.:CD000363, 2004.

[15] G. F. Killeen, U. Fillinger, and B. G. Knols, "Advantages of larval control for African malaria vectors: Low mobility and behavioural responsiveness of immature mosquito stages allow high effective coverage," *Malaria J.*, vol. 1, pp. 8–14, 2002.

[16] R. Muirhead-Thomson, *Mosquito Behaviour in relation to Malaria Transmission and Control in the Tropics.* London: Edward Arnold & Co., 41, Maddox Street, WI, 1951.

[17] J. Webster, J. Hill, J. Lines, and K. Hanson, "Delivery systems for insecticide treated and untreated mosquito nets in Africa: categorization and outcomes achieved," *Health Policy Plann.*, vol. 22, pp. 277–293, 2007.

[18] S. L. Hoffman, L. M. Goh, T. C. Luke, I. Schneider, T. P. Le, D. L. Doolan, J. Sacci, P. de la Vega, M. Dowler, C. Paul, D. M. Gordon, J. A. Stoute, L. W. P. Church, M. Sedegah, G. Heppner, W. R. Ballou, and T. L. Richie1, "Protection of Humans against Malaria by Immunization with Radiation-Attenuated *Plasmodium falciparum* Sporozoites," *J. Infect. Dis.*, vol. 185, pp. 1155–64, 2002.

[19] P. L. Alonso, J. Sacarlal, J. J. Aponte, A. Leach, E. Macete, J. Milman, I. Mandomando, B. Spiessens, C. Guinovart, M. Espasa, Q. Bassat, P. Aide, O. Ofori-Anyinam, M. M. Navia, S. Corachan, M. Ceuppens, M.-C. Dubois, M.-A. Demoitie, F. Dubovsky, C. Menendez, N. Tornieporth, W. R. Ballou, R. Thompson, and J. Cohen, "Efficacy of the RTS,S/As02A vaccine against *Plasmodium falciparum* infection and disease in young African children: randomised controlled trial," *Lancet*, vol. 364, pp. 1411–20, 2004.

[20] P. L. Alonso, J. Sacarlal, J. J. Aponte, A. Leach, E. Macete, P. Aide, B. Sigauque, J. Milman, I. Mandomando, Q. Bassat, C. Guinovart, M. Espasa, S. Corachan, M. Lievens, M. M. Navia, M.-C. Dubois, C. Menendez, F. Dubovsky, J. Cohen, R. Thompson, and W. R. Ballou, "Duration of protection with RTS,S/AS02A malaria vaccine in prevention of *Plasmodium falciparum* disease in Mozambican children: single-blind extended follow-up of a randomised controlled trial," *Lancet*, vol. 366, pp. 2012–18, 2005.

[21] R. Nussenzweig, J. Vanderberg, H. Most, and C. Orton, "Protective immunity produced by the injection of x-irradiated sporozoites of *Plasmodium berghei*," *Nature*, vol. 216, pp. 160–2, 1967.

[22] M. P. Girard, Z. H. Reed, M. Friede, and M. P. Kieny, "A review of human vaccine research and development: Malaria," *Vaccine*, vol. 25, pp. 1567–1580, 2007.

[23] M. F. Good, H. Xu, M. Wykes, and C. R. Engwerda, "Development and regulation of cell-mediated immmune responses to the blood stages of Malaria: Implications for Vaccine Research," *Annu. Rev. Immunol.*, vol. 23, pp. 69–99, 2005.

[24] E. Malkin, F. Dubovsky, and M. Moree, "Progress towards the development of malaria vaccines," *Trends Parasitol.*, vol. 22, pp. 292–295, 2006.

[25] T. Kaufman and E. Ruveda, "The Quest for Quinine: Those Who Won the Battles and Those Who Won the War," *Angew. Chem. Int. Ed.*, vol. 44, pp. 854–885, 2005.

[26] J. Burckhalter, F. Tendick, E. Jones, P. A. Jones, W. Holcolm, and A. Rawlins, "Aminoalkylphenols as Antimalarials. II. (Heterocyclic-amino)-α-amino-o-cresols. The Synthesis of Camoquin2," *J. Amer. Chem. Soc.*, vol. 70, pp. 1363–1373, 1948.

[27] P. O'Neill, P. Bray, S. R. Hawley, S. Ward, and B. Park, "4-Aminoquinolines-Past, Present and Future: A Chemical Perspective," *Pharmacol. Ther.*, vol. 77, no. 1, pp. 29–58, 1998.

[28] T. E. Wellems, "Plasmodium Chloroquine Resistance and the Search for a Replacement Antimalarial Drug," *Science*, vol. 298, no. 5591, pp. 124–126, 2002.

[29] K. Krafts, E. Hempelmann, and A. Skorska-Stania, "From methylene blue to chloroquine: a brief review of the development of an antimalarial therapy," *Parasitol. Res.*, vol. 111, pp. 1–6, 2012.

[30] D. Fidock, T. Nomura, A. K. Talley, R. Cooper, S. Dzekunov, M. Ferdig, L. Ursos, A. bir Singh Sidhu, B. Naude, K. Deitsch, X. Su, J. Wootton, P. Roepe, and T. Wellems, "Mutations in the *P. falciparum* Digestive Vacuole Transmembrane Protein PfCRT and Evidence for Their Role in Chloroquine Resistance," *Mol. Cell*, vol. 6, pp. 861–871, 2000.

[31] L. H. Miller and X. Su, "Artemisinin: Discovery from the Chinese Herbal Garden," *Cell*, vol. 146, pp. 855–858, 2011.

[32] R. Ridley, "Medical need, scientific opportunity and the drive for antimalarial drugs," *Nature*, vol. 415, pp. 686–693, 2002.

[33] A. Nzila and R. Chilengi, "Modulators of the efficacy and toxicity of drugs in malaria treatment," *Trends Pharmacol. Sci.*, vol. 31, no. 6, pp. 277–283, 2010.

[34] I. M. Kompis, K. Islam, and R. L. Then, "DNA and RNA synthesis: Antifolates," *Chem. Rev.*, vol. 105, no. 2, pp. 593–620, 2005.

[35] Y. Yuthavong, "The malarial folate pathway and molecular targets for antimalarial development," *J. Sci. Soc. Thailand*, vol. 22, pp. 181–186, 1996.

[36] V. Schirch and W. Strong, "Interaction of folylpolyglutamates with enzymes in one-carbon metabolism," *Arch. Biochem. Biophys.*, vol. 269, no. 2, pp. 371–380, 1989.

[37] M. McBurney and G. Whitmorea, "Characterization of a chinese hamster cell with a temperature-sensitive mutation in folate metabolism," *Cell*, vol. 2, pp. 183–188, 1974.

[38] A. Nzila, "Inhibitors of *de novo* folate enzymes in *Plasmodium falciparum*," *Drug Discov. Today*, vol. 11, no. 19/20, pp. 939–944, 2006.

[39] C. H. Sibley, J. E. Hyde, P. F. Sims, C. V. Plowe, J. G. Kublin, E. K. Mberu, A. F. Cowman, P. A. Winstanley, W. M. Watkins, and A. M. Nzila, "Pyrimethamine-sulfadoxine resistance in *Plasmodium falciparum*: what next?," *Trends Parasitol.*, vol. 17, pp. 582–588, 2001.

[40] P. Chitnumsub, J. Yavaniyama, J. Vanichtanankul, S. Kamchonwongpaisan, M. D. Walkinshaw, and Y. Yuthavong, "Characterization, crystallization and preliminary X-ray analysis of bifunctional dihydrofolate reductase-thymidylate synthase from *Plasmodium falciparum*," *Acta Crystallogr. D*, vol. 60, pp. 780–783, 2004.

[41] J. Yuvaniyama, P. Chitnumsub, S. Kamchonwongpaisan, J. Vanichtanankul, W. Sirawaraporn, P. Taylor, M. D. Walkinshaw, and Y. Yuthavong, "Insights into antifolate resistance from malarial DHFR-TS structures," *Nat. Struct. Biol.*, vol. 10, pp. 357–365, 2003.

[42] Y. Yuthavong, J. Yuvaniyama, P. Chitnumsub, J. Vanichtanankul, S. Chusacultanachai, B. Tarnchompoo, T. Vilaivan, and S. Kamchonwongpaisan, "Malarial (*Plasmodium falciparum*) dihydrofolate reductase-thymidylate synthase: structural basis for antifolate resistance and development of effective inhibitors," *Parasitology*, vol. 130, pp. 249–259, 2005.

[43] B. Maegraith, A. Adams, J. King, M. Tottey, D. Rigby, and R. Sladden, "Paludrine in the treatment of malaria," *Brit. Med. J.*, vol. 1, pp. 903–905, 1946.

[44] "No authors listed," *Drug Ther. Bull.*, vol. 33, pp. 92–3, 1995.

[45] A. Mital, "Recent Advances in Antimalarial Compounds and their Patents," *Curr. Med. Chem.*, vol. 14, pp. 759–773, 2007.

[46] M. Hurly, "Potentiation of pyrimethamine by sulphadiazine in human malaria," *Trans. R. Soc. Trop. Med. Hyg.*, vol. 53, pp. 412–413, 1959.

[47] W. Chin, P. Contacos, G. Coatney, and H. King, "The evaluation of sulfonamides, alone or in combination with pyrimethamine, in the treatment of multi-resistant *falciparum* malaria.," *Am. J. Trop. Med. Hyg.*, vol. 15, pp. 823–829, 1966.

[48] P. Wang, Q. Wang, Y. Yang, J. Coward, A. Nzila, P. Sims, and J. Hyde, "Characterization of the bifunctional dihydrofolate synthase-folylpolyglutamate synthase from *Plasmodium falciparum*; a potential novel target for antimalarial antifolate inhibition," *Mol. Biochem. Parasit.*, vol. 172, pp. 41–51, 2010.

[49] J. Curtis, M. Duraisingh, and D. Warhurst, "*In Vivo* selection for a specific genotype of dihydropteroate synthetase of *Plasmodium falciparum* by Pyrimethamine-Sulfadoxine but Not Chlorproguanil-Dapsone Treatment," *J. Individ. Dif.*, vol. 177, pp. 1429–1433, 1998.

[50] T. Jelinek1, A. Ronn, M. Lemnge, J. Curtis, J. Mhina, M. Duraisingh, I. Bygbjerg, and D. Warhurst, "Polymorphisms in the dihydrofolate reductase (DHFR) and dihydropteroate synthetase (DHPS) genes of *Plasmodium falciparum* and *in vivo* resistance to sulphadoxine/pyrimethamine in isolates from Tanzania," *Trop. Med. Int. Health*, vol. 3, pp. 605–609, 1998.

[51] L. Luzzatto, "The rise and fall of the antimalarial Lapdap: a lesson in pharmacogenetics," *Lancet*, vol. 376, pp. 739–41, 2010.

[52] O. Daramola, P. Alonso, T. O'Dempsey, P. Twumasi, T. McArdle, and B. Greenwood, "Sensitivity of *Plasmodium falciparum* in Gambia to co-trimoxazole.," *Trans. R. Soc. Trop. Med. Hyg.*, vol. 85, pp. 345–8, 1991.

[53] P. J. Rosenthal, "Antimalarial drug discovery: old and new approaches," *J. Exp. Biol.*, vol. 206, pp. 3735–3744, 2003.

[54] L. von Seidlein, P. Milligan, M. Pinder, K. Bojang, C. Anyalebechi, R. Gosling, R. Coleman, J. I. Ude, A. Sadiq, M. Duraisingh, P. D. Warhurst, A. Alloueche, P. G. Targett, P. K. McAdam, P. B. Greenwood, G. Walraven, P. Olliaro, and T. Doherty, "Efficacy of artesunate plus pyrimethamine-sulphadoxine for uncomplicated malaria in Gambian children: a double-blind, randomised, controlled trial," *Lancet*, vol. 355, pp. 352–357, 2000.

[55] A. Farnert, J. Lindberg, P. Gil, G. Swedberg, Y. Berqvist, M. M. Thapar, N. Lindegardh, S. Berezcky, and A. Bjorkman, "Evidence of *Plasmodium falciparum* malaria resistant to atovaquone and proguanil hydrochloride: case reports," *Brit. Med. J.*, vol. 326, pp. 628–9, 2003.

[56] D. G. Dorsey, D. Njama, M. R. Kamya, A. Cattamanchi, D. Kyabayinze, S. G. Staedke, A. Gasasira, and P. J. Rosenthal, "Sulfadoxine/pyrimethamine alone or with amodiaquine or artesunate for treatment of uncomplicated malaria: a longitudinal randomised trial," *Lancet*, vol. 360, pp. 1998–1999, 2002.

[57] C. Fanello, C. Karema, D. Ngamije, A. Uwimana, V. Ndahindwa, C. V. Overmeir, W. V. Doren, J. Curtis, and U. D'Alessandro, "A randomised trial to assess the efficacy and safety of chlorproguanil/dapsone + artesunate for the treatment of uncomplicated *Plasmodium falciparum* malaria.," *Trans. R. Soc. Trop. Med. Hyg.*, vol. 102, pp. 412–20, 2008.

[58] S. M. Kiara, J. Okombo, V. Masseno, L. Mwai, I. Ochola, S. Borrmann, and A. Nzila, "In Vitro Activity of Antifolate and Polymorphism in Dihydrofolate Reductase of *Plasmodium falciparum* Isolates from the Kenyan Coast: Emergence of Parasites with Ile-164-Leu Mutation," *Antimicrob. Agents Chemother.*, vol. 53, pp. 3793–3798, 2009.

[59] W. Sirawaraporn, T. Sathikul, R. Sirawaraporn, Y. Yuthavong, and D. V. Santi, "Antifolate-resistant mutants of *Plasmodium falciparum* dihydrofolate reductase," *Proc. Natl. Acad. Sci.*, vol. 94, pp. 1124–1129, 1997.

[60] D. C. Warhurst, "Antimalarial drug discovery: development of inhibitors of dihydrofolate reductase active in drug resistance," *Drug Discov. Today*, vol. 3, pp. 538–546, 1998.

[61] K. H. Rieckmann, A. E. Yeo, and M. D. Edstein, "Activity of PS-15 and its metabolite, WR99210, against *Plasmodium falciparum* in an *in vivo-in vitro* model," *Trans. R. Soc. Trop. Med. Hyg.*, vol. 90, pp. 568–571, 1996.

[62] D. Gravestock, A. L. Rousseau, A. C. Lourens, S. S. Moleele, R. L. V. Zyl, and P. A. Steenkamp, "Expeditious synthesis and biological evaluation of novel 2,N^6-disubstituted 1,2-dihydro-1,3,5-triazine-4,6-diamines as potential antimalarials," *Eur. J. Med. Chem.*, vol. 46, pp. 2022–2030, 2011.

[63] N. P. Jensen, A. L. Ager, R. A. Bliss, C. J. Canfield, B. M. Kotecka, K. H. Rieckmann, J. Terpinski, and D. P. Jacobus, "Phenoxypropoxybiguanides, prodrugs of DHFR-inhibiting diaminotriazine antimalarials," *J. Med. Chem.*, vol. 44, no. 23, pp. 3925–3931, 2001.

[64] A. Nzila, J. Okombo, R. P. Becker, R. Chilengi, and T. Lang, "Anticancer agents against malaria: time to revisit?," *Trends Parasitol.*, vol. 26, no. 3, pp. 125–129, 2010.

[65] M. A. Howard, A. B. Hibbard, D. R. Terrell, P. J. Medina, S. K. Vesely, and J. N. George, "Quinine allergy causing acute severe systemic illness: report of 4 patients manifesting multiple hematologic, renal, and hepatic abnormalities," *Proc. (Bayl. Univ. Med. Cent.)*, vol. 16, pp. 21–26, 2003.

[66] J. Sibilia and J. Pasquali, "Systemic lupus erythematosus: news and therapeutic perspectives," *Presse Med.*, vol. 37, pp. 444–59, 2008.

[67] O. Dar, M. Khan, and I. Adagu, "The potential Use of Methotrexate in the Treatment of *Falciparum* Malaria: In Vitro Assays against Sensitive and Multidrug-Resistant *Falciparum* Strains," *Jpn. J. Infect. Dis.*, vol. 61, pp. 210–211, 2008.

[68] R. Chilengi, R. Juma, A. M. Abdallah, M. Bashraheil, H. Lodenyo, P. Nyakundi, E. Anabwani, A. Salim, G. Mwambingu, E. Wenwa, J. Jemutai, C. Kipkeu, G. O. Oyoo, S. N. Muchohi, G. Kokwaro, T. Niehues, T. Lang, and A. Nzila, "A phase I trial to evaluate the safety and pharmacokinetics of low-dose methotrexate as an anti-malarial drug in Kenyan adult healthy volunteers," *Malaria J.*, vol. 10, p. 63, 2011.

[69] J. Swierkot and J. Szechinski, "Methotrexate in rheumatoid arthritis," *Pharmacol. Rep.*, vol. 58, pp. 473–92, 2006.

[70] B. Irungu, D. Kiboi, B. Langat, G. Rukunga, S. Wittlin, and A. Nzila, "Methotrexate and aminopterin lack *in vivo* antimalarial activity against murine malaria species," *Exp. Parasitol.*, vol. 123, pp. 118–121, 2009.

[71] B. N. Cronstein, "Low-Dose Methotrexate: A Mainstay in the Treatment of Rheumatoid Arthritis," *Pharmacol. Rev.*, vol. 57, pp. 163–172, 2005.

[72] R. Kalb, B. Strober, G. Weinstein, and M. Lebwohl, "Methotrexate and psoriasis: 2009 National Psoriasis Foundation Consensus Conference," *J. Am. Acad. Dermatol.*, vol. 60, pp. 824–37, 2009.

[73] E. Nduati, A. Diriye, S. Ommeh, L. Mwai, S. Kiara, V. Masseno, G. Kokwaro, and A. Nzila, "Effect of folate derivatives on the activity of antifolate drugs used against malaria and cancer," *Parasitol. Res.*, vol. 102, pp. 1227–1234, 2008.

[74] D. S. Walsh, S. Looareesuwan, P. Wilairatana, J. D. Gray Heppner, D. B. Tang, T. G. Brewer, W. Chokejindachai, P. Viriyavejakul, D. E. Kyle, W. K. Milhous, B. G. Schuster, J. Horton, D. J. Braitman, , and R. P. Brueckner, "Randomized Dose-Ranging Study of the Safety and Efficacy of WR238605 (Tafenoquine) in the Prevention of Relapse of *Plasmodium vivax* Malaria in Thailand," *J. Inf. Dis.*, vol. 180, pp. 1282–7, 1999.

[75] B. Lell, J. Faucher, M. Missinou, S. Borrmann, O. Dangelmaier, J. Horton, and P. Kremsner, "Malaria chemoprophylaxis with tafenoquine: a randomised study.," *Lancet*, vol. 355, pp. 2041–2045, 2000.

[76] P. A. Stocks, K. J. Raynes, P. G. Bray, B. K. Park, P. M. O'Neill, and S. A. Ward, "Novel Short Chain Chloroquine Analogues Retain Activity Against Chloroquine Resistant K1 *Plasmodium falciparum*," *J. Med. Chem.*, vol. 45, pp. 4975–4983, 2002.

[77] L. Gordon Tech. Rep. WO0153276, Isis Innovation, 2001.

[78] E. F. F. da Cunha, T. C. Ramalho, E. R. Maia, and R. B. de Alencastro, "The search for new DHFR inhibitors: a review of patents, January 2001- February 2005," *Expert Opin. Ther. Patents*, vol. 15, pp. 1–20, 2005.

[79] B. Tarnchompoo, C. Sirichaiwat, W. Phupong, C. Intaraudom, W. Sirawaraporn, S. Kamchonwongpaisan, J. Vanichtanankul, Y. Thebtaranonth, and Y. Yuthavong, "Development of 2, 4-Diaminopyrimidines as Antimalarials Based on Inhibition of the S108N and C59R + S108N Mutants of Dihydrofolate Reductase from Pyrimethamine-Resistant *Plasmodium falciparum*," *J. Med. Chem.*, vol. 45, pp. 1244–1252, 2002.

[80] A. Rousseau, D. Gravestock, A. Lourens, R. van Zyl, H. van Hoppe, L. Nkabinde, and S. Kamchonwongpaisan, "Novel Dihydrotriazines With Potent Antimalarial activity." Manuscript in preparation.

[81] E. Nduati, S. Hunt, E. M. Kamau, and A. Nzila, "2,4-Diaminopteridine-Based Compounds as Precursors for *De Novo* Synthesis of Antifolates: a Novel Class of Antimalarials," *Antimicrob. Agents and Chemother.*, vol. 49, no. 9, pp. 3652–3657, 2005.

[82] A. Rousseau, D. Gravestock, and A. Lourens, "WO2011018742." patent lodged, 2010.

[83] D. Seeger, J. S. Jr., and M. Hultquist, "Antagonist for pteroylglutamic acid," *J. Am. Chem. Soc.*, vol. 69, p. 2567, 1947.

[84] R. Elliot, J. C. Temple, and J. Montgomery, "Potential Folic Acid Antagonists. IV. Synthetic Approaches to Analogs of Aminopterin and Methotrexate. IV. The Preparation of p-[(2,4-Diamino-6-pteridinyl)methyl]amino-benzoic Acids," *J. Org. Chem*, vol. 35, pp. 1676–1680, 1970.

[85] C. M. Baugh and E. Shaw, "The synthesis of 6-Hydroxymethylpteridines," *J. Org. Chem.*, vol. 29, pp. 3610–3612, 1964.

[86] M. Chaykovsky, A. Rosowsky, N. Papathanasopoulos, K. K. Chen, E. J. Modest, R. L. Kisliuk, and Y. Gaumont, "Methotrexate analogs. 3. Synthesis and biological properties of some side-chain altered analogs," *J. Med. Chem.*, vol. 17, pp. 1212–1216, 1974.

[87] A. Rosowsky, J. H. Freisheim, H. Bader, R. A. Forsch, S. S. Susten, C. A. Cucchi, and E. Frei, "Methotrexate Analogues. 25. Chemical and Biological Studies on the γ-*tert*-Butyl Esters of Methotrexate and Aminopterin," *J. Med. Chem.*, vol. 28, pp. 660–667, 1985.

[88] R. C. Reynolds, C. A. Johnson, J. R. Piper, and F. M. Sirotnak, "Synthesis and antifolate evaluation of the aminopterin analogue with a bicyclo[2.2.2]octane ring in place of the benzene ring," *Eur. J. Med. Chem.*, vol. 36, pp. 237–242, 2001.

[89] C. Waller, A. Goldman, R. Angier, J. Boothe, B. Hutchings, J. Mowat, and J. Semb, "2-Amino-4-hydroxy-6-pteridinecarboxaldehyde," *J. Am. Chem. Soc.*, vol. 72, p. 4630, 1950.

[90] W. P. Tong, J. Rosenberg, and D. B. Ludlum, "Purity of Methotrexate," *Lancet*, vol. 306, p. 719, 1975.

[91] P. H. Boyle and Wolfganleiderer, "Pteridine, LXIX. Synthese und Reaktivitat des 2,4-Diamino-6-(hydroxymethyl)-pteridins," *Chem. Ber.*, vol. 113, pp. 1514–1523, 1980.

[92] W. Traube, "Zur Kenntniss der γ, δ-Dioxypropylmalonsaure," *Chem. Ber.*, vol. 37, p. 4544, 1904.

[93] M. Mallette, E. Taylor, and C. Cain, "Pyrimido[4,5-b]pyrazines. II. 2,4-Diaminopyrimido[4,5-b]pyrazine and Derivatives," *J. Am. Chem. Soc.*, vol. 69, pp. 1814–1816, 1947.

[94] L. B. Tulloch, V. P. Martini, J. Iulek, J. K. Huggan, J. H. Lee, C. L. Gibson, T. K. Smith, C. J. Suckling, and W. N. Hunter, "Structure-based design of pteridine reductase inhibitors targeting African sleeping sickness and the leishmaniases," *J. Med. Chem.*, vol. 53, no. 1, pp. 221–229, 2009.

[95] C. W. van der Westhuyzen, A. L. Rousseau, and C. J. Parkinson, "Effect of substituent structure on pyrimidine electrophilic substitution," *Tetrahedron*, vol. 63, pp. 5394–5405, 2007.

[96] D. E. O'Brien, F. Baiocchi, R. K. Robins, and C. Cheng, "Pyrimidines. IX. 4-and 5-(Substituted-anilino) pyrimidines," *J. Med. Chem.*, vol. 5, no. 6, pp. 1085–1103, 1962.

[97] J. R. Piper and J. A. Montgomery, "Preparation of 6-(Bromomethyl)-2,4-pteridinediamine Hydrobromide and Its Use in Improved Synthesis of Methotrexate and Related Compounds," *J. Org. Chem.*, vol. 42, pp. 208–211, 1977.

[98] E. Taylor and H. Patel, "Synthesis of pyrazolo(3,4,-d)pyrimidine analogues of the potent antitumor agent n-4-(2-(2-amino-4(3H)-oxo-7H-pyrrolo(2,3-d)pyrimidin-5-yl)methyl)," *Tetrahedron Lett.*, vol. 48, pp. 8089–8100, 1992.

[99] C. J. Barnett, T. M. Wilson, and M. E. Kobierski, "A Practical Synthesis of Multitargeted Antifolate LY231514," *Org. Proc. Res. Dev.*, vol. 3, p. 184, 1999.

[100] R. C. Larock, W.-Y. Leung, and S. Stolz-Dunn, "Synthesis of aryl-substituted aldehydes and ketones via palladium-catalyzed coupling or aryl halides and non-allylic unsaturated alcohols," *Tetrahedron Lett.*, vol. 30, pp. 6629–6632, 1989.

[101] T. Mizoroki, K. Mori, and A. Ozaki, "Arylation of Olefin with Aryl Iodide Catalyzed by Palladium," *A. Bull. Chem. Soc. Jpn.*, vol. 44, p. 581, 1971.

[102] R. Heck and J. Nolley, "Palladium-catalyzed vinylic hydrogen substitution reactions with aryl, benzyl, and styryl halide," *J. Org. Chem.*, vol. 14, pp. 2320–2322, 1972.

[103] H. Dieck and R. Heck, "Organophosphinepalladium complexes as catalysts for vinylic hydrogen substitution reactions," *J. Am. Chem. Soc.*, vol. 96, p. 1133, 1974.

[104] I. P. Beletskaya and A. V. Cheprakov, "The Heck Reaction as a Sharpening Stone of Palladium Catalysis," *Chem. Rev.*, vol. 100, pp. 3009–3066, 2000.

[105] A. J. Chalk and S. A. Magennis, "Palladium-catalyzed vinyl substitution reactions. II. Synthesis of aryl substituted allylic alcohols, aldehydes, and ketones from aryl halides and unsaturated alcohols," *J. Org. Chem*, vol. 41, pp. 1206–1209, 1976.

[106] D. P. Kjell, B. J. Slattery, and M. J. Semo, "A Novel, Nonaqueous Method for Regeneration of Aldehydes from Bisulfite Adducts," *J. Org. Chem.*, vol. 64, pp. 5722–5724, 1999.

[107] A. Stadler, B. h. Yousefi, D. Dallinger, P. Walla, E. V. der Eycken, N. Kaval, and C. O. Kappe, "Scalability of Microwave-Assisted Organic Synthesis. From Single-Mode to Multimode Parallel Batch Reactors," *Org. Process Res. Dev.*, vol. 7, pp. 707–716, 2003.

[108] E. C. Taylor and P. M. Harrington, "A convergent synthesis of 5, 10-dideaza-5, 6, 7, 8-tetrahydrofolic acid and 5, 10-dideaza-5, 6, 7, 8-tetrahydrohomofolic acid. An effective principle for carbonyl group activation," *J. Org. Chem.*, vol. 55, no. 10, pp. 3222–3227, 1990.

[109] S. D. Meyer and S. L. Schreiber, "Acceleration of the Dess-Martin Oxidation by Water," *J. Org. Chem.*, vol. 59, pp. 7549–7552, 1994.

[110] C. J. Barnett and T. M. Wilson, "Process for preparing 5-substituted pyrrolo-[2,3-d]pyrimidines," Tech. Rep. US 5416211 A, Eli Lilly and Co., 1995.

[111] P. Prabhakar, N. Suryakiran, M. Narasimhulu, and Y. Venkateswarlu, "A mild and efficient 1,4-addition of thiols and phenols to α,β-unsaturated carbonyl compounds using $La(NO_3)_3 \cdot 6\,H_2O$ as a catalyst under solvent-free conditions," *J. Mol. Catal. A: Chem.*, vol. 274, pp. 72–77, 2007.

[112] G. Jenner, "Synthesis of hindered functionalised ethers via high-pressure addition of alcohols to acrylic compounds," *Tetrahedron Lett.*, vol. 41, pp. 4807–4810, 2001.

[113] I. Stewart, F. Toste, and R. Bergman, "Phosphine-catalyzed Hydration and Hydroalkoxylation of Activated Olefins: Use of a Strong Nucleophile to Generate a Strong Base," *J. Am. Chem. Soc.*, vol. 125, pp. 8696–8697, 2003.

[114] A. Cook and K. Reed, "Some aryl di-β-amidinoethyl ethers," *J. Chem. Soc.*, pp. 920–921, 1945.

[115] Y.-L. Zhong, D. T. Boruta, D. R. Gauthier, and D. Askin, "An efficient synthesis of 4-chromanones," *Tetrahedron Lett.*, vol. 52, no. 38, pp. 4824–4826, 2011.

[116] J. Greiner, E. Rouvier, R. Pastor, and A. Cambon, "Etudes Conformationnelles par Resonance Magnetique Nucleaire d'Ethanes Disubstitue par un Heteroatome appartenant aux Colonnes IV, V et VI et par un Groupement Fonctionnel," *Org. Magn. Reson.*, vol. 11, pp. 329–332, 1978.

[117] T. Weiske and H. Schwarz, "Pseudo-einstufige C-C-Spaltungen beim Zerfall von ionisierten Carbonsauren. Radikaltypische Reaktionen in der Massenspektrometrie," *Chem. Ber.*, vol. 116, pp. 323–347, 1983.

[118] P. B. Russell and G. H. Hitchings, "2,4-Diaminopyrimidines as Antimalarials. III. 5-Aryl Derivatives," *J. Am. Chem. Soc.*, vol. 73, pp. 3763–3770, 1951.

[119] A. Park and S. Lee, "Synthesis of Benzoylacetonitriles from Pd-Catalyzed Carbonylation of Aryl Iodides and Trimethylsilylacetonitrile," *Org. Lett.*, vol. 14, pp. 1118–1121, 2012.

[120] G. F. Starkulla, E. Kapatsina, A. Baro, F. Giesselmann, S. Tussetschläger, M. Kaller, and S. Laschat, "Influence of spacer chain lengths and polar terminal groups on the mesomorphic properties of tethered 5-phenylpyrimidines," *Beilstein. J. Org. Chem.*, vol. 5, p. 63, 2009.

[121] D. D. Holsworth, "An Expeditious Synthesis of 6-Alkyl-5-(4'-amino-phenyl)-pyrimidine-2,4-diamines," *Synth. Commun.*, vol. 33, pp. 3467–3475, 2003.

[122] M. D. Serby, H. Zhao, B. G. Szczepankiewicz, C. Kosogof, Z. Xin, B. Liu, M. Liu, L. T. Nelson, W. Kaszubska, H. D. Falls, V. Schaefer, E. N. Bush, R. Shapiro, B. A. Drox, V. E. Knourek-Segel, T. A. Fey, M. E. Brune, D. W. A. Beno, T. M. Turner, C. A. Collins, P. B. Jacobson, H. L. Sham, and G. Liu, "2,4-Diaminopyrimidine Derivatives as Potent Growth Hormone Secretagogue Receptor Antagonists," *J. Med. Chem.*, vol. 49, pp. 2568–2578, 2006.

[123] S. Ahmad, K. Ngu, D. W. Combs, S. C. Wu, D. S. Weinstein, W. Liu, B.-C. Chen, G. Chandrasena, C. R. Dorso, M. Kirby, and K. S. Atwal, "Aminoimidazoles as bioisosteres of acylguanidines: novel, potent, selective and orally bioavailable inhibitors

of the sodium hydrogen exchanger isoform-1," *Bioorg. Med. Chem. Lett.*, vol. 14, pp. 177–180, 2004.

[124] T. de Boer and H. Backer, "Diazomethane," *Org. Synth.*, vol. 36, p. 250, 1963.

[125] A. Salahuddin, A. Inam, R. L. van Zyl, D. C. Heslop, C.-T. Chen, F. Avecilla, S. M. Agarwal, and A. Azam, "Synthesis and evaluation of 7-chloro-4-(piperazin-1-yl) quinoline-sulfonamide as hybrid antiprotozoal agents," *Bioorg. Med. Chem.*, 2013.

[126] D. Perrin and W. Armarego, *Purification of Laboratory Chemicals*. Pergamon Press, Oxford, 1998.

[127] R. D. Elliott, C. Temple Jr, and J. A. Montgomery, "Potential folic acid antagonists. IV. Synthetic approaches to analogs of aminopterin and methotrexate. IV. preparation of p-{[(2, 4-diamino-6-pteridinyl) methyl] amino} benzoic acids," *J. Org. Chem.*, vol. 35, pp. 1676–1680, 1970.

[128] S. Al-Awadi, M. Abdallah, H. Dib, M. Ibrahim, N. Al-Awadi, and O. El-Dusouqui, "Kinetics and mechanism of thermal gas-phase elimination of β-substituted carboxylic acids," *Tetrahedron*, vol. 61, no. 24, pp. 5769–5777, 2005.

[129] G. Roda, S. Riva, and B. Danieli, "Almond oxynitrilase-catalyzed transformation of aldehydes is strongly influenced by naphthyl and alkoxy substituents," *Tetrahedron asymmetr.*, vol. 10, pp. 3939–3949, 1999.

[130] Y. Ji, W. C. Trenkle, and J. V. Vowles, "A High-Yielding Preparation of β-Ketonitriles," *Org. Lett.*, vol. 8, pp. 1161–1163, 2006.

[131] H. Yoshida, K. Yoshida, H. Totani, T. Ogata, and K. Matsumoto, "Some Properties of Cyclopropenone Oximes under Beckmann Reaction Conditions," *Bull. Chem. Soc. Jpn.*, vol. 63, pp. 3579–3582, 1990.

[132] W. Broser and U. Bollert, "Reaktion von α-Benzoyl-benzylcyanid mit 1.1-disubstituierten Hydrazinen," *Chem. Ber.*, vol. 104, pp. 2053–2062, 1971.

[133] L. Huang, A. Shi, F. He, and X. Li, "Synthesis, biological evaluation, and molecular modeling of berberine derivatives as potent acetylcholinesterase inhibitors," *Bioorg. Med. Chem.*, vol. 18, no. 3, pp. 1244–1251, 2010.

[134] A. Schmitz, A. Sankaranarayanan, P. Azam, K. Schmidt-Lassen, D. Homerick, W. Hänsel, and H. Wulff, "Design of PAP-1, a Selective Small Molecule Kv1. 3 Blocker, for the Suppression of Effector Memory T Cells in Autoimmune Diseases," *Mol. Pharmacol.*, vol. 68, pp. 1254–1270, 2005.

[135] Shiongi and L. Co., "Cyclic amine derivatives and use thereof," Tech. Rep. US6649623, 2003.

[136] E. Ljubovic and V. Sunjic, "Effect of Distant Groups on the Enantioselectivity in Kinetic Resolution of sec-Alcohols Catalyzed by Microbial Lipases," *Croat. Chem. Acta*, vol. 71, pp. 99–117, 1998.

[137] M. Rivara, V. Zuliani, G. Cocconcelli, G. Morini, M. Comini, S. Rivara, M. Mor, F. Bordi, E. Barocelli, V. Ballabeni, *et al.*, "Synthesis and biological evaluation of new non-imidazole h3-receptor antagonists of the 2-aminobenzimidazole series," *Bioorg. Med. Chem.*, vol. 14, pp. 1413–1424, 2006.